DESIGN, ANALYSIS AND CHARACTERIZATION OF DIFFERENT TYPES OF FREQUENCY SELECTIVE SURFACES AND ABSORBER

A THESIS SUBMITTED IN PARTIAL FULFILLMENT OF THE REQUIREMENTS FOR THE DEGREE OF DOCTOR OF PHILOSOPHY

SAPTARSIKA DAS

MZU REGISTRATION NO.: 2200050

Ph.D. REGISTRATION NO.: MZU/Ph.D./1935 of 15.09.2021

DEPARTMENT OF PHYSICS

SCHOOL OF PHYSICAL SCIENCE

AUGUST 2025

DESIGN, ANALYSIS AND CHARACTERIZATION OFDIFFERENT TYPES OF FREQUENCY SELECTIVE SURFACES AND ABSORBER

By

SAPTARSIKA DAS

DEPARTMENT OF PHYSICS

Supervisor

Prof. RAMESH CHANDRA TIWARI

Joint Supervisor

Prof. L. LOLIT KUMAR SINGH

Submitted

In partial fulfillment of the requirement of the Degree of Doctor of Philosophy in Physics of Mizoram University, Aizawl

DEPARTMENT OF PHYSICS

MIZORAM UNIVERSITY, AIZAWL-796004, MIZORAM

CERTIFICATE

This is to certify that the thesis entitled '**DESIGN, ANALYSIS AND CHARACTERIZATION OF DIFFERENT TYPES OF FREQUENCY SELECTIVE SURFACES AND ABSORBER'** *submitted by Saptarsika Das for the degree* of *Doctor of Philosophy under Mizoram University, Aizawl, embodies the record of original investigations carried out by her under our supervision. She has been duly registered and the thesis presented is worthy of being considered for the award of Ph.D Degree. This work has not been submitted for any degree at any other university.*

(Prof. RAMESH CHANDRA TIWARI)
Supervisor

(Prof. L.LOLIT KUMAR SINGH)
Joint Supervisor

DECLARATION

MIZORAM UNIVERSITY

AUGUST, 2025

I **SAPTARSIKA DAS,** hereby declare that the subject matter of this thesis is the record of work done by me, that the contents of this thesis did not form basis of the award of any previous degree to me or to do the best of my knowledge to anybody else, and that the thesis has not been submitted by me for any research degree in any other University/ Institute.

This is being submitted to the Mizoram University for the **Degree of Doctor of Philosophy in Physics.**

(SAPTARSIKA DAS)
Candidate

(Prof. RAMESH CHANDRA TIWARI)
Supervisor

(Head of the Department)

(Prof. L.LOLIT KUMAR SINGH)
Joint Supervisor

Acknowledgement

I would like to express my sincere and heartfelt gratitude to the individuals and institutions who have played a significant role in completion of this research work.

I would like to express my gratefulness and indebtedness to my supervisor Prof. Ramesh Chandra Tiwari, Professor, Department of Physics, Mizoram University, Aizawl, Mizoram and Joint supervisor Prof. L.Lolit Kumar Singh, Dean FW, Department of Electronics and Communication Engineering, National Institute of Technology, Imphal, Manipur for enlighten me with their extensive experiential knowledge. Their constant encouragement and support, insightful suggestions and open discussions advance to the effectual outcome of this research work.

I am also grateful to Prof. Partha Pratim Sarkar, Professor, Department of Engineering and Technological Studies, University of Kalyani, Kalyani, West Bengal for being my guiding light. He generously extended his cooperation to conduct the experimental part of this research work in his esteemed laboratory. His valuable suggestions and support facilitate and enhances the research work to a great extent. I am equally thankful to the research scholars in his team, whose assistance and time to time cultivation of ideas through discussion greatly enrich the learning experience during this research work.

I would like to convey my special thanks to all who have extended their assistance directly or indirectly to complete this academic journey. This includes my family, colleagues and friends whose constant encouragement and understanding have been a great source of strength. Lastly, I beg to be excused for not mentioning their individual names.

(Saptarsika Das)

Table of Contents

Certificate i

Declaration ii

Acknowledgement iii

Contentsi v - vii

List of Tables viii

List of Figures ix - xiii

Chapter 1 Introduction 1-23

1.1 Introduction 1

1.2 Application 3

1.3 Surveyof Literature 6

1.3.1 Previous Work on Method of Moment (MOM) Based FSS 7

1.3.2 Previous Work on Compact FSS 8

1.3.3 Previous Work on Curved FSS 10

1.3.4 Previous Work on Absorber 11

1.4 Objective 13

1.5 Organisation of Thesis 13

1.6 References 15

Chapter 2 Method of Moment and Its Application for Theoretical Analysis of an FSS Structure 24 - 70

2.1 Introduction 24

2.2 Concept of The Method of Moment 25

2.3 Formulation of the Problem 27

2.4 General Solution of the Operator Equation 36

2.5 Theoretical Analysis of Printed Cross dipole Array as an FSS Structure by MOM 39

2.6 Development of Algorithm and Programming 40

2.7 Experimental Verification 43

2.8 Conclusion 47

2.9 References 69

Chapter 3 Planar and Curved FSS: Enhancement of Flatness and Roll of Factor of Transmission Characteristic 71 - 105

3.1 Introduction 71

3.2 Design of the Planar and Curved FSS 72

3.2.1 Design of Planar FSS 73

3.2.2 Design of Curved FSS 77

3.3 Results and Discussion 79

3.3.1 Study of Planar FSS 79

3.3.2 Study of Curved FSS 81

3.4 Conclusion 83

3.5 References 103

Chapter 4 Design of a Reduced Size Frequency Selective Surface 106 - 145

4.1 Introduction 106

4.2 Design of FSSs 107

4.2.1 Modification of circular type patch element to reduce the size of the FSS 107

4.2.2 Modification of square type patch element with loop type slots to reduce the size of the FSS 109

4.2.3 Modification of square type patch element with rectangular s lots and slits to reduce the size of the FSS 112

4.3 Results & Discussion 115

4.3.1 Study of compactness of modified circular patch type element 116

4.3.1.1 Calculation of size reduction of the final modified circular patch type FSS 118

4.3.2 Study of compactness of modified square patch type element with loop type slot 118

4.3.2.1 Calculation of size reduction of the final modified square patch type FSS 120

4.3.2.2 Comparative study of the designed square patch with the contemporary works 121

4.3.3 Study of compactness of modified square patch type element with rectangular slot and slits 122

4.3.3.1 Effect of periodicity P on compactness of the FSS 122

4.3.3.2 Study of the transmission characteristic of rectangular slots and slits loaded square patch FSS 123

4.3.3.3Calculation of size reduction of the final modified rectangular

slits and slots loaded square patch type FSS 126

4.3.3.4 Comparative study of the designed square patch with the contemporary works 127

4.4 Conclusion 128

4.4 References 144

Chapter 5 Design of a Frequency Selective Surface as Absorber 146 - 164

5.1 Introduction 146

5.2 Design of FSS absorber 147

5.2.1 Design of three layer FSS absorber 148

5.2.2 Design of two layer FSS absorber 151

5.3 Results & Discussion 154

5.3.1 Study of three layer FSS absorber 154

5.3.2 Study of two layer FSS absorber 157

5.4 Conclusion 161

5.5 References 162

Chapter 6 Conclusion and Future Scope of Studies 165 - 168

6.1 Conclusion 165

6.2 Future scope of studies 168

Bio – Data of the Candidate

Particulars of the Candidate

LIST OF TABLES

Table 2.1 Comparative Study of Results 45

Table 2.2 Parametric Study of the FSS by changing the periodicity 46

Table 3.1 Parametric study of planar FSS by varying the air gap between the two layers 79

Table 3.2 Comparison of contemporary works with the presented work for planar FSS 80

Table 3.3 Comparison of contemporary works with the presented work for curved FSS 82

Table 4.1 Dimensions of finally modified square patch FSS 111

Table 4.2 Dimensions of slits and slots of the final modified square patch 114

Table 4.3 Overview of all the simulated results 121

Table 4.4 Comparison of the designed square patch with the related works 121

Table 4.5 Study of compactness by changing the periodicity 122

Table 4.6 Overview of all the stages of modification of the square patch 127

Table 4.7 Comparison of the designed square patch with the related works 128

Table 5.1 Overview of the study of FSS absorber 161

LIST OF FIGURES

Fig.1.1 Patch type FSS and its characteristics 2

Fig.1.2 Aperture type FSS and its characteristics 2

Fig.1.3 Typical shapes of FSS element 3

Fig.1.4 Sub reflector based on FSS 4

Fig.1.5 FSS based radome 5

Fig.2.1 Diagram showing the projection of the incident wave on XY plane with X-axis 36

Fig.2.2 Part of frequency selective surface 39

Fig.2.3 Unit cell of FSS structure 39

Fig.2.4 Fabricated frequency selective surface 44

Fig.2.5 Transmission coefficient vs frequency graph 44

Fig.2.6 Transmission coefficient vs frequency graph for periodicity 18 mm 46

Fig.3.1 Unit cell of layer-1of the planar FSS 73

Fig.3.2 Unit cell of layer-2of the planar FSS 74

Fig.3.3 Layer-1of Planar FSS 74

Fig.3.4 Layer-2 of Planar FSS 75

Fig.3.5 Fabricated Frequency Selective Surfaces a) Layer-1 b) Layer-2 75

Fig.3.6 Laser cutting machine 76

Fig.3.7 Measurement set up of planar FSS 76

Fig.3.8 Semi cylindrical FSS structure from different perspectives

a) Front view of duallayer curved FSS 77
b) b) Side view of dual layer curved FSS 78

Fig.3.9 Measurement set up of dual layer curved FSS 78
Fig.3.10 Transmission coefficient vs frequency plot of composite planar FSS 79
Fig.3.11 Transmission coefficient vs frequency plot of composite planar FSS 81
Fig.4.1 Unit cell of reference circular patch FSS 108
Fig.4.2 Intermediate step of circular and cross dipole slots loaded patch for the modification of circular patch 108
Fig.4.3 Final modified circular patch 109
Fig.4.4 Unit cell of reference square patch FSS 110
Fig.4.5 Unit cell of modified square patch FSS (1^{st} step) 110
Fig.4.6 Unit cell of final modified square patch FSS 111
Fig.4.7 Unit cell of reference square patch FSS 112
Fig.4.8 An intermediate step of modification of the square patch unit cell loaded withslits and slots 113
Fig.4.9 Second intermediate step of modification of the square patch unit cell loaded with slits and slots 113
Fig.4.10 Final and optimized modification of square patch unit cell loaded with slits andslots 114
Fig.4.11 Fabricated square patch FSS loaded with slits and slots 115
Fig.4.12 Measurement set up of the fabricated FSS 115
Fig.4.13 Transmission characteristics of reference circular patch FSS by simulation 116

Fig.4.14 Simulated transmission characteristics of intermediate step of circular and crossdipole slots loaded patch for the modification of circular patch FSS 116

Fig.4.15 Simulated transmission Characteristics of finally modified circular patch FSS 117

Fig.4.16 Transmission characteristics of reference square patch FSS by simulation 119

Fig.4.17 Transmission characteristics of the first modified square patch FSS by simulation 119

Fig.4.18 Transmission characteristics of finally modified square patch FSS by simulation 120

Fig.4.19 Transmission characteristics by changing the periodicity of rectangular slotsand slits loaded square patch FSS structure 123

Fig.4.20 Transmission characteristics of reference square patch 124

Fig.4.21 Transmission characteristics of an intermediate step of modification of thesquare patch loaded with slits and slots 124

Fig.4.22 Transmission characteristics of second intermediate step of modification of thesquare patch loaded with slits and slots 125

Fig.4.23 Transmission characteristics of finally modified square patch loaded with slitsand slots 126

Fig.5.1 Square patch imprinted on top of the substrate representing unit cell of the bottom layer of the FSS absorber 149

Fig.5.2 Square patch imprinted on top of the substrate representing unit cell of the middle layer of the FSS absorber 149

Fig.5.3 Square patch imprinted on bottom of the substrate representing unit cell of themiddle layer of the FSS absorber 150

Fig.5.4 Square patch imprinted on top of the substrate representing unit cell of the toplayer of the FSS absorber 150

Fig.5.5 Square patch imprinted on bottom of the substrate representing unit cell of the top layer of the FSS absorber 151

Fig.5.6 Unit cell representation of composite FSS absorber 151

Fig.5.7 Patch imprinted on top of the substrate representing unit cell of the top of the lower layer of the FSS absorber 152

Fig.5.8 Patch imprinted on bottom of the substrate representing unit cell of the bottom oflower layer of the FSS absorber 153

Fig.5.9 Unit cell representation of the superstrate where the square patch is imprinted onthe bottom of the substrate 153

Fig.5.10 Unit cell representation of composite FSS absorber 154

Fig.5.11 Transmission/ Reflection Characteristic of top layer of the three layer FSS absorber by combining Fig.5.4 & Fig.5.5 155

Fig.5.12 Transmission/ Reflection Characteristic of middle layer of the three layer FSS absorber by combining Fig. 5.2 & Fig. 5.3 155

Fig.5.13 Transmission/ Reflection Characteristic of bottom layer of the three layer FSS absorber shown in Fig.5.1 156

Fig.5.14 Transmission/ Reflection Characteristic of three layer FSS absorber 156

Fig.5.15 Absorption percentage vs frequency plot of three layer FSS absorber 157

Fig.5.16 Transmission/ Reflection Characteristic of the patch shown in Fig.5.7 158

Fig.5.17 Transmission/ Reflection Characteristic of the patch shown in Fig.5.8 159

Fig.5.18 Transmission/ Reflection Characteristic of the combination of patches shown inFig.5.7 & Fig.5.8 159

Fig.5.19 Transmission/ Reflection Characteristics of the two layer FSS absorber 160

Fig.5.20 Absorption percentage vs frequency plot of the two layer Absorber 160

CHAPTER 1

Introduction

1.1 Introduction

The advancement of satellite communication and wireless technology demand new microwave devices. The development accelerates focusing on the demand of handheld devices. These demands in lieu superannuated the traditional devices that build up the conventional communication systems. Likewise, the development of periodic structures gradually replaced the conventional filters in microwave and optical frequency spectrum. The substitution helps in the progression of wireless and satellite communication systems to a great extent. Light weight, easy to fabricate, cost effectiveness are some of the ample factors of the frequency selective surface that ignite the research minds to take the challenge to overcome the drawback of narrow bandwidth. Hence, the periodic structure also known as frequency selective surface (FSS) necessities an extensive study to meet the demand of the technological advancement in microwave and optical systems.

Frequency Selective Surface (FSS) is a two dimensional placement of indistinguishable elements in a periodic fashion. Fundamentally there are two types of FSS- patch type and aperture type. The periodic arrangement of elemental metal patches on a dielectric substrate is known as patch type FSS. The cutting of elemental structures on conducting plane supported by dielectric substrate is known as aperture type FSS.The FSS works on the principle of resonance of a filter. When an FSS structure is excited by a plane electromagnetic wave, the incident plane wave is partly transmitted through the structure and partly reflected by the structure. The dominance of transmission or reflection entirely depends on the harmonization of frequency of incident wave with the frequency of resonance of the FSS elements.Patch type elements reflect a certain frequency band of the incoming electromagnetic wave at resonant frequency, hence similitude bandstop filter.

The aperture type FSS resemble bandpass filter as it passes a certain frequency band of the incident electromagnetic wave. Both types of FSS are exactly

complementary to each other having the difference in excitement of currents in patch and aperture elements. In patch type elements excitement of electric current have been done and in aperture type elements magnetic current has been excited.

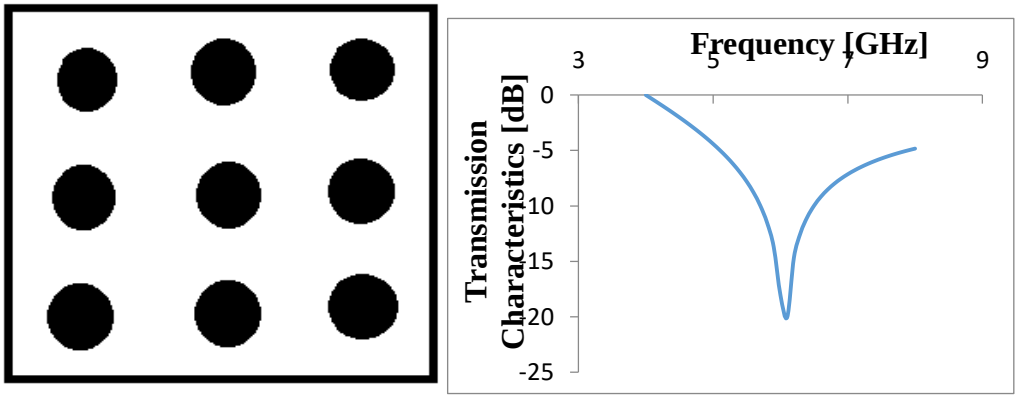

Fig.1.1.Patch type FSS and its characteristics

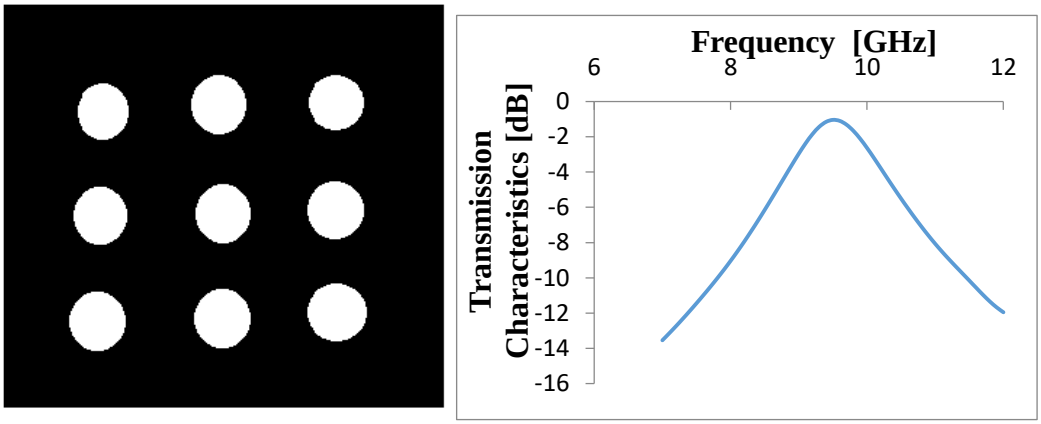

Fig.1.2.Aperture type FSS and its characteristics

The performance and behaviour of the FSS primarily depends on the geometry of the FSS element. Furthermore, the operating frequency depends on the thickness of the dielectric substrate and the characteristics of the dielectric material. The frequency response of the FSS is also controlled by the conductivity, inter spacing of the elements, incident angle and polarisation of the incident wave. The resonant frequency and the bandwidth are influenced by the permittivity of the substrate and the period of the elements of the FSS array is responsible for the grating lobes which

administer the bandwidth of the FSS. All these factors have to be considered and should be methodically characterised to obtain the desired performance of an FSS. FSS can be designed utilizing solid interior or plate type element, centre connected structure, loop type element and by combining any of the documented elements. All type of elements are shown in Fig.1.3.

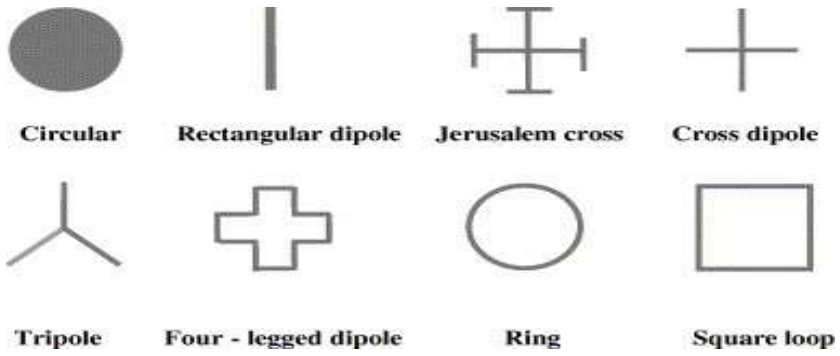

Fig.1.3.Typical shapes of FSS element

Frequency Selective Surfaces are theoretically analysed by numerical methods like FDTD, FEM, MOM. MOM is extensively used for the analysis of the FSS structures due to its high precision in the frequency domain. The characteristic basis functions are used in MOM to reduce the matrix significantly and converge quickly. Consequently it can electrically solve large problems knowing fewer unknowns. This features of MOM keep it ahead of other numerical methods while studying an FSS. We will use softwares like ANSOFT designer version 2.2 (based on MOM), HFSS (based on FEM) and FEKO (based on MOM) for simulating the FSS structure theoretically. FSS designed is then will be fabricated to perform experiment and measurement using Standard Microwave Test Bench.

1.2 Application

Frequency Selective Surface is the foremost cynosure of the researchers since last five decades and has numerous appealing applications.

Reflector antenna system includes atleast one FSS sub reflector that provides multifrequency operation in the desired frequency range of S band, X band, Ka and Ku band. Dual band parabolic reflector antenna was manufactured incorporating FSS based hyperbolic sub reflectors [1]. In 1993, the requirement of multiple microwave

frequencies for NASA's Cassimi project signifies the application of FSS as sub reflector with a single high gain antenna [2].

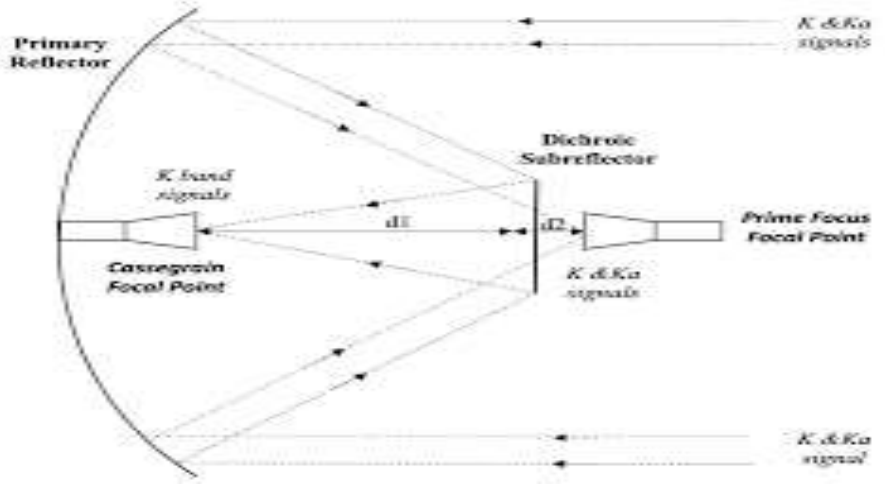

Fig.1.4.Sub reflector based on FSS

FSS sub reflector structure has been designed combining dichrocity and conformal geometry for Cassegrain systems [3]. Sub reflectors are used to produce multibeam coverage needed for broadband satellite missions [4]. Miniaturized sub-reflector is possible due to FSS and it also enhances the gain of sub-reflector based Cassegrain antenna [5,6]. This results in enhancement of longevity of the satellite due to decrease of its weight.

Aperture type FSS, which is also known as bandpass FSS has its application as polariser as it is capable to pass the desired frequency band and reflect back the other frequencies [7]. FSS has the capability to convert the linear polarised sub-millimeter wave to circularly polarised wave [8]. Conventionally, polarisation transformation had been done by cascading more than one surface. Later, a single planar surface has been reported, where closely arranged metallic meander lines impedance is loaded with rectangular metal patches. Circularly polarised transformers have its significance in microwave communication and radar systems where linearly polarised signals cannot be predicted reliably [9,10]. FSS polariser has extensive usage in remote sensing applications; isolate communication systems etc. [11,12].

FSS is used in radomes to reduce the enclosed antenna radar cross section. Bandpass FSS is used for the purpose, that allows in band frequency, ie. the frequency of the

incident wave that matches the operating frequency of the antenna, and divert the outband frequencies in another direction from the incident wave direction. A two layer rectangular aperture type FSS Separated by a low-loss dielectric medium has

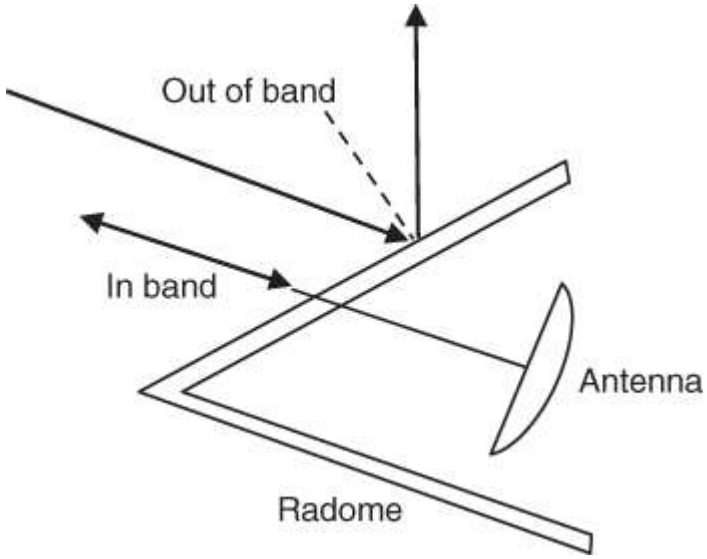

Fig.1.5. FSS based Radome

been analysed using MM-GSM technique [13]. The authors presented the technique that has less computational complexity in compare to the numerical techniques that are used to analyse FSS structure. The structure proposed is suitable for airborne radome application. The FSS radomes of insertion loss less than 1 dB have been studied with single slot element for linear polarisation and Jerusselum slot element for circular polarisation [14]. The lower insertion loss would increase the bandpass performance of the FSS which in lieu stabilised the system performance. A square loop configured with Jerruselum cross FSS structure exhibits sharp roll-off characteristics that help in out of band RCS reduction [15,16]. The authors proposed ray tracing technique and flat model to analyse FSS radomes. The investigation of Bore sight error (BSE) has been performed by analysing the phase distortion of the flat model and curved radome. The results obtained proved worthy to improve the electromagnetic performances of FSS radomes.

FSS reflector is integrated with microstrip antenna to enhance the gain and directivity of the antenna by reducing the back lobe losses. (Chatterjee, 2016) [17] enhance the gain of the antenna to 8-10 dBi by placing two reflective FSS at angle of

90° maintaining a specific distance from the antenna. The introduction of FSS improves the performance of dual band microstrip patch antenna, ie. it enhance the gain from 0.772 dBi to 0.915 dBi and improves return loss at WLAN frequency [18]. (Swetha et.al, 2020) [19] reported the enhancement of the gain of a ultra wideband antenna from 4.9 dB to 10.9 dB by employing FSS reflector below the UWB (Ultra Wide Band) antenna.

FSS tie up with monopole antenna transforms the bidirectional radiation pattern into unidirectional radiation pattern and increases the radiation efficiency upto 97.88% [20]. FSS reduces the free space radiation when inserted between two dielectric resonator antennas (DRA) and provides high isolation. The integrated system reported by (Karimian et.al, 2016) [21] contributes to increase the data capacity of wireless communication systems at millimetre waves. FSS is efficiently used to alleviate electromagnetic interference that badly affects the portable communication devices [22, 23]. FSS absorbers have wide contribution in stealth technology. Absorbers are designed utilizing resistive films, magnetic films etc. as absorbing material [24, 25]. FSS alongwith integrated limiter provides a protection to the receiver from high power signals [26]. FSS enhances the power transmission [27] and energy transmission [28] that contributes to high power microwave protection.

FSS is favoured in diverse applications due to its light weight, low volume and low cost. A notable advantage of FSS is, it can be fabricated using typical printed circuit technology.

1.3 Survey of Literature

The study of periodic structure first started to assist military application and since last five decades it has been extensively explored, as a consequence quickly absorbed for consumption.

R Mittra proposed the entire domain type of basis function for typical FSS unit cell geometries that reduces the moment method matrix and efficiently solves problems for electrically large structure. His work is the backbone to analyse FSS structures theoretically [29].

1.3.1 Previous Work on Method of Moment (MOM) Based FSS

In 2001, P.P.Sarkar investigated the property of an array of printed dipole experimentally. The dipole structure was theoretically analysed following the moment method and establishing MATLAB coding. The experimental verification satisfied the theory in good agreement [30]. In 2005, Blackburn presented a sub domain formulation of the periodic method of moment with wire elements to analyse FSS [31].

An aperture type FSS had been studied based on method of moment (MOM) by Don. In the study, the authors reported a method for electromagnetic analysis of FSS with an arbitrary shaped aperture element. The design strategy of dual band arc shaped slots had also been discussed [32].

Dardenne described a MOM technique to analyse complex elements that involves both metal and dielectric part. An algorithm has been established to compute singly and doubly periodic Green's functions and their gradients [33].

In 2010, Fallahi introduced a new technique known as sub domain MOM to analyse FSS. In this technique a large number of sub patches overlapped each of the separate patches in the unit cell. The shape of the sub patch is simple enough for obtaining an appropriate set of basis functions analytically from an eigen value problem. It has been showed that the method exhibit better convergence than the standard MOM [34]. In the same year, Mehta suggested dipole moment method that follows the matrix based approach of MOM to solve the unknown currents whereas avoids the direct usage of Green's function to analyse an FSS structure [35].

The Rao-Wilton-Glisson (RWG) sub domain basis function is applied for the representation of distribution of current to arbitrary FSS geometry in spectral domain method of moments [36]. Maehly approximation is applied for accurate representation of the response of the structure over broad bandwidth. MOM based Maehly approximation, proposed for the analysis of FSS had been considered more efficient than traditional MOM.

Yardim and team examined the shielding effect of square patch elements in a frequency band of 5 GHz by using Green's function and moment method. At $\theta = 0^{\circ}$ and 30° vertical polarisation, the FSS structure exhibits best shielding effect [37].

In 2021, Corcoles and Boix considered spectral domain method of moment for the formulation of a multilayered periodic structure having a number of metallized interfaces alternating patches and apertures. The results obtained are verified using CST microwave studio software. The analysis of non rectangular periodic lattices with tightly packed elements has been done using non-uniform fast fourier transform in the spectral MOM [38].

1.3.2 Previous Work on Compact FSS

A compact triple band bandstop spatial filter in the frequency bands 824 MHz, 1.75 GHz to 1.87 GHz and 1.92 GHz to 2.17 GHz had been proposed in 2008. The proposition involves a three layer FSS placed on a glass plane with air gap between them. Two square loops are designed as patch type unit cell and are meandered to reduce the size [39].

In 2014, Yan reported an anchor shaped loop unit cell structure for compact FSS. The structure resonates at 2.4 and 5 GHz. It manifests dual band behaviour of bandwidth 230 MHz and 300 MHz. The miniaturisation had been shown with 0.065 λ X 0.076 λ unit cells, where λ represents the free space wavelength [40].

A group of Iranian researchers, in 2017 reported a compact multiband FSS with wideband spurious rejection. Four small patches were added to a square loop to reduce the size of the FSS, whereas multiband operation was attained by adding lumped inductor elements between the parasitic patches and main loop. The proposed structure acts as a band stop filter at 7.2GHz and are able to eliminate spurious frequency upto 30GHz [41].

The size reduction of an FSS was not circumscribing to band stop filters. Miniaturization had been attained by the elements loaded with capacitive structures. The equivalent capacitance of pass band was increased by implementing convoluted slot grids, which in lieu resonates at lower frequency [42]. In 2019, P.P.Sarkar reported the compactness in curved FSS keeping in mind the necessity of the present

era [43]. Although it's challenging to reduce size in curved FSS but under his guidance the team successfully designed and fabricated semi-cylindrical bandstop curved FSS with square slit and achieved compactness of 50.31%. In 2020, R.Atla and fellows proposed a compact polarization independent band pass FSS for a frequency of 2.4GHz to 5GHz [44]. They cut two slots, a circular outer loop and a diamond shaped inner loop on FR4 substrate to achieve bandpass response. The total slot length created in the proposed structure was inversely proportional to frequency, thus resonance frequency decreases with increase in total slot length resulting into the reduction of FSS size.

A polarisation insensitive compact FSS of unit cell dimension $0.13\lambda_0$X$0.13\lambda_0$X $0.020\lambda_0$presented by Katoch exhibits triple band notches at WiMAX and satellite communication bands. A metallic square loop and four identical rotational symmetric square split ring resonator (SSRR1) have been incorporated on the upper part of the substrate, and another four identical rotational symmetric square split ring resonators (SSRR2) have been introduced in the lower part of the substrate to attain insensitiveness to polarisation [45]. A single layer bandstop FSS comprises of a symmetrically modified square loop was introduced by Abidin in 2022. The polarisation independence was established by arranging the square loop in C4 rotation symmetry. The size of the unit cell being $0.09\lambda_0$X $0.09\lambda_0$X $0.007\lambda_0$attains the lowest operating frequency of 5.54 GHz [46]. (λ_0– wavelength corresponding to lowest operating frequency)

In 2023, Karimi introduced pixelated patterns on a single layer unit cell to reduce the size of the unit cell. 50 X 50 pixels with resolution of 0.2 mm X 0.2 mm have been incorporated on the surface to miniaturise the unit cell. The structure resonates at 1.8 GHz and attains compactness by creating a long path to pass the surface current [47]. A compact FSS was developed by Natarajan by modifying the arms of the conventional crossed dipole element. The dimension of the unit cell is 6mm X 6mm embossed on substrate of thickness 1.6 mm which resonate at 5 GHz showcasing bandstop behaviour with angular stability upto 60° [48].

1.3.3 Previous Work on Curved FSS

During 90's the study of curved FSS up rear with the curiosity of Parker, Philips and Langley on the subject.Characteristic comparison of curved FSS has been done by them with finite and infinite planar arrays [49]. Ray tracing approach was preliminary adopted to study the transmission performance of curved FSS [50]. In 2009 Su and Xu reported RWG basis function based MOM analysis for finite dipole array FSS taking account of both planar and cylindrically curved structure [51]. In 2010, the hybrid technique to volume surface integral equation was proposed by Prof. Chen and team to analyse the transmission and reflection characteristics of finite and curved FSS structures [52]. These techniques build the backbone of further studies of mathematically complex finite curved structures.

In 2014, Jeong studied the scattering characteristics of infinite and finite cylindrical dipole array considering MOM with entire domain basis function and cylindrical floquet harmonics [53]. (Mattiello et.al, 2015)[54] presented a literature on research outcomes in last 50 years on finite and curved FSS.The analysis and characterization of both the FSSs areserved as the foundation for the investigation. Park and team designed a curved frequency selective radome. The structure had been analyzed by using characteristics basis function method (CBFM). The work was aimed to establish CBFM an appropriate method to analyze electrically large problem [55]. In 2017, Lei designed a cylindrical conformal FSS utilising the mechanical bending cover method. The structure proves itself a better candidate for the RCS reduction performance of single and double stations in comparison to the conventional one. Its operating range is from 5-20 GHz [56]. Son, Hyun and Lee designed a curved radar absorbing structure with FSS. The performance of the RAS has been predicted using equivalent circuit model and ray tracking method. The validation has been done by the free space measurement with the structure [57]. An elemental structure for curved FSS unit cell had been developed following parametric scanning method. The development started considering the traditional circular structure; the inside and outside of the circular structure was then cut by many semicircles. The designed unit cell effectively enhances the gain and directivity of a flexible cylindrical antenna [58].

In 2019, P.P.Sarkar focused on miniaturization of curved FSS. The lowering of resonant frequency was attained by incorporating slit in patch elements of the curved FSS. Circular, hexagonal and square patches were considered for the purpose. A maximum of 50.31% reduction had been reported for the slit loaded square patch element [59]. In the consecutive year, Wei reported a miniaturised FSS for conformal application utilising the property that the size of the element can be altered by using different thickness of the substrate. The structure manifests stable resonant frequency on curved surfaces with different curvatures. The reported size reduction of element was 5.2% of free space wavelength [60].

In 2022, Kima studied the bandpass and bandstop characteristics of hemispherical FSS with circular hole and circular patch element respectively in the frequency range of 5-25 GHz [61]. Govindarajan and Purusothaman reported a cylindrical curved FSS for radar application. They proposed a unit cell comprising of a rhombus slot consist of a head slot and a meander line. The structure exhibits angular stabilization, linear polarisation and wide passband frequency in 7.98-12.10 GHz range [62].

1.3.4 Previous Work on Absorber

Salisbury screen first put forward the absorbing idea in FSS. Henceforth, numerous researches have been done with the absorbing material. In 2010, high impedence surface is used to design absorber [63]. The paper documented wideband absorption in a reduced thickness. They used resistive inks instead of conventional printing technique.

Absorbing characteristics were observed by combining resistive and conductive type FSS and documented stable frequency response and absorbing characteristics for 5GHz [64, 65].

During 2014, magnetic materials were used for absorbing purpose. Zhou Xu designed an FSS comprising of square patch surrounded by square loop as unit cell and loaded the back of the FSS with magnetic microwave absorbing film [66]. The proposed FSS shows good bandpass performance at lower frequencies and absorbs some out band signals; the absorber also suppressed the grating lobes. Yijung Feng proposed absorber depending on ferromagnetic nano films and obtained absorption

bandwidth of 11GHz in 2GHz to 18GHz frequency range [67]. In 2015, Jiang developed a broadband microwave absorber by sandwiching a resistive FSS between two magnetic sheets and attained a bandwidth of 11.4GHz in the frequency range 6.6GHz to 18GHz [68].

A multi resonant gridded square FSS reported by Xie and fellow researchers has wideband absorbing capability having multi resonant mechanism [69]. In 2017, Panwar developed a sugarcane bagasse based agricultural waste composite. The composite integrated with Minkowski loop FSS enhances the absorption bandwidth upto 3.6 GHz [70]. Next year, a nano composite sheet had been reported by Chakradhary. The conducting carbon black nano powder and a dielectric sheet are embedded into epoxy matrix resultant in a hybrid absorber that is capable to enhance the -10 dB absorption bandwidth upto 3.5 GHz [71].

Resistive loaded FSS are extensively studied for absorbing purpose in recent past. A remarkable absorbing bandwidth of 2.98GHz to 16.62 GHz was reported by Y.L.Yulu and team using double layered resistor loaded FSS in 2019 [72]. In the next year, a letter was published by B.Z.Wang, where they reported a single layer absorber with two square loop arrays with embedded lumped resistor at the four edges of the loop [73]; printed the structure on both side of the substrate backed by a metal ground and documented a fractional bandwidth of 132.3%.The squad explored the same square loop structure loaded with two resistors and reported a fractional bandwidth of 171.2% [74].

120% absorption bandwidth had been reported by Zheng. They used magnetic material based substrate and superstrate and the elements of the FSS are embossed using resistive ink [75]. In 2022, Jha reported an absorber utilizing dielectric substrate and magnetic superstrate suitable for planar and conformal applications [76].

Manokaran in 2024 designed an absorber based on dual layer FSS. Split ring resonator, square loop are etched on top and bottom part of Jean's material substrate which is then backed by metal ground plane. The structure attains 90% absorptivity

suitable for shielding technology in military application at X-band frequency range [77].

1.4 Objective

Frequency Selective Surface demands a comprehensive study till date due to its large scale application emerging from home based microwave appliances to satellite communication. The main objective of the work is to explore the basic properties of the FSSs concerning the present requirement for consolidation with various devices.

- A cross dipole structure has been theoretically established employing MOM based algorithm. The characteristic of the structure has been determined by formulating MATLAB code followed by simulated results and practical measurements.
- Emphasize will be given on double layer curved structure to design a curved FSS to improve the roll-off and bandpass property with minimum insertion loss.
- To achieve compactness, foreground will be loaded with slits and slots on the patch; consequently it may result in multiband due to multi electrical path. Broadband is attained due to staggering effect.
- To achieve absorbent property with stable bandwidth without using any absorbing material like magnetic superstrate or resistive ink etc. will be the endeavour of the work.

1.5 Organisation of Thesis

In Chapter 1 the fundamentals of FSS are put forward to understand the characteristic behaviour of an FSS. Its dependence on structure of the unit cell elements. The methods applied to theoretically analyse an FSS and the softwares used for the purpose. The areas that substantiate the importance of FSS as spatial filter. A thorough literature survey has been done to track down the objective of our work.

In Chapter 2 a theoretical analysis of a cross dipole structure is put forward following the technique known as method of moment (MOM). The algorithm developed is supported by MATLAB coding to establish the transmission characteristics of the

structure. The structure is simulated by ANSOFT software to obtain the transmission characteristics. The experiment performed by Microwave Test Bench validated that the algorithm developed by us is in closure proximity to its result then the same obtained by the simulation of the structure.

In Chapter 3 a dual layer aperture type planar and curved cylindrical FSS is investigated focussing on the characteristics like roll-off and insertion loss. The planar structure with sharp roll-off, wide band and low insertion loss is easy to design whereas, it is challenging to attain the same for curved structure. The main dedication of the chapter is to improve the performance of the cylindrical curved FSS.

In Chapter 4 the focus has been given in the designing of multiband compact FSS considering simple elemental structure. The reduction in size has been achieved by using conventional method, that is, by incorporating slits and slots on the patch element. The introduction of the slots and slits increases the path of the current that has a direct relation with the lowering of resonant frequency. Circular and rectangular patch elements have been modified to attain compactness. A good compactness have been achieved for all the studied structure by simulation or measurement.

In Chapter 5 study of FSS has been focussed on development of FSS absorber without using any absorbing material. The bandstop property of the conventional FSS has been utilised for the purpose. Technological development forces living beings to live amidst microwave frequency, so, on regular basis they have to face undesired frequencies that are harmful for their health. Microwave absorbers can reduce the ill effects to health caused by microwave frequency. FSS designed and studied in this chapter put forward a cost effective and light weight microwave absorber. The same FSS absorber can also be incorporated with radar systems or airborne systems for stealth purpose.

In Chapter 6 the summary and conclusion of the entire research work has been set forth and a discussion of future scope has been set down.

1.6 References

C. K. Lee and R. J. Langley, “Performance of a dual-band reflector antenna incorporating a frequency selective subreflector”, *International Journal of Electronics Theoretical and Experimental*, vol. 61, no. 5, pp. 607-616,1986.

T. K. Wu and S. W. Lee, "Evaluation of multi-band reflector antennas with frequency selective subreflectors," Proceedings of IEEE Antennas and Propagation Society International Symposium, Ann Arbor, MI, USA, pp. 262-265 vol.1, 1993.doi: 10.1109/APS.1993.385354.

M. G. Floreani, R. E. Zich, G. Aulisio, P. Besso and A. Somma, "Design and experimental validations of a new FSS conformal subreflector structure for Cassegrain systems," *IEEE Antennas and Propagation Society International Symposium. 2001 Digest*. Held in conjunction with: USNC/URSI National Radio Science Meeting (Cat. No.01CH37229), Boston, MA, USA, pp. 304-307 vol.2, 2001.doi: 10.1109/APS.2001.959724.

N. J. G. Fonseca, "Dual-band (Tx/Rx) multiple-beam reflector antenna using a frequency selective sub-reflector for Ka-band applications," *2015 9th European Conference on Antennas and Propagation (EuCAP)*, Lisbon, Portugal, pp. 1-5,2015.

S. Khan and T. F. Eibert, "A miniaturized frequency selective surface sub-reflector for X and Ku-bands," *2018 11th German Microwave Conference (GeMiC)*, Freiburg, Germany, pp. 184-186, 2018.doi: 10.23919/GEMIC.2018.8335060

S. Guo, Y. Wang and M. Zhu, "Design of FSS Sub-reflector based Dual Band Cassegrain Antenna," *2024 IEEE International Conference on Computational Electromagnetics (ICCEM)*, Nanjing, China, pp. 1-3, 2024.doi: 10.1109/ICCEM60619.2024.10558946

Dickie, R. Cahill, H. S. Gamble, V. F. Fusco, N. Grant and S. P. Rea, "Dual Polarised Sub-mm Wave Frequency Selective Beamsplitter," *2006 First European Conference on Antennas and Propagation, Nice*, France, pp. 1-7,2006.doi: 10.1109/EUCAP.2006.4584535

M. Euler and V. Fusco, "Sub-millimetre wave linear to circular polariser converter," *2008 Loughborough Antennas and Propagation Conference, Loughborough*, UK, pp. 77-80, 2008.doi: 10.1109/LAPC.2008.4516870

L. Morrow and P. Thomas, “Compact frequency selective surface for polarisation transform”, Electronics Letters, 2014.

Q Zeng, W Ren, H Zhao, Z Xue, “Dual-band transmission-typecircular polariser based on frequency selective surfaces”, *IET Microwaves, Antennas,* 2019.

Xia Bu.G. *et al.*, “Tetrahertz Frequency Selective Surface for Space Borne Passive Remote Sensing Application”, *Electronics Letters,*vol.49, no.22, pp. 1398-1399, 2013.

MaY., *et al.*, “A Wideband Frequency Selective Surface Based on Vias for Communication Systems”, *IEEE Antennas and Wireless Propagation Letters,* vol.17, no.12**,**pp. 2517- 2520, 2018.

Shiv Narayan,Kurapati Prasad,Raveendranath Nair,Rakesh Mohan Jha, “A Novel EM Analysis of Double-Layered Thick FSS Based on mm -GSM Technique for Radome Applications”,*Progress In Electromagnetics Research Letters*, vol. 28, pp.53-62, 2012.doi:10.2528/PIERL11101710

C. Sudhendra, A. R. Madhu, A. Mahesh, A. C. R. Pillai, “FSS RADOMES FOR ANTENNA RCS REDUCTION”, *International Journal of Advances in Engineering & Technology*, vol.6, no.4, pp.1464-1473, 2013.

P. Mahima, B. Sangeetha, S. Narayan and R. U. Nair, "EM design of hybrid-element FSS structure for radome application," *2016 IEEE Annual India Conference (INDICON)*, Bangalore, India, pp. 1-4, 2016.doi: 10.1109/INDICON.2016.7839051

H. Shin, D. Yoon, D. -Y. Na and Y. B. Park, "Analysis of Transmission Loss and Boresight Error of a Curved FSS Radome-Enclosed Antenna", *IEEE Access*, vol. 9, pp. 95843-95852, 2021.doi: 10.1109/ACCESS.2021.3094526.

A. Chatterjee and S. K. Parui, "Performance Enhancement of a Dual-Band Monopole Antenna by Using a Frequency-Selective Surface-Based Corner Reflector", *IEEE Transactions on Antennas and Propagation*, vol. 64, no. 6, pp. 2165-2171, June 2016.doi: 10.1109/TAP.2016.2552543

F. N. M. Zaid, S. N. Azemi, C. B. M. Rshidi, " Application of FSS for microstrip antenna for gain enhancement" , *IOP Conference Series: Materials Science and Engineering,* vol. 767, no.1, 2020.

A. Swetha, K. R. Naidu, " Gain enhancement of an UWB antenna based on a FSS reflector for broadband applications", *Progress In Electromagnetics Research C,* vol.99, pp.193-208, 2020.

S. Ara, P. K. Nunna, " Gain enhancement of a monopole antenna using frequency selective surface for sub-6 GHz band applications" , *International Journal of Advanced Technology and Engineering Exploration,* 10 (104), 2023.

R. Karimian, A. Kesavan, M. Nedil and T. A. Denidni, "Low-Mutual-Coupling 60-GHz MIMO Antenna System With Frequency Selective Surface Wall", *IEEE Antennas and Wireless Propagation Letters,* vol. 16, pp. 373-376, 2017.doi: 10.1109/LAWP.2016.2578179.

Bilal M. et al., Miniature and Flexible Frequency Selective Surface based EM-Shields for Conformal Applications, IEEE Transactions on Electromagnetic Compatibility, vol.62, no.5, pp.1703-1710, 2020.

Jain C., Sharma M., Smartphone Frequency Shielding with Penta Band Stop FSS for Security and Electromagnetic Health Applications, IEEE Transactions on Electromagnetic Compatibility,vol.61, no.3, pp.887-892, 2019.

D Wan, S Bie, J Zhou, H Xu, Y Xu, J Jiang, "A thin and broadband microwave absorber based on magnetic sheet and resistive FSS.", Progress in Electromagnetics Research, 56, 93-100, 2015.

S.N. Zabri, R. Cahill, A. Schuchinsky, "Compact FSS absorber design using resistively loaded quadruple hexagonal loops for bandwidth enhancement", Electronics Letters, vo.51, no.2, pp.162-164, 2015.

S. Scott *et al., "* A frequency selective surface with integrated limiter for receiver protection", *Proceedings of the 2012 IEEE International Symposium on Antennas and Propagation,* pp.1-2, 2012.

L. Scorrano *et al.,* " FSS- based approach for the power transmission enhancement through electrically small apertures", *Applied Physics,* vol.103, pp.927-931, 2011.

N. Hu *et al.,* " Design of Ultrawide Band Energy Selective Surface for High Power Microwave Protection", *IEEE Antennas and Wireless Propagation Letters,* vol.18, no. 4, pp. 669-673, 2019.

R. Mittra *et al.,* "Techniques for Analysing Frequency Selective Surface- A Review", *Proceedings IEEE,* vol.76, no.12, pp.1593-1615, 1988.

P.P.Sarkar, S.Sarkar, S.Das, S.K.Chowdhury, "Experimental Investigation on the frequency Selective Property of an array Printed Dipole", *Proc. National Conf. on Microwave, Antenna and Propagation,* Jaipur,pp 115-116, 2001.

John Blackburn and Luk R. Arnaut, "Numerical Convergence in Periodic Method of Moments Analysis of Frequency-Selective Surfaces Based on Wire Elements", *IEEE TRANSACTIONS ON ANTENNAS AND PROPAGATION,* Vol. 53, no. 10, OCTOBER 2005.

Nataliya Don, Maurizio Bozzi, Anatoly Kirilenko, andLuca Perregrini , "Analysis Of Inductive Frequency Selective Surfaces by the Method Of Moments With Entire Domain Basis Functions", *Microwave and Optical Technology Letters,* vol. 49, no.12, pp. 2929-2932, 2007.

Xavier Dardenne and Christophe Craeye, "Method of moments simulation of infinitely periodic structurs combining metal with connected dielectric objects", *IEEE Tranactions on Antennas nd Propagation,* vol.56, no.8, pp. 2372-2380, 2008.

A Fallahi, A Yahaghi, H Abiri, M Shahabadi, C Hafner, "Large Overlapping subdomain Method for the Analysis of Frequency Selective Surface", *IEEE Transactions on Microwave Theory and Techniques,* vol. 58, no.8, pp. 2175-2187, 2010.

N Mehta, "Numerical Analysis of Frequency Selective Surfaces", *A thesis in Electrical Engineering,* Master of Science, The Pennysylvania State University,2010.

Xin Ma, Guo Bin Wan, Wei Wan, "Efficient analysis of FSS using the MOM based Maehly approximation", *Proc. 2011 Cross Strait Quadregional Radio Science and Wireless Technology Conference 1,* pp. 21-24,2011.

F E Yardim, N Akcam, M Bayraktar, “Shielding Effect Analysis of Various Configurations of the Square Patch Elements”, *Gazi University Journal of Sciene,* vol.30 no.2, 2017.

Juan Corcoles, Rafael R Boix, “Spectral MOM NUFFT- based formulation for the efficient analysis of high-order bandpass FSSs with thightly packed non resonant elements in skewed grid”, *IEEE Transactions on Antennas and Propagation,* ol. 69, no.9, pp.6099-6104, 2021.

Kim D. *et al.*, “Compact Spatial Triple Band Stop Filter for Cellular/ PCS/ IMT-2000 Systems”, *ETRI Journal,* vol.30, no.5, pp.735-737, 2008.

M Yan, S Qu, J Wang, J Zhang, H Zhou, H Chen, L Zheng, “A miniaturized dual-band FSS with stable resonance frequencies of 2.4 GHz/ 5 GHz for WLAN applications”, *IEEE Antennas and Wireless Propagation Letters,* vol.13, pp.895-898, 2014.

Narsollahi H. *et al.*,“Compact, Dual, Polarised Multiband FSS with Wideband Spurious Rejection”, *Microwave and Optical Technology Letters,* vol. 59, no.4, pp. 888-893, 2017.

P. C. Zhao, Z. Zong, W. Wu, B. Li, D. Fang, “ Miniaturized- element bandpass FSS by loading capacitive structures”, *IEEE Transactions on Antennas and Propagation,* vol.67, no.5, pp.3539-3544, 2019.

Begam N. *et al.*, “Design of Compact Patch Type Curved Frequency Selective Surface”, *International Journal of RF and Microwave Computer-Aided Engineering,* vol.29, no.9, 2019.

Krishnan R. *et al.*, “A Compact Polarisation Independent Dual Band FSS for Smart Phone Safety Application”, *IEEE* 7th International Conference on Smart Structures and Systems (ICSSS), 2020.

K Katoch, N Jaglan, S Dev Gupta, M S Sharawi, “Design of a triple band notched polarization independent compact FSS at UWB frequency range”, *International Journal of RF and Microwave Computer-Aided Engineering,* vol.31, no.6, e22631,2021.

Z U Abidin, Q Cao, G Shah, “Design of a compact single layer frequency selective surface with high oblique stability”, *IEEE Transactions on Electromagnetic Compatibility,* vol. 64, no.6, pp.2060-2066, 2022.

A Karimi, M Nadi, “A Miniaturized Band- Stop FSS Based on pixelated unit cell”, *Progress in Electromagnetics Research Letters*, vol.109, pp.111-117, 2023.

R Natarajan, R Sivasamy, A Gunasekar, “A compact polarization independent stop band frequency selective surface for WLAN shielding”, *Microwave and Optical Technology Letters*, vol.66, no.3,e34097,2024.

Philips B. *et al.*, “Finite Curved Frequency Selective Surface”, *Electronics Letters,* vol.29, no.10, pp.882-883, 1993.

Philips B. *et al.*, “Ray Tracing Analysis of The Transmission Performance of Curved FSS”, *IEEE Proceedings-Microwaves, Antennas and Propagation,* vol.142, no.3, pp.193-200,1995.

Su J., Xu X., “MOM Analysis of The Planar and Curved FSS Based on Dipole Elements”, *International Conference on Microwave Technology and Computational Electromagnetics* (ICMTCE), 2009.

24. Ding D. *et al.*, “Fast Analusis of Finite and Curved FSS using the VSIE with MLFMA”, *International Journal of Numerical Modelling,* vol.24, no.5, pp.425-436, 2011.

Y R Jeong, I P Hong, H J Chun, Y B Park, Y J Kim, J Gwan, “Scattering analysis of curved FSS using Floquet harmonics and asymptotic waveform evaluation technique”, *Steel and composite structures*, vol.17, no.5, pp.561-572, 2014.

F Mattiello, G Leone, G Ruvio , “Analysis and characterisation of finite-size curved frequency selective surfaces”, *Technological University Dublin,*2015.

C S Park, Y R Jeong, I P Hong, H J Chun, Y B Park, Y Jae, “Analysis of Curved Frequency selective surface for radome using characteristic basis function method”, *10^{th} European Conference on Antennas and Propagation (EUCAP),* pp.1-4, 2016.

W Xin-lei, Y Yan-ling, Z De-hua, X Wei, C Yi-feng, C Yu, “Design and modelling of the cylindrical conformal FSS with mechanical bending cover method”, *Procedia Computer Science,* vol.107, pp.824-829,2017.

D S Son, J M Hyun, J R Lee, “Prediction and validation of electromagnetic performance of curved radar-absorbing structures based on equivalent circuit model and ray tracking method”, *Composites Science and Technology,* vol.167, pp. 547-554,2018.

Hua Jing, Ge He ,and Shengyao Wang, “Design of a Flexible Cylindrical Antenna with Rotatable Curved Frequency Selective Surface for

Omnidirectional HighGain Applications”, *International Journal of Antennas and Propagation,* Volume 2023, Article ID 6553980, 15 pages https://doi.org/10.1155/2023/6553980.

N Begam, S Saha, S Sarkar, D C Sarkar, P P Sarkar, “Design of compact patch type curved frequency selective surface*”, International Journal of RF and Microwave Computer-Aided Engineering*, vol.29, no.9, e21803, 2019.

P S Wei, C N Chiu, C C Chou, T L Wu, “Miniaturized dual-band FSS suitable for curved surface application”, *IEEE Antennas and Wireless Propagation Letters*, vol.19, no.12, pp. 2265-2269, 2020.

Jiyeon Kima, , Hyeon-Seo Choia, , Wook Ki Jungb, Kisu Leeb , and Chang-Hee Choa, “Curved Frequency-Selective Surface on Hemispherical Dome for Wave Bandpass Filters”, *Appl. Sci. Converg. Technol.,* vol.31, no.6, pp. 137-140, 2022.https://doi.org/10.5757/ASCT.2022.31.6.137

Geethanjali Govindarajan and Preetha Purusothaman, “Novel Polyimide-Based Conformal Bandpass FSS for X-band RADAR Communications” ,*JOURNAL OF HIGH-FREQUENCY COMMUNICATION TECHNOLOGIES*, vol. 2,no.1, pp.130-139,2024. https://doi.org/10.58399/BAAG2904.

Costa F. *et al.*, “Analysis and Design of Ultra Electromagnetic Absorbers Comprising Resistively Loaded High Impedance Surface”, *IEEE Transactions on Antennas and Propagation,*vol.58, no.5, pp.1551-1558, 2010.

Kiani G. *et al.*, “Oblique Incidence Performance of a Novel FSS Absorber”, *IEEE Transactions on Antennas and Propagation,*vol.55, no.10**,**pp.2931-2934, 2007.

Rafique U. *et al.*, “Frequency Selective Surface Absorber for WLAN Security”, *Proceedings of the 5th European Conference on Antennas and Propagation (EUCAP),*pp.872- 875, 2011.

Zhou H. *et al.*, “Experimental Demostration of an Absorptive/ Transmissive FSS with Magnetic Material”, *IEEE Antennas and Wireless Propagation Letters,*vol.13, 2014.

Zhang M. *et al.*, “Design and Measurement of Microwave Absorbers Comprising Resistive Frequency Selective Surface”, *Journal of Electromagnetic Analysis and Applications,*vol.6**,** pp.203-208, 2014.

Wan D. *et al.*, “A Thin and Broadband Microwave Absorber Based on Magnetic Sheet and Resistive FSS”, *Progress in Electromagnetics Research,* vol.56, pp.93-100, 2015.

D Xie, X Liu, H Guo, X Yang, C Liu, L Zhu, “A wideband absorber with a multiresonant gridded square FSS for antenna RCS reduction*”, IEEE Antennas and Wireless Propagation Letters*, vol.16, pp.629-632, 2016.

R Panwar, S Puthucheri, D Singh, V Agarwala, J R Lee, “Microwave absorption properties of FSS-impacted composites as a broadband microwave absorber”, *Advanced Composite Materials*, vol.26, no.2, pp. 99-113, 2017.

V Chakradhary, H B Baskey, R Roshan, A Pathik, M. J Akhtar, “Design of Frequency Selective Surface Based Hybrid Nanocomposite Absorber for Stealth Applications”, *IEEE Transactions on Microwave Theory and Techniques*, vol.66, no.11, pp.4737-4744, 2018.

Wei J. *et al.*, “Flexible Design and Realization of Wideband Microwave Absorber with Double Layered Resistor Loaded FSS”, *Journal of Physics D:Applied Physics,* vol.52, no.18, 2019.

Yao Z. *et al.*, “On the Design of Ultrawide band Circuit Analog Absorber Based on Quasi-Single Layer FSS”, *IEEE Antennas and Wireless Propagation Letters,*vol.19, no.4**,**pp.591-595, 2020.

Yao Z. *et al.*, “On The Design Of Wideband Absorber Based on Multilayer and Multi Resonant FSS Array”, *IEEE Antennas and Wireless Propagation Letters,*vol.20, no.3**,**pp.284-288, 2020.

L Zheng, X Yang, W Gong, M Qiao, X Li, “Ultralow thickness- bandwidth ratio magnetic absorber with printed FSS for S & C bands”, *IEEE Antennas and Wireless Propagation Letters*, vol.21, no.3, pp. 576-580,2021.

K R Jha, Z P Jibran, S K Sharma, “Absorption peak controlled low frequency wideband flexible FSS absorber”, *IEEE Transactions on Electromagnetic Compatibility*, vol. 64, no.4, pp.975-986,2022.

S Manokaran, J Shweatha, R Sivasamy, P Geethika, “An Ultrathin FSS Absorber for X Band Applications”, *9th International Conference on Science Technology Engineering and Mathematics (ICONSTEM),* pp.1-6, 2024.

CHAPTER 2

Method of Moment and Its Application for Theoretical Analysis of an FSS Structure

2.1 Introduction

The concept of filtering white light into distinct wavelength bands was put forward by David Rittenhouse in 1786, popularly known as principle of diffraction grating [1]. He performed the experiment by uniformly spacing the hair and descried that six equidistant different frequency bands of light were visible on both sides of the central maxima and it had dependence on the spacing between the hairs. Rittenhouse's experiment was the eye opener of a simple spatial filtering process, his mind altering idea later set forth the fundamentals of frequency selective surface (FSS). In FSS, the characteristic of the scattered field depends on the geometry of each elements and the spacing between them. When element size corresponds to an integer multiple of half wavelength,FSS exhibits either total reflection or transmission of the incoming electromagnetic field. Respective dependence on the total reflection or transmission of the incident field, FSS is classified as patch type or aperture type FSS.

The numerical methods associated with the investigation of an FSS theoretically are Finite difference time domain method (FDTD), Finite element method (FEM), Method of moment (MOM) [2-4]. It is intricate to formulate the electromagnetic scattering problem for normal incidence by moment method, howbeit it is substantially used for the purpose because of its perfect accuracy in spectral domain. Theoretical analysis of an FSS structure employing moment method and its worthiness have been appreciated throughout the literature [5-8]. MOM is the best numerical technique to solve electromagnetic scattering problem in comparison to FDTD and FEM, as it focuses on electromagnetic sources. It is capable to solve larger structures and complex geometries utilizing fewer meshes, hence MOM take less computational time than FDTD and FEM, and is the fastest solver of electromagnetic scattering problem. MOM has been effectively applied to analyze planar and conformal FSS [9,10].

The chapter is dedicated to study the characteristic behavior of a cross dipole FSS making use of MOM numerical technique. An algorithm has been developed to calculate the transmission coefficient and respective MATLAB coding is established. The theoretical formulation is eventually validated by simulation and measured results.

Numerous assumptions have been framed to construct the method of moment:-

(i) The FSS is considered as infinite, to disregard the diffraction from surface's edges, in practical scenario.

(ii) A monochromatic plane wave is considered as incident wave and

(iii) Infinitesimally thinconducting patches or the conducting screen has been considered.

2.2 Concept of The Method of Moment

The method of moment, a general process for solving the linear equations is explored here. The inhomogeneous equation considered here is:-

$$L(f) = g \qquad (2.1)$$

Where L is a linear operator, g is known and f is to be determined. Let f be expanded in a series of functions f1, f2, f3,.....in the domain of L, as

$$f = \sum_n \alpha_n f_n \qquad (2.2)$$

Where, α_n- constants

f_n- the expansion function or basis function

For precise solution, equation (2.2) is typically an infinite summation and f_n constitute a full set of basis functions. Equation (2.2) is generally a finite summation for an approximate solution, replacing equation (2.2) in equation (2.1) and applying the linearity of L, we have

$$\sum_n \alpha_n L(f_n) = g \qquad (2.3)$$

Presumably, an appropriate inner product <f,g> has been deduced for the problem. After defining a set of weighting functions or testing functions; w_1, w_2, w_3....in the range of L, and considering the inner product of (2.3) with each $w_m$yields the result

$$\sum_n \alpha_n < w_m, Lf_n > = < w_m, g > \qquad (2.4)$$

If m=l,2,3..... ; these collection of equations can be written in matrix form as

$$[l_{mn}][\alpha_n] = [g_m] \qquad (2.5)$$

where,

$$l_{mn} = \begin{bmatrix} < w_1, Lf_1 > & < w_1, Lf_2 > & < w_1, Lf_3 > & \dots\dots. \\ < w_2, Lf_1 > & < w_2, Lf_2 > & < w_2, Lf_3 > & \dots\dots.. \\ \dots\dots\dots & \dots\dots\dots & \dots\dots\dots & \dots\dots\dots \\ \dots\dots.. & \dots\dots\dots & \dots\dots\dots & \dots\dots.. \end{bmatrix} \qquad (2.6)$$

$$\alpha_n = \begin{bmatrix} \alpha_1 \\ \alpha_2 \\ \alpha_3 \\ . \\ . \\ . \end{bmatrix} \quad and \quad g_m = \begin{bmatrix} < w_1, g > \\ < w_2, g > \\ < w_3, g > \\ . \\ . \\ . \end{bmatrix} \qquad (2.7)$$

If the matrix $[l]$ is non singular its inverse $[l]^{-1}$ exists. The α_n are then given by

$$[\alpha_n] = [l_{mn}]^{-1}[g_m] \qquad (2.8)$$

and equation (2.2) gives the solution for f. To get an incisive expression of this result,

we may define the matrix of functions

$$[\widetilde{f_n}] = [f_1, f_2, f_3 \dots..] \qquad (2.9)$$

So, we can write,

$$f = [\widetilde{f_n}][\alpha_n] = [\widetilde{f_n}][l_{mn}]^{-1}[g_m] \qquad (2.10)$$

Depending upon the choice of f_n and w_n, the solution may be exact or approximate. The specific consideration w_n-f_n is known as Galerkin's method.

In any particular problem, the main assignment is the choice of fn and wn.The choice of fn and w_n are influenced by certain factors, that are:-

(i) The accuracy of the expected solution.

(ii) Simplified technique to evaluate the matrix elements.

(iii) An invertible size of the matrix.

(iv) Accomplishment of a well-conditioned matrix of [l_{mn}].

2.3 Framing of the Problem

Let us start from the well- known Maxwell's field equations

$$\nabla \text{X } \vec{H} = \vec{J} + \frac{\partial \vec{D}}{\partial t} \qquad (2.11)$$

$$\nabla \text{X } \vec{E} = -\frac{\partial \vec{B}}{\partial t} \qquad (2.12)$$

Where, $\vec{H}$ -the magnetic field vector (ampere per meter)

$\vec{E}$- the electric field vector (volt per meter)

$\vec{D}$ - the electric flux density vector (coulomb per square meter)

$\vec{B}$ - the magnetic flux density vector (weber per square meter)

We can write equation (2.11) as,

$\nabla X \vec{H} = \vec{J} + \varepsilon \frac{\partial \vec{E}}{\partial t}$ [As $\vec{D} = \varepsilon\vec{E}$, where ε is the electric permittivity (farad per meter)]

$= \vec{J} + \varepsilon j\omega\vec{E}$ [As $\vec{E}$ is of the form $E_0 e^{jwt}$]

$= \vec{J} + j\,\omega\varepsilon\vec{E}$ (2.13)

From equation (2.12), we can write,

$\nabla X \vec{E} = -\mu \frac{\partial \vec{H}}{\partial t}$ [As, $\vec{B} = \mu\vec{H}$, where μ is the magnetic

permeability (Henry per meter)]

$= -\mu j\omega\vec{H}$ [As $\vec{H}$ is of the form $H_0 e^{j\omega t}$]

$$= -j\omega\mu\vec{H} \qquad (2.14)$$

Now, consider $\vec{J}$as the surface current density induced on the frequency selective surface because of a given incident field and as a result the current density at the z plane is 0 [i.e. xy- plane]; $\vec{A}$is the magnetic vector potential,

$$\text{Let, } \vec{H} = \nabla X \vec{A} \qquad (2.15)$$

Substituting the expression of $\vec{H}$ from (2.15)in equation (2.14) we get,

$$\nabla X \vec{E} = -j\omega\mu\left(\nabla X \vec{A}\right)$$

$$or, \nabla X \left(\vec{E} + j\omega\mu\vec{A}\right) = 0 \qquad (2.16)$$

We know that, Curl of a vector is 0, which must be the grad of a scalar quantity (say ϕ).Hence it can be written as,

$$\vec{E} + j\omega\mu\vec{A} = -\nabla\phi$$

$$or, \vec{E} = -j\omega\mu\vec{A} - \nabla\phi \qquad (2.17)$$

Now putting the value of $\vec{H}$ from the equation (2.15) into equation (2.13) we get;

$$\nabla X \nabla X\vec{A} = \vec{J} + j\omega\varepsilon\vec{E} \qquad (2.18)$$

substituting the equation (5.17) in equation (5.18),

$$\nabla X \nabla X\vec{A} = \vec{J} + j\omega\varepsilon(-j\omega\mu\vec{A} - \nabla\phi)$$

$$\text{or, } \nabla(\nabla.\overrightarrow{A}) - \nabla^2\vec{A} = \omega^2\mu\varepsilon\vec{A} - j\omega\varepsilon\nabla\phi + \vec{J}$$

$$or, \nabla\left(\nabla.\vec{A} + j\omega\varepsilon\,\phi\right) = \nabla^2\vec{A} + \vec{J} + \omega^2\mu\varepsilon\vec{A}$$

$$\text{or, } \nabla\left(\nabla.\vec{A} + j\omega\varepsilon\,\phi\right) = \nabla^2\vec{A} + \vec{J} + k^2\vec{A} \qquad (2.19)$$

[Where, k - the wave number;$k^2 = \omega^2\mu\varepsilon$]

From Lorentz Condition,

we can choose,

$$\nabla.\vec{A} + j\omega\varepsilon\,\phi = 0$$

$$or, \phi = -\frac{1}{j\omega\varepsilon}\vec{A} \qquad (2.20)$$

substituting the equation (2.20) into equation (2.17),

$$\vec{E} = -j\omega\mu\vec{A} - \nabla[-\frac{1}{j\omega\varepsilon}(\nabla.\overrightarrow{A})\ ]$$

$$\text{or,}\quad \vec{E} = -j\omega\mu\vec{A} + \nabla[\frac{1}{j\omega\varepsilon}(\nabla.\overrightarrow{A})\ ]$$

$$\text{or,}\qquad \vec{E} = -j\omega\mu\vec{A} + \frac{1}{j\omega\varepsilon}\nabla(\nabla.\overrightarrow{A}) \qquad (2.21)$$

The magnetic vector potential at a distance r due to unit current at a distance r', is given by free space Green's function,as

$$G(r,r') = \frac{e^{-jk_0|r-r'|}}{4\pi|r-r'|} \qquad (2.22)$$

So, due to current J at a distance r', the magnetic vector potential at a distance r, is given as,

$$A(r) = G * J = \int G(r,r')J(r')dr'$$

If we consider r'=0 i.e. current J is assumed to be at the origin, then

$$G(r) = \frac{e^{-jk_0r}}{4\pi r} \qquad (2.23)$$

[$k = k_0$ in free space, k_0- the free space wave number]

In the plane z=0; $r = \sqrt{x^2 + y^2}$

So, we can write,

$$\vec{G}(x,y) = \frac{e^{-jk_0 r}}{4\pi r}\vec{I} = \frac{e^{-jk_0\sqrt{x^2+y^2}}}{4\pi\sqrt{x^2+y^2}}\vec{I} \qquad (2.23a)$$

$$\vec{A}(x,y) = \vec{G}(x,y) * \vec{J}(x,y) \qquad (2.24)$$

[* sign means the convolution operation]

From equation (2.21), we can write scattered electric field in free space,

$$E^s(x,y) = \frac{1}{j\omega\varepsilon_0}\{\nabla(\nabla.\vec{A}) - j\omega\mu_0(j\omega\varepsilon_0)\vec{A}\}$$

$$= \frac{1}{j\omega\varepsilon_0}\{\nabla(\nabla.\vec{A}) + \omega^2\mu_0\varepsilon_0\vec{A}\}$$

$$= \frac{1}{j\omega\varepsilon_0}\{\nabla(\nabla.\overrightarrow{A}) + k_0^2\vec{A}\} \qquad (2.25)$$

Considering a planar thin surface, only surface current Jx and Jy exist. Thus, only Ax and Ay are non-zero and Az=0.

$$So, \nabla.\vec{A} = \left(\frac{\partial}{\partial x}\vec{I} + \frac{\partial}{\partial y}\vec{J} + \frac{\partial}{\partial z}\vec{K}\right).\left(A_x\vec{I} + A_y\vec{J} + 0.\vec{K}\right)$$

$$= \frac{\partial}{\partial x}A_x + \frac{\partial}{\partial y}A_y$$

$$So, \nabla(\nabla.\vec{A}) = \nabla\left(\frac{\partial}{\partial x}A_x + \frac{\partial}{\partial y}A_y\right)$$

$$= \left(\frac{\partial}{\partial x}\vec{I} + \frac{\partial}{\partial y}\vec{J} + \frac{\partial}{\partial z}\vec{K}\right)\left(\frac{\partial}{\partial x}A_x + \frac{\partial}{\partial y}A_y\right)$$

$$= \frac{\partial^2}{\partial x^2}A_x\vec{I} + \frac{\partial^2}{\partial x\partial y}A_y\vec{I} + \frac{\partial^2}{\partial y\partial x}A_x\vec{J} + \frac{\partial^2}{\partial y^2}A_y\vec{J}$$

[Since there is no variation in z direction, $\vec{K}$ components are zero]

$$= \left(\frac{\partial^2}{\partial x^2}A_x + \frac{\partial^2}{\partial x\partial y}A_y\right)\vec{I} + \left(\frac{\partial^2}{\partial y\partial x}A_x + \frac{\partial^2}{\partial y^2}A_y\right)\vec{J}$$

$$So, \left\{\nabla(\nabla.\overrightarrow{A}) + k_0^2\vec{A}\right\} =$$

$$\left(\frac{\partial^2}{\partial x^2}A_x + \frac{\partial^2}{\partial x\partial y}A_y\right)\vec{I} + \left(\frac{\partial^2}{\partial y\partial x}A_x + \frac{\partial^2}{\partial y^2}A_y\right)\vec{J} + k_0^2 A_x\vec{I} + k_0^2 A_y\vec{J}$$

$$= \left(\frac{\partial^2}{\partial x^2} + k_0^2\right)A_x\vec{I} + \left(\frac{\partial^2}{\partial y^2} + k_0^2\right)A_y\vec{J} + \frac{\partial^2}{\partial x\partial y}A_y\vec{I}$$

$$+ \frac{\partial^2}{\partial y\partial x}A_x\vec{J} \qquad (2.26)$$

Now replacing equation (2.26) into equation (2.25) we get,

$$\overrightarrow{E^s}(x,y) = \frac{1}{j\omega\varepsilon_0}\left\{\left(\frac{\partial^2}{\partial x^2} + k_0^2\right)A_x\vec{I} + \left(\frac{\partial^2}{\partial y^2} + k_0^2\right)A_y\vec{J} + \frac{\partial^2}{\partial x\partial y}A_y\vec{I} + \frac{\partial^2}{\partial y\partial x}A_x\vec{J}\right\}$$

(2.27)

It can be written in matrix form as,

$$\begin{bmatrix}\overrightarrow{E_x^s}(x,y)\\ \overrightarrow{E_y^s}(x,y)\end{bmatrix} = \frac{1}{j\omega\varepsilon_0}\begin{bmatrix}\frac{\partial^2}{\partial x^2} + k_0^2 & \frac{\partial^2}{\partial x\partial y}\\ \frac{\partial^2}{\partial y\partial x} & \frac{\partial^2}{\partial y^2} + k_0^2\end{bmatrix}\begin{bmatrix}A_x\\ A_y\end{bmatrix} \qquad (2.28)$$

Two dimensional Fourier transform of a function f(x,y) is defined as,

$$\tilde{f}(\alpha,\beta) = \int_{-\infty}^{+\infty}\int_{-\infty}^{+\infty} f(x,y)e^{-j\alpha x}e^{-j\beta y}dxdy \qquad (2.29)$$

Similarly two-dimensional Fourier inverse transform of *f(α,β)* is defined as,

$$f(x,y) = \frac{1}{(2\pi)^2}\int_{-\infty}^{+\infty}\int_{-\infty}^{+\infty}\tilde{f}(\alpha,\beta)e^{-j\alpha x}e^{-j\beta y}d\alpha d\beta \qquad (2.30)$$

From equation 2.28 we get,

$$\overrightarrow{E_x^s}(x,y) = \frac{1}{j\omega\varepsilon_0}\left\{\left(\frac{\partial^2}{\partial x^2} + k_0^2\right)\overrightarrow{A_x}(x,y) + \frac{\partial^2}{\partial x\partial y}\overrightarrow{A_y}(x,y)\right\} \qquad (2.31)$$

Performing fourier transform of both sides of equation (5.31),

$$\widetilde{\overrightarrow{E_x^s}}(\alpha,\beta) = \frac{1}{j\omega\varepsilon_0}\left[\{(j\alpha)^2 + k_0^2\}\widetilde{\overrightarrow{A_x}}(\alpha,\beta) + (j\alpha)(j\beta)\widetilde{\overrightarrow{A_y}}(\alpha,\beta)\right]$$

$$= \frac{1}{j\omega\varepsilon_0}\left[(k_0^2 - \alpha^2)\widetilde{\overrightarrow{A_x}}(\alpha,\beta) - \alpha\beta\widetilde{\overrightarrow{A_y}}(\alpha,\beta)\right] \qquad (2.32)$$

Similarly,

$$\widetilde{\overrightarrow{E_y^s}}(\alpha,\beta) = \frac{1}{j\omega\varepsilon_0}\left[(k_0^2 - \beta^2)\widetilde{\overrightarrow{A_y}}(\alpha,\beta) - \alpha\beta\widetilde{\overrightarrow{A_x}}(\alpha,\beta)\right] \qquad (2.33)$$

Where, $\widetilde{\overrightarrow{E_x^s}}(\alpha,\beta), \widetilde{\overrightarrow{E_y^s}}(\alpha,\beta), \widetilde{\overrightarrow{A_x}}(\alpha,\beta), \widetilde{\overrightarrow{A_y}}(\alpha,\beta)$ are the Fourier transforms of the functions $\overrightarrow{E_x^s}(x,y), \overrightarrow{E_y^s}(x,y), \overrightarrow{A_x}(x,y), \overrightarrow{A_y}(x,y)$ respectively.

In matrix form it can be written as,

$$\begin{bmatrix}\widetilde{\overrightarrow{E_x^s}}(\alpha,\beta)\\ \widetilde{\overrightarrow{E_y^s}}(\alpha,\beta)\end{bmatrix} = \frac{1}{j\omega\varepsilon_0}\begin{bmatrix}k_0^2 - \alpha^2 & -\alpha\beta\\ -\alpha\beta & k_0^2 - \beta^2\end{bmatrix}\begin{bmatrix}\widetilde{\overrightarrow{A_x}}(\alpha,\beta)\\ \widetilde{\overrightarrow{A_y}}(\alpha,\beta)\end{bmatrix} \qquad (2.34)$$

As, $\vec{A}(x,y) = \vec{G}(x,y) * \vec{J}(x,y)$ [From eqn.(2.24)]

Performing Fourier transform of both sides we get,

$$\tilde{\vec{A}}(\alpha,\beta) = \tilde{\vec{G}}(\alpha,\beta)\tilde{\vec{J}}(\alpha,\beta) \qquad (2.35)$$

So, $$\widetilde{\overrightarrow{A_x}}(\alpha,\beta) = \tilde{\vec{G}}(\alpha,\beta)\widetilde{\overrightarrow{J_x}}(\alpha,\beta) \qquad (2.36)$$

And $$\widetilde{\overrightarrow{A_y}}(\alpha,\beta) = \tilde{\vec{G}}(\alpha,\beta)\widetilde{\overrightarrow{J_y}}(\alpha,\beta) \qquad (2.37)$$

Substituting equations (2.36) and (2.37) into equation (2.34) we get,

$$\begin{bmatrix}\widetilde{\overrightarrow{E_x^s}}(\alpha,\beta)\\ \widetilde{\overrightarrow{E_y^s}}(\alpha,\beta)\end{bmatrix} = \frac{1}{j\omega\varepsilon_0}\begin{bmatrix}k_0^2 - \alpha^2 & -\alpha\beta\\ -\alpha\beta & k_0^2 - \beta^2\end{bmatrix}\tilde{\vec{G}}(\alpha,\beta)\begin{bmatrix}\widetilde{\overrightarrow{J_x}}(\alpha,\beta)\\ \widetilde{\overrightarrow{J_y}}(\alpha,\beta)\end{bmatrix} \qquad (2.38)$$

From equation (2.23a),

$$\vec{G}(x,y) = \frac{e^{-jk_0\sqrt{x^2+y^2}}}{4\pi\sqrt{x^2+y^2}}\vec{I}$$

So, $\tilde{\tilde{G}}(\alpha,\beta) = \int_{-\infty}^{+\infty}\int_{-\infty}^{+\infty} \frac{e^{-jk_0\sqrt{x^2+y^2}}}{4\pi\sqrt{x^2+y^2}} \vec{I} e^{-j\alpha x} e^{-j\beta y} dx\, dy$

$$\tilde{\tilde{G}}(\alpha,\beta) = \frac{-j}{2\sqrt{k_0^2-\alpha^2-\beta^2}}\vec{I} \qquad (2.39)$$

[for, $k_0^2 > \alpha^2+\beta^2$]

$$\tilde{\tilde{G}}(\alpha,\beta) = \frac{-j}{2\sqrt{\alpha^2+\beta^2-k_0^2}}\vec{I} \qquad (2.40)$$

[for, $k_0^2 < \alpha^2+\beta^2$]

Performing inverse fourier transforms on both sides of equation (2.38) we have,

$$\begin{bmatrix} \widetilde{\widetilde{E_x^s}}(\alpha,\beta) \\ \widetilde{\widetilde{E_y^s}}(\alpha,\beta) \end{bmatrix}$$
$$= \frac{1}{(2\pi)^2}\int_{-\infty}^{+\infty}\int_{-\infty}^{+\infty} \frac{1}{j\omega\varepsilon_0}\begin{bmatrix} k_0^2-\alpha^2 & -\alpha\beta \\ -\alpha\beta & k_0^2-\beta^2 \end{bmatrix} \tilde{\tilde{G}}(\alpha,\beta) \begin{bmatrix} \widetilde{\widetilde{J_x}}(\alpha,\beta) \\ \widetilde{\widetilde{J_y}}(\alpha,\beta) \end{bmatrix} e^{-j\alpha x} e^{-j\beta y} d\alpha\, d\beta \qquad (2.41)$$

As the tangential electric field vanishes on the conducting patch.

So, $E^s + E^{inc} = 0$ [on the conducting patch]

ie, $E^s = -E^{inc}$

Thus, equation (2.41) can be written as,

$$-\begin{bmatrix} \widetilde{\widetilde{E_x^{inc}}}(\alpha,\beta) \\ \widetilde{\widetilde{E_y^{inc}}}(\alpha,\beta) \end{bmatrix} =$$
$$\frac{1}{(2\pi)^2}\int_{-\infty}^{+\infty}\int_{-\infty}^{+\infty} \frac{1}{j\omega\varepsilon_0}\begin{bmatrix} k_0^2-\alpha^2 & -\alpha\beta \\ -\alpha\beta & k_0^2-\beta^2 \end{bmatrix} \tilde{\tilde{G}}(\alpha,\beta) \begin{bmatrix} \widetilde{\widetilde{J_x}}(\alpha,\beta) \\ \widetilde{\widetilde{J_y}}(\alpha,\beta) \end{bmatrix} e^{-j\alpha x} e^{-j\beta y} d\alpha\, d\beta \qquad (2.42)$$

It is to be noted that the above formulation has been done for a single patch only.The periodicity in x-direction is considered only to comprehend the spectral domain

method to a regular periodic array of patches. To satisfy Floquet's theorem for periodic structure, the current must be of the form:

$$J(x+a) = J(x)e^{jk_x^{inc}a} \qquad (2.43)$$

Where, k_x^{inc}-the incident wave number ,

a - periodicity in the x-direction

A new function is defined as,

$$J'(x) = J(x)e^{-jk_x^{inc}x} \qquad (2.44)$$

Substituting x = x+a in equation (2.44)

$$J'(x+a) = J(x+a)e^{-jk_x^{inc}(x+a)}$$

$$= J(x)e^{jk_x^{inc}a}e^{-jk_x^{inc}(x+a)}$$

[Putting the expression of J(x+a) from equation 2.43]

$$= J(x)e^{-jk_x^{inc}x}$$

So, $J'(x+a) = J'(x)$ (2.45) [By equation (2.44)]

Hence, $J'(x)$ is a periodic function with period a.

Thus,$J'(x)$can be represented by the sum of its Fourier components.

$$J'(x) = \frac{1}{a}\sum_{m=-\infty}^{+\infty} \widetilde{J_m} e^{j\left(\frac{2m\pi}{a}\right)x} \qquad (2.46)$$

Hence, J(x) can be written as,

$$J(x) = J'(x)e^{jk_x^{inc}x}$$

[By equation (2.44)]

$$= \frac{1}{a}\sum_{m=-\infty}^{+\infty} \tilde{J}_m e^{j\left(\frac{2m\pi}{a}\right)x} e^{jk_x^{inc}x}$$

[By equation (2.46)]

$$= \frac{1}{a} \sum_{m=-\infty}^{+\infty} \tilde{J}_m e^{j\left(\frac{2m\pi}{a} + k_x^{inc}\right)x} \qquad (2.47)$$

Similarly, considering the periodicity in the y-direction, we can write,

$$J(y) = \frac{1}{b} \sum_{n=-\infty}^{+\infty} \tilde{J}_n e^{j\left(\frac{2n\pi}{b} + k_y^{inc}\right)y} \qquad (2.48)$$

Where,k_y^{inc}- the incident wave number,

b - periodicity in the y-direction.

For the periodic structure, $\overrightarrow{J_x}(x,y)$ and $\overrightarrow{J_y}(x,y)$ have the discrete spectra in the transformed domain, which means, for discrete values of α,β,$\overrightarrow{\tilde{J}_x}(\alpha,\beta)$ and $\overrightarrow{\tilde{J}_y}(\alpha,\beta)$ are non-zeros.Thus, we can convert the integral equation (2.42) in to a summation form and assuming the infinite regular periodicity in x and y directions. The equation (2.42) can be reconfigured as,

$$-\begin{bmatrix} \overrightarrow{E_x^{inc}} \\ \overrightarrow{E_y^{inc}} \end{bmatrix}$$

$$= \frac{1}{j\omega\varepsilon_0} X \frac{1}{(2\pi)^2 ab} \sum_{m=-\infty}^{+\infty} \sum_{n=-\infty}^{+\infty} \begin{bmatrix} k_0^2 - \alpha_m^2 & -\alpha_m\beta_n \\ -\alpha_m\beta_n & k_0^2 - \beta_n^2 \end{bmatrix} \tilde{\tilde{G}}(\alpha_m,\beta_n)\, X \begin{bmatrix} \overrightarrow{\tilde{J}_x}(\alpha_{m,}\beta_n) \\ \overrightarrow{\tilde{J}_y}(\alpha_m,\beta_n \end{bmatrix} e^{j\alpha_m x} e^{j\beta_n y}$$

(2.49)

Where,

$$\alpha_m = \frac{2m\pi}{a} + k_x^{inc} \qquad (2.50)$$

and $\beta_n = \frac{2n\pi}{b} + k_y^{inc}$ (2.51)

$$k_x^{inc} = k_0 \sin\theta \cos\emptyset \qquad (2.52)$$

$$k_y^{inc} = k_0 \, sin\theta \, sin\emptyset \qquad (2.53)$$

Where, θ- the angle of incident wave with the z-axis

∅- the angle of the projection of the incident wave on the xy plane with the x-axis (Fig. 2.1).

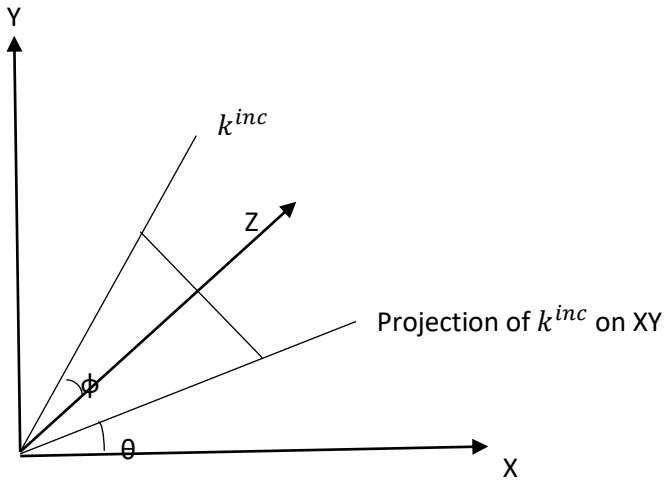

Fig.2.1. Diagram showing the incident wave projected on XY plane with X-axis

Now our goal is to solve the equation (2.49) with the help of method of moment to calculate the surface current density.

2.4 General Solution of the Operator Equation

Let,the matrix equation (2.49) is written in the symbolic diadic form.

L(u) = g , where g is the recognised matrix $\begin{bmatrix} \vec{E}_x^{inc} \\ \vec{E}_y^{inc} \end{bmatrix}$

U is the matrix that has to be determined $\begin{bmatrix} \widetilde{\vec{J}_x}(\alpha_m, \beta_n) \\ \widetilde{\vec{J}_y}(\alpha_m, \beta_n) \end{bmatrix}$

and L is the total operator included in matrix equation (2.49).

Thus, we can write,

$$\left(\hat{x}\hat{x}L_{xx} + \hat{x}\hat{y}L_{xy} + \hat{y}\hat{x}L_{yx} + \hat{y}\hat{y}L_{yy}\right)\left(\hat{x}u_x + \hat{y}u_y\right) = \hat{x}g_x + \hat{y}g_y \tag{2.54}$$

Here u is the basis function that has to be choosen. In generalised form,

$$u = \sum_{i=1}^{n}\left(\hat{x}C_{xi}f_{xi} + \hat{y}C_{yi}f_{yi}\right) \tag{2.55}$$

From equation (2.54) we have,

$$L_{xx}\,u_x + L_{xy}u_y = g_x$$

$$\text{or, } L_{xx}\sum_{j=1}^{N} C_{xj}f_{xj} + L_{xy}\sum_{j=1}^{N} C_{yj}f_{yj} = g_x \tag{2.56}$$

Similarly,

$$L_{yx}\sum_{j=1}^{N} C_{xj}f_{xj} + L_{yy}\sum_{j=1}^{N} C_{yj}f_{yj} = g_y \tag{2.57}$$

Considering the inner product of f_{xi} and equation (2.56) we obtained,

$$\langle f_{xi}, L_{xx}\sum_{j=1}^{N} C_{xj}f_{xj}\rangle + \langle f_{xi}, L_{xy}\sum_{j=1}^{N} C_{yj}f_{yj}\rangle = \langle f_{xi}, g_x\rangle \tag{2.58}$$

Similarly, considering the inner product of f_{yi} and equation (2.57) we obtained,

$$\langle f_{yi}, L_{yx}\sum_{j=1}^{N} C_{xj}f_{xj}\rangle + \langle f_{yi}, L_{yy}\sum_{j=1}^{N} C_{yj}f_{yj}\rangle$$
$$= \langle f_{yi}, g_y\rangle \tag{2.59}$$

From equation (2.58) we get,

$$\sum_{j=1}^{N}\langle f_{xi}, L_{xx}f_{xj}\rangle C_{xj} + \sum_{j=1}^{N}\langle f_{xi}, L_{xy}f_{yj}\rangle = \langle f_{xi}, g_x\rangle \tag{2.60}$$

From equation (2.59) we get,

$$\sum_{j=1}^{N}\langle f_{yi}, L_{yx}f_{xj}\rangle C_{xj} + \sum_{j=1}^{N}\langle f_{yi}, L_{yy}f_{yj}\rangle = \langle f_{yi}, g_y\rangle \tag{2.61}$$

Concisely, equations (2.60) and (2.61) can be written as,

$$\sum_{j=1}^{N} a_{ij}^{xx} C_{xj} + \sum_{j=1}^{N} b_{ij}^{xy} C_{yj} = \lambda_i^x \tag{2.62}$$

$$\sum_{j=1}^{N} a_{ij}^{yx} C_{xj} + \sum_{j=1}^{N} b_{ij}^{yy} C_{yj} = \lambda_i^y \tag{2.63}$$

Where,

$$a_{ij}^{xx} = \langle f_{xi}, L_{xx} f_{xj} \rangle;\ b_{ij}^{xy} = \langle f_{xi}, L_{xy} f_{yj} \rangle$$

$$a_{ij}^{yx} = \langle f_{yi}, L_{yx} f_{xj} \rangle;\ b_{ij}^{yy} = \langle f_{yi}, L_{yy} f_{yj} \rangle$$

$$\lambda_i^x = \langle f_{xi}, g_x \rangle;\ \lambda_i^y = \langle f_{yi}, g_y \rangle$$

Taking account of whole, in matrix form it can be represented as,

$$\begin{bmatrix} a_{11}^{xx} & a_{12}^{xx} \dots\dots\dots\dots a_{1N}^{xx} & b_{11}^{xy} & b_{12}^{xy} \dots\dots\dots\dots b_{1N}^{xy} \\ a_{21}^{xx} & a_{22}^{xx} \dots\dots\dots\dots a_{2N}^{xx} & b_{21}^{xy} & b_{22}^{xy} \dots\dots\dots\dots b_{2N}^{xy} \\ \vdots & \vdots & \vdots & \vdots \\ a_{N1}^{xx} & a_{N2}^{xx} \dots\dots\dots\dots a_{NN}^{xx} & b_{N1}^{xy} & b_{2N}^{xy} \dots\dots\dots\dots b_{NN}^{xy} \\ a_{11}^{yx} & a_{12}^{yx} \dots\dots\dots\dots a_{1N}^{yx} & b_{11}^{yy} & b_{12}^{yy} \dots\dots\dots\dots b_{1N}^{yy} \\ a_{21}^{yx} & a_{22}^{yx} \dots\dots\dots\dots a_{2N}^{yx} & b_{21}^{yy} & b_{22}^{yy} \dots\dots\dots\dots b_{2N}^{yy} \\ \vdots & \vdots & \vdots & \vdots \\ a_{N1}^{yx} & a_{N2}^{yx} \dots\dots\dots\dots a_{NN}^{yx} & b_{N1}^{yy} & b_{N2}^{yy} \dots\dots\dots\dots b_{NN}^{yy} \end{bmatrix} \begin{bmatrix} C_{x1} \\ C_{x2} \\ \vdots \\ C_{xn} \\ C_{y1} \\ C_{y2} \\ \vdots \\ C_{yn} \end{bmatrix} = \begin{bmatrix} \lambda_1^x \\ \lambda_2^x \\ \vdots \\ \lambda_N^x \\ \lambda_1^y \\ \lambda_2^y \\ \vdots \\ \lambda_N^y \end{bmatrix}$$

(2.64)

Now, $C_{x1}, C_{x2}, C_{x3}, \dots\dots\dots\dots\dots\dots\dots, C_{xN}$ and $C_{y1}, C_{y2}, C_{y3}, \dots\dots\dots\dots\dots\dots, C_{yN}$ are to be calculated

There from the function u can be evaluated

$$u = \sum_{i=1}^{N} \left(\hat{x} C_{xi} f_{xi} + \hat{y} C_{yi} f_{yi} \right) \tag{2.65}$$

Hence; $\begin{bmatrix} \widetilde{\vec{J}}_x(\alpha_m, \beta_n) \\ \widetilde{\vec{J}}_y(\alpha_m, \beta_n) \end{bmatrix}$ is known now.

2.5 A Printed Cross dipole Array is Analysed Theoretically as an FSS Structure by MOM

The chapter is dedicated to the theoretical analysis of a cross dipole FSS structure. For the purpose, an FSS structure with metallic cross dipole patch element has been taken into account of dimension 15mm X 1.5mm, having the periodicity of 29.7 mm in both x and y direction. An FR4- epoxy material of dimension 150mm X 150mm X 1.6mm having relative permittivity of 4.4, has been considered as substrate, which is shown in Fig.2.2 The unit cell of the FSS under consideration is depicted in Fig.2.3.

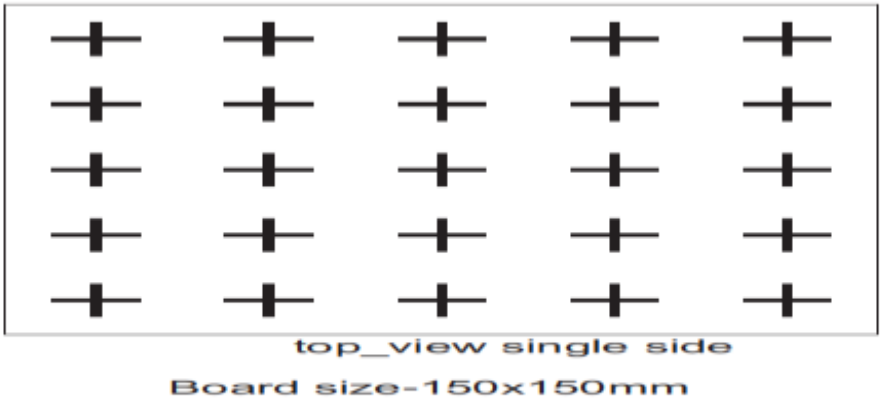

Fig.2.2. Section of frequency selective surface

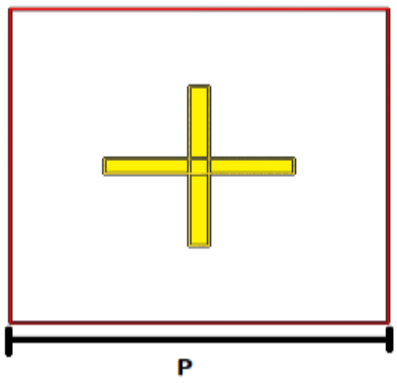

Fig.2.3. The unit cell representation of cross dipole patch type FSS structure

2.6 Development of Algorithm and Programming

In 1988, R. Mittra put forward a summary to calculate the scattered field from the incident field to the FSS by utilising spectral domain method of moment technique [11]. R Mittra also proposed entire domain basis function for standard geometry of FSS element, like dipole, cross dipole, Jerusalem cross, circular rings etc. Entire domain type of basis functions are preferred as in this case the matrix size reduces considerably, and thus converges quickly. Hence, larger problems can be solved knowing fewer unknowns.

The basis function, that is u has to be choosen. In generalised form, from equation (2.55)

$$u = \sum_{i=1}^{n} \left(\hat{x} C_{xi} f_{xi} + \hat{y} C_{yi} f_{yi} \right) \qquad (2.66)$$

C_{xi} and C_{yi} can be determined by knowing the transferred basis function and λ in x and y direction.

Considering the proposal put forward by R.Mittra, for cross dipole or slot type FSS, basis function may be assumed as [11],

$$J_{xp} = \hat{x} \left\{ c_{1q} \sin \left[\frac{P\pi}{L} \left(x + \frac{L}{2} \right) \right] + Sgn(x)\, B \cos \left(\frac{\pi}{L} x \right) \right\}$$

$$P_x(0, L) P_y(0, W)$$

$$J_{yp} = \hat{y} \left\{ c_{2q} \sin \left[\frac{P\pi}{L} \left(y + \frac{L}{2} \right) \right] - Sgn(y)\, B \cos \left(\frac{\pi}{L} y \right) \right\}$$

$$P_x(0, W) P_y(0, L) \qquad (2.67)$$

Where p=1,2,3,- - - - - -

The transferred basis function in y-direction is determined as:-

$$T_{Basis}(P,\alpha_m,\beta_n) = \int_{-\alpha}^{+\alpha}\int_{-\alpha}^{+\alpha} J_y\, e^{-j\beta y} e^{-j\alpha x}\, dy\, dx$$

$$=\frac{LW}{2j}\left[c_{2q}\left\{e^{jP\frac{\pi}{2}}\, sinc\left(\frac{P\pi}{L}-\beta\right)\frac{L}{2\pi} - e^{-jP\frac{\pi}{2}}\, sinc\left(\frac{P\pi}{L}+\beta\right)\frac{L}{2\pi}\right\} + B\left\{sinc\left(\frac{\pi}{L}-\beta\right)\frac{L}{4\pi}\sin\left(\frac{\pi}{L}-\beta\right)\frac{L}{4} - sinc\left(\frac{\pi}{L}+\beta\right)\frac{L}{4\pi}\sin\left(\frac{\pi}{L}+\beta\right)\frac{L}{4}\right\}\right]\, \text{sinc}\left(\frac{\alpha W}{2\pi}\right) \quad (2.68)$$

The transferred basis function in x-direction is determined as:

$$T^*_{Basis}(P,\alpha_m,\beta_n) = \int_{-\alpha}^{+\alpha}\int_{-\alpha}^{+\alpha} J_x\, e^{-j\beta y} e^{-j\alpha x}\, dy\, dx$$

$$=\frac{LW}{2j}\left[c_{1q}\left\{e^{jP\frac{\pi}{2}}\, sinc\left(\frac{P\pi}{L}-\alpha\right)\frac{L}{2\pi} - e^{-jP\frac{\pi}{2}}\, sinc\left(\frac{P\pi}{L}+\alpha\right)\frac{L}{2\pi}\right\} + B\left\{sinc\left(\frac{\pi}{L}+\alpha\right)\frac{L}{4\pi}\sin\left(\frac{\pi}{L}+\alpha\right)\frac{L}{4} - sinc\left(\frac{\pi}{L}-\alpha\right)\frac{L}{4\pi}\sin\left(\frac{\pi}{L}-\alpha\right)\frac{L}{4}\right\}\right]\, \text{sinc}\left(\frac{\beta W}{2\pi}\right) \quad (2.69)$$

So in matrix equation (2.64)

$$a^{xx}_{mn} = \langle f_{xm}, L_{xx} f_{xn}\rangle$$

$$= \frac{1}{j\omega\varepsilon_0} X \frac{1}{(2\pi)^2 ab} \sum_{m=-\infty}^{+\infty}\sum_{n=-\infty}^{+\infty} (k_0^2 - \alpha_m^2)\tilde{\tilde{G}}(\alpha_m,\beta_n)\, T^*_{Basis}(m,-\alpha_m,-\beta_n) T^*_{Basis}(n,\alpha_m,\beta_n)$$

(2.70)

$$a^{yx}_{mn} = \langle f_{ym}, L_{yy} f_{xn}\rangle$$

$$= \frac{1}{j\omega\varepsilon_0} X \frac{1}{(2\pi)^2 ab} \sum_{m=-\infty}^{+\infty}\sum_{n=-\infty}^{+\infty} (-\alpha_m\beta_n)\tilde{\tilde{G}}(\alpha_m,\beta_n)\, T_{Basis}(m,-\alpha_m,-\beta_n) T^*_{Basis}(n,\alpha_m,\beta_n)$$

(2.71)

$$b^{xy}_{mn} = \langle f_{xm}, L_{xy} f_{yn}\rangle$$

$$= \frac{1}{j\omega\varepsilon_0} X \frac{1}{(2\pi)^2 ab} \sum_{m=-\infty}^{+\infty} \sum_{n=-\infty}^{+\infty} (-\alpha_m \beta_n) \tilde{\tilde{G}}(\alpha_m, \beta_n)\, T^*_{Basis}(m, -\alpha_m, -\beta_n) T_{Basis}(n, \alpha_m, \beta_n)$$

(2.72)

$$b_{mn}^{yy} = \langle f_{ym}, L_{yy} f_{yn} \rangle$$

$$= \frac{1}{j\omega\varepsilon_0} X \frac{1}{(2\pi)^2 ab} \sum_{m=-\infty}^{+\infty} \sum_{n=-\infty}^{+\infty} (k_0^2 - \beta_n^2) \tilde{\tilde{G}}(\alpha_m, \beta_n)\, T_{Basis}(m, -\alpha_m, -\beta_n) T_{Basis}(n, \alpha_m, \beta_n)$$

(2.73)

The expression for λ in y direction can be written as,

$$\lambda_i^y = \frac{LW}{2} e^{-j(\omega t + \emptyset)} \left[\frac{c_{2q}}{j} \left\{ e^{ji\frac{\pi}{2}}\, sinc2(i-1) - e^{ji\frac{\pi}{2}}\, sinc2(i+1) \right\} - B \right] \quad (2.74)$$

where, i=1, 2, 3,----------

The expression for λ in x direction can be written as,

$$\lambda_i^x = \frac{LW}{2} e^{-j(\omega t + \emptyset)} \left[\frac{c_{1q}}{j} \left\{ e^{ji\frac{\pi}{2}}\, sinc2(i-1) - e^{ji\frac{\pi}{2}}\, sinc2(i+1) \right\} + B \right] \quad (2.75)$$

where, i=1, 2, 3,----------

Thus, Knowing λ_i^y andλ_i^x ; anda_{ij}^{xx} ,a_{ij}^{yx} ,b_{ij}^{xy} ,b_{ij}^{yy}, we can calculate$\sum_{i=1}^{N} C_{xi}$ and $\sum_{i=1}^{N} C_{yi}$. Hence, $\begin{pmatrix} \widetilde{\overrightarrow{J_{x(\alpha_m,\beta_n)}}} \\ \widetilde{\overrightarrow{J_{y(\alpha_m,\beta_n)}}} \end{pmatrix}$ can be determined by using equation (2.68) to (2.75).

Now, using these values of $\widetilde{\overrightarrow{J_x}}$ and $\widetilde{\overrightarrow{J_y}}$ into equation (2.49) can calculate scattered electric fields$\begin{pmatrix} E_x^s \\ E_y^s \end{pmatrix}$.

The transmission coefficients of the structure of mode mn due to mode kl incident can be obtained from these scattered electric fields E_x^s and E_y^s as,

$$T_{TM} = \frac{j\omega\epsilon_0 E_z^t}{(k_0^2+\gamma_{mn}^2)}\sqrt{\frac{\gamma_{mn\,(k_0^2+\gamma_{mn}^2)}}{\gamma_{kl}(k_0^2+\gamma_{kl}^2)}} \qquad (2.76)$$

Where, $E_z^t = j\frac{(\alpha_{m\,E_x^s}+\beta_n E_y^s)}{\gamma_{mn}}$

$\gamma_{mn} = -j(k_0^2 - \alpha_m^2 - \beta_n^2)^{1/2}$ for $k_0^2 > \alpha_m^2 + \beta_n^2$

$= -(\alpha_m^2 + \beta_n^2 - k_0^2)^{1/2}$ for $k_0^2 < \alpha_m^2 + \beta_n^2$

The equations (2.67) to (2.75) have been programmed in MATLAB to obtain the transmission characteristics plot of the cross dipole patch type FSS structure, therefrom the resonating frequency is theoretically achieved, which is depicted in Fig.2.5

2.7 Experimental Verification

The cross dipole structure is theoretically verified by establishing the coding based on the algorithm explained in section 2.6 and the same structure is again theoretically verified by simulation done by means of available software.For the experimental verification of the structure microwave test bench has been used. The simulation softwares that are developed based on moment method are ANSOFT, FEKO; the transmission characteristics of an FSS structure can be generated by exploiting these softwares.The chapter presents a cross dipole structure that has been simulated by ANSOFT version 2.2.The transmission characteristic curve has been generated for the cross dipole structure; wherefrom the frequency of resonance has been obtained. The fabricated cross dipole has been measured in the laboratory using microwave test bench as shown in Fig.2.4.Transmitting and receiving antenna are connected to a variable RF generator and to a power meter with power sensor respectively.The cross dipole FSS structure is mountedbetween the receiving and transmitting antenna at far field distance. The observation revealed that the FSS structureunder consideration blocks the frequency band 6.02 GHz to 6.20 GHz and radiates all other frequencies.The frequency of

resonance is obtained from the plot of experimentally obtained data of transmitted electric field and frequency. The frequency of resonanceobtained by the established algorithm and MATLAB coding proposed here to study the dipole structure are then verified with the frequency of resonanceobtained by simulation and experiment. The theoretical, simulated and experimentally obtainedtransmitted characteristic curve of thecross dipole structure (Fig.2.3) are plotted on the same graph as shown in Fig.2.5. The designed and documented work presented here is published in a reputed journal [11].

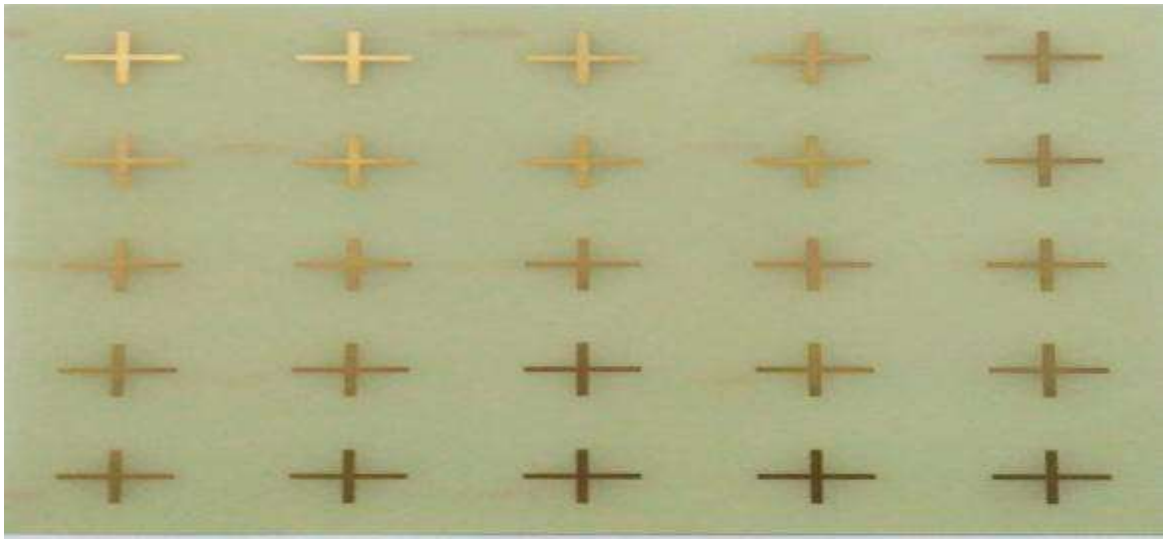

Fig.2.4. Fabricated cross dipole FSS structure

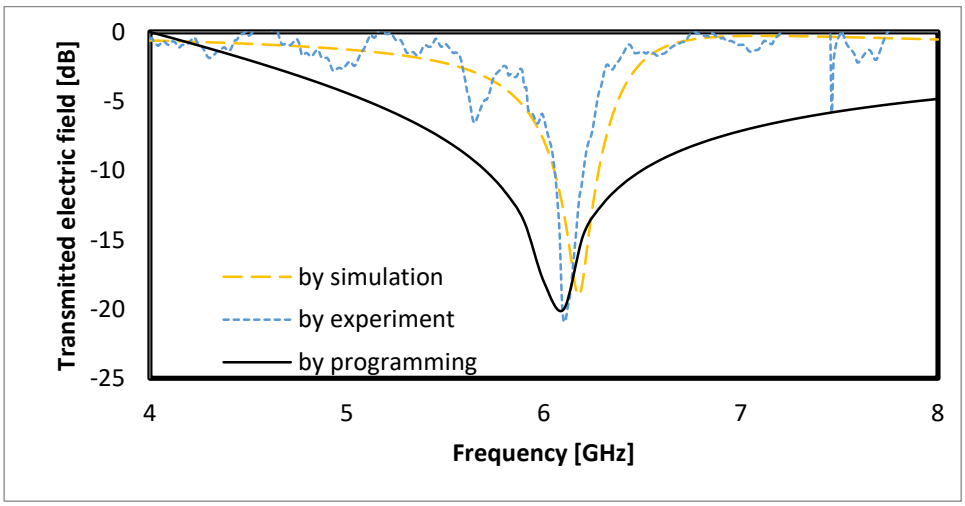

Fig.2.5. Transmission coefficient vs frequency graph

The transmission characteristic shown in Fig.2.5 make it evident that the cross dipole structure of dimension 15 mmX 1.5 mm formulated by using MOM and its realization by programming in MATLAB attains a frequency of resonance of 6.10 GHz considering the periodicity in both the plane of two dimension as 29.7 mm. The simulation of the cross dipole FSS under consideration, by ANSOFT achieved a frequency of resonance at 6.18 GHz.The measurement of the cross dipole FSS utilizing microwave test bench attains frequency of resonance at 6.13 GHz.

The comparative analysis of the results obtained by the three different approach to study a cross dipole FSS has been furnished in Table 2.1.

Table2.1.Comparative Analysis of the Findings

FSS Structure	**Resonant Frequency (GHz)**	**Transmission Coefficient (dB)**
Theoretical	6.10	-20.02
Simulated	6.18	-18.99
Experimental	6.13	-20.92

The comparative study presented in Table 2.1 set out the fact that the resonant frequency achieved theoretically and experimentally are in close proximity. It delineates the worthiness of the algorithm and MATLAB coding established to analyse the cross dipole FSS. Thus, the validation of the FSS has been successfully completed.

In Table 2.2, the parametric investigation of the cross dipole FSS has been conducted by altering the periodicity to increase the bandwidth of the FSS.The study intensify the fact that the bandwidth increases when the periodicity is decreased; as the bandwidth increases from 100 MHz to 820 MHz while the periodicity is changed from 37.5 mm to 18 mm .At 18 mm periodicity, 820 MHz bandwidth is achieved, which is maximum, additionally at 6.40 GHz resonant frequency a good band separation is noticed having a transmission coefficient of -28.31 dB.The variation of

transmission characteristic as a function of frequency at a periodicity of 18 mm is shown inFig.2.6.

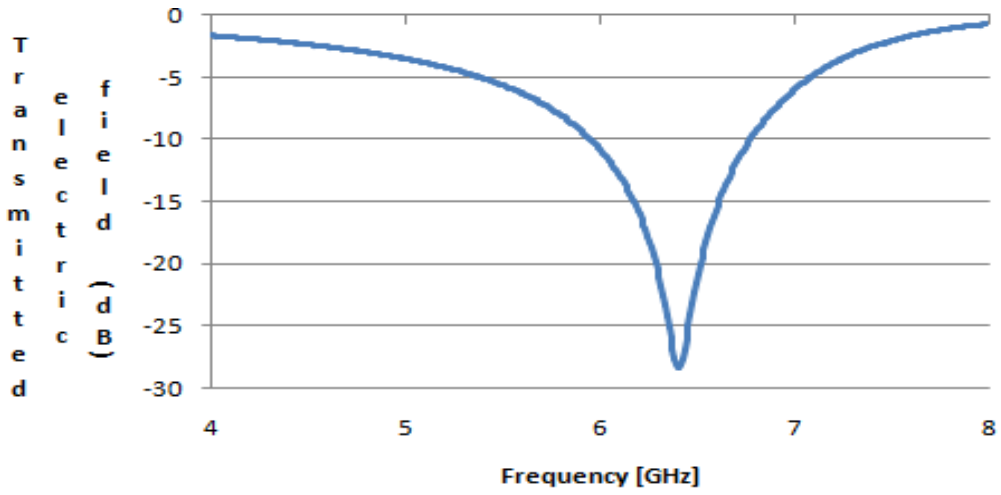

Fig.2.6.Transmission coefficient vs frequency graph at a periodicity of 18mm

Table 2.2.The effect on bandwidth on changing the periodicity

Periodicity P(mm)	Resonant Frequency (GHz)	Transmission Coefficient (dB)	Bandwidth (MHz)
37.5	**5.90**	**-14.50**	**100**
30	**6.12**	**-18.60**	**223**
29.7	**6.18**	**-19.00**	**230**
29	**6.22**	**-19.29**	**250**
28	**6.25**	**-20.00**	**270**
27	**6.27**	**-20.61**	**290**
26	**6.32**	**-21.26**	**320**
25	**6.34**	**-22.00**	**360**
24	**6.37**	**-22.81**	**400**
23	**6.39**	**-23.52**	**440**
22	**6.41**	**-24.37**	**480**
21	**6.44**	**-25.20**	**540**
20	**6.44**	**-26.28**	**620**
19	**6.44**	**-27.22**	**700**
18	**6.40**	**-28.31**	**820**

2.8 Conclusion

The theoretical formulation of cross dipole FSS has been established by MOM and MATLAB programming which depicts good agreement with the experimental results than the result generated by using ANSOFT simulation software.During the analysis of a structure, the simulation result is dependent on the choice of number of steps in the frequency range of study or on typeof choosing a mess; whereas, the algorithm developed by us is independent of such type of consideration.Thus, the established theory and MATLAB coding presented throughout the chapter is skilful and impactful to analyse any type of FSS.The analysis of the cross dipole FSSby varying the periodicity shows that optimum bandwidth has been achieved with minimal change of operating frequency. The same approach can be implement to analyse any typical FSS structure.

2.9 Experimental datasheet of fabricated cross dipole FSS structure

Table 2.3 Designed cross dipole experiment data

Frequency[Hz]	S_{21} [dB]
4.00E+09	-4.64E-01
4.00E+09	-4.43E-01
4.01E+09	-4.38E-01
4.01E+09	-5.45E-01
4.02E+09	-7.20E-01
4.02E+09	-8.36E-01
4.03E+09	-8.51E-01
4.03E+09	-9.38E-01
4.04E+09	-1.00E+00
4.04E+09	-1.01E+00
4.04E+09	-9.67E-01
4.05E+09	-9.24E-01
4.05E+09	-8.81E-01
4.06E+09	-7.79E-01
4.06E+09	-6.99E-01
4.07E+09	-6.71E-01
4.07E+09	-7.24E-01
4.08E+09	-7.95E-01
4.08E+09	-8.40E-01

Frequency[Hz]	S_{21} [dB]
4.09E+09	-9.10E-01
4.09E+09	-9.57E-01
4.10E+09	-9.00E-01
4.10E+09	-7.75E-01
4.11E+09	-6.99E-01
4.11E+09	-6.86E-01
4.12E+09	-6.83E-01
4.12E+09	-6.83E-01
4.13E+09	-7.88E-01
4.13E+09	-9.24E-01
4.13E+09	-1.01E+00
4.14E+09	-1.05E+00
4.14E+09	-1.10E+00
4.15E+09	-1.11E+00
4.15E+09	-1.05E+00
4.16E+09	-9.56E-01
4.16E+09	-9.35E-01
4.17E+09	-9.24E-01
4.17E+09	-8.98E-01
4.18E+09	-8.81E-01
4.18E+09	-8.93E-01
4.19E+09	-8.74E-01
4.19E+09	-8.18E-01
4.20E+09	-7.08E-01
4.20E+09	-6.31E-01
4.21E+09	-5.76E-01
4.21E+09	-4.75E-01
4.22E+09	-3.99E-01
4.22E+09	-3.77E-01
4.22E+09	-4.06E-01
4.23E+09	-4.74E-01
4.23E+09	-5.94E-01
4.24E+09	-7.46E-01
4.24E+09	-8.70E-01
4.25E+09	-9.01E-01
4.25E+09	-9.31E-01
4.26E+09	-1.00E+00
4.26E+09	-1.10E+00
4.27E+09	-1.20E+00
4.27E+09	-1.31E+00
4.28E+09	-1.44E+00

Frequency[Hz]	S_{21} [dB]
4.28E+09	-1.61E+00
4.29E+09	-1.74E+00
4.29E+09	-1.81E+00
4.30E+09	-1.87E+00
4.30E+09	-1.88E+00
4.31E+09	-1.83E+00
4.31E+09	-1.77E+00
4.31E+09	-1.72E+00
4.32E+09	-1.68E+00
4.32E+09	-1.66E+00
4.33E+09	-1.59E+00
4.33E+09	-1.47E+00
4.34E+09	-1.40E+00
4.34E+09	-1.38E+00
4.35E+09	-1.37E+00
4.35E+09	-1.33E+00
4.36E+09	-1.29E+00
4.36E+09	-1.23E+00
4.37E+09	-1.14E+00
4.37E+09	-1.10E+00
4.38E+09	-1.12E+00
4.38E+09	-1.21E+00
4.39E+09	-1.30E+00
4.39E+09	-1.33E+00
4.40E+09	-1.36E+00
4.40E+09	-1.37E+00
4.40E+09	-1.36E+00
4.41E+09	-1.25E+00
4.41E+09	-1.11E+00
4.42E+09	-9.20E-01
4.42E+09	-7.59E-01
4.43E+09	-6.25E-01
4.43E+09	-5.71E-01
4.44E+09	-5.71E-01
4.44E+09	-5.06E-01
4.45E+09	-3.55E-01
4.45E+09	-2.19E-01
4.46E+09	-1.65E-01
4.46E+09	-1.64E-01
4.47E+09	-1.42E-01
4.47E+09	-8.24E-02

Frequency[Hz]	S_{21} [dB]
4.48E+09	-3.11E-02
4.48E+09	1.08E-02
4.49E+09	1.52E-02
4.49E+09	-8.58E-02
4.49E+09	-1.94E-01
4.50E+09	-2.54E-01
4.50E+09	-2.40E-01
4.51E+09	-1.87E-01
4.51E+09	-1.30E-01
4.52E+09	-3.73E-02
4.52E+09	1.15E-01
4.53E+09	2.93E-01
4.53E+09	3.42E-01
4.54E+09	3.26E-01
4.54E+09	2.70E-01
4.55E+09	2.15E-01
4.55E+09	1.41E-01
4.56E+09	1.04E-01
4.56E+09	1.12E-01
4.57E+09	1.62E-01
4.57E+09	2.07E-01
4.58E+09	2.52E-01
4.58E+09	2.71E-01
4.58E+09	2.94E-01
4.59E+09	3.39E-01
4.59E+09	3.10E-01
4.60E+09	2.25E-01
4.60E+09	1.45E-01
4.61E+09	8.99E-02
4.61E+09	7.64E-02
4.62E+09	1.19E-01
4.62E+09	1.76E-01
4.63E+09	2.14E-01
4.63E+09	2.50E-01
4.64E+09	2.61E-01
4.64E+09	1.72E-01
4.65E+09	-7.81E-02
4.65E+09	-3.50E-01
4.66E+09	-5.83E-01
4.66E+09	-7.74E-01
4.67E+09	-8.87E-01

Frequency[Hz]	S_{21} [dB]
4.67E+09	-9.22E-01
4.67E+09	-9.19E-01
4.68E+09	-8.96E-01
4.68E+09	-8.76E-01
4.69E+09	-8.48E-01
4.69E+09	-8.70E-01
4.70E+09	-9.04E-01
4.70E+09	-9.34E-01
4.71E+09	-9.47E-01
4.71E+09	-9.12E-01
4.72E+09	-8.53E-01
4.72E+09	-7.97E-01
4.73E+09	-6.96E-01
4.73E+09	-5.67E-01
4.74E+09	-5.06E-01
4.74E+09	-4.96E-01
4.75E+09	-5.91E-01
4.75E+09	-7.44E-01
4.76E+09	-9.69E-01
4.76E+09	-1.24E+00
4.76E+09	-1.50E+00
4.77E+09	-1.65E+00
4.77E+09	-1.69E+00
4.78E+09	-1.65E+00
4.78E+09	-1.56E+00
4.79E+09	-1.52E+00
4.79E+09	-1.51E+00
4.80E+09	-1.55E+00
4.80E+09	-1.63E+00
4.81E+09	-1.70E+00
4.81E+09	-1.77E+00
4.82E+09	-1.77E+00
4.82E+09	-1.71E+00
4.83E+09	-1.60E+00
4.83E+09	-1.49E+00
4.84E+09	-1.40E+00
4.84E+09	-1.32E+00
4.85E+09	-1.27E+00
4.85E+09	-1.26E+00
4.85E+09	-1.32E+00
4.86E+09	-1.48E+00

Frequency[Hz]	S_{21} [dB]
4.86E+09	-1.69E+00
4.87E+09	-1.83E+00
4.87E+09	-1.91E+00
4.88E+09	-1.90E+00
4.88E+09	-1.88E+00
4.89E+09	-1.87E+00
4.89E+09	-1.87E+00
4.90E+09	-1.88E+00
4.90E+09	-1.97E+00
4.91E+09	-2.12E+00
4.91E+09	-2.32E+00
4.92E+09	-2.55E+00
4.92E+09	-2.71E+00
4.93E+09	-2.81E+00
4.93E+09	-2.80E+00
4.94E+09	-2.75E+00
4.94E+09	-2.72E+00
4.94E+09	-2.70E+00
4.95E+09	-2.65E+00
4.95E+09	-2.59E+00
4.96E+09	-2.58E+00
4.96E+09	-2.60E+00
4.97E+09	-2.63E+00
4.97E+09	-2.67E+00
4.98E+09	-2.66E+00
4.98E+09	-2.59E+00
4.99E+09	-2.49E+00
4.99E+09	-2.40E+00
5.00E+09	-2.31E+00
5.00E+09	-2.22E+00
5.01E+09	-2.16E+00
5.01E+09	-2.11E+00
5.02E+09	-2.13E+00
5.02E+09	-2.23E+00
5.03E+09	-2.38E+00
5.03E+09	-2.47E+00
5.03E+09	-2.50E+00
5.04E+09	-2.44E+00
5.04E+09	-2.35E+00
5.05E+09	-2.19E+00
5.05E+09	-2.02E+00

Frequency[Hz]	S_{21} [dB]
5.06E+09	-1.84E+00
5.06E+09	-1.69E+00
5.07E+09	-1.54E+00
5.07E+09	-1.42E+00
5.08E+09	-1.33E+00
5.08E+09	-1.22E+00
5.09E+09	-1.11E+00
5.09E+09	-9.54E-01
5.10E+09	-7.75E-01
5.10E+09	-6.30E-01
5.11E+09	-4.57E-01
5.11E+09	-2.94E-01
5.12E+09	-1.97E-01
5.12E+09	-1.92E-01
5.12E+09	-2.50E-01
5.13E+09	-3.38E-01
5.13E+09	-3.85E-01
5.14E+09	-4.05E-01
5.14E+09	-3.54E-01
5.15E+09	-2.14E-01
5.15E+09	-4.03E-02
5.16E+09	1.11E-01
5.16E+09	1.84E-01
5.17E+09	2.24E-01
5.17E+09	2.19E-01
5.18E+09	1.43E-01
5.18E+09	4.23E-02
5.19E+09	-5.38E-02
5.19E+09	-1.13E-01
5.20E+09	-1.42E-01
5.20E+09	-1.61E-01
5.21E+09	-1.51E-01
5.21E+09	-9.99E-02
5.21E+09	-5.28E-02
5.22E+09	-6.01E-02
5.22E+09	-1.10E-01
5.23E+09	-2.01E-01
5.23E+09	-3.01E-01
5.24E+09	-4.28E-01
5.24E+09	-5.43E-01
5.25E+09	-6.05E-01

Frequency[Hz]	S_{21} [dB]
5.25E+09	-6.44E-01
5.26E+09	-6.52E-01
5.26E+09	-6.23E-01
5.27E+09	-5.70E-01
5.27E+09	-6.20E-01
5.28E+09	-7.47E-01
5.28E+09	-9.08E-01
5.29E+09	-1.07E+00
5.29E+09	-1.27E+00
5.30E+09	-1.43E+00
5.30E+09	-1.53E+00
5.30E+09	-1.53E+00
5.31E+09	-1.52E+00
5.31E+09	-1.50E+00
5.32E+09	-1.45E+00
5.32E+09	-1.45E+00
5.33E+09	-1.49E+00
5.33E+09	-1.56E+00
5.34E+09	-1.65E+00
5.34E+09	-1.67E+00
5.35E+09	-1.67E+00
5.35E+09	-1.64E+00
5.36E+09	-1.58E+00
5.36E+09	-1.44E+00
5.37E+09	-1.27E+00
5.37E+09	-1.10E+00
5.38E+09	-1.01E+00
5.38E+09	-9.72E-01
5.39E+09	-9.36E-01
5.39E+09	-9.69E-01
5.39E+09	-1.04E+00
5.40E+09	-1.07E+00
5.40E+09	-1.05E+00
5.41E+09	-1.01E+00
5.41E+09	-8.89E-01
5.42E+09	-7.24E-01
5.42E+09	-5.67E-01
5.43E+09	-4.89E-01
5.43E+09	-5.25E-01
5.44E+09	-6.27E-01
5.44E+09	-7.81E-01

Frequency[Hz]	S_{21} [dB]
5.45E+09	-9.19E-01
5.45E+09	-1.03E+00
5.46E+09	-1.07E+00
5.46E+09	-1.03E+00
5.47E+09	-9.37E-01
5.47E+09	-8.73E-01
5.48E+09	-8.52E-01
5.48E+09	-8.77E-01
5.48E+09	-9.96E-01
5.49E+09	-1.16E+00
5.49E+09	-1.30E+00
5.50E+09	-1.37E+00
5.50E+09	-1.45E+00
5.51E+09	-1.52E+00
5.51E+09	-1.52E+00
5.52E+09	-1.48E+00
5.52E+09	-1.49E+00
5.53E+09	-1.52E+00
5.53E+09	-1.58E+00
5.54E+09	-1.65E+00
5.54E+09	-1.80E+00
5.55E+09	-2.07E+00
5.55E+09	-2.42E+00
5.56E+09	-2.78E+00
5.56E+09	-3.12E+00
5.57E+09	-3.46E+00
5.57E+09	-3.86E+00
5.57E+09	-4.30E+00
5.58E+09	-4.74E+00
5.58E+09	-5.19E+00
5.59E+09	-5.63E+00
5.59E+09	-6.05E+00
5.60E+09	-6.38E+00
5.60E+09	-6.54E+00
5.61E+09	-6.56E+00
5.61E+09	-6.43E+00
5.62E+09	-6.21E+00
5.62E+09	-6.05E+00
5.63E+09	-5.86E+00
5.63E+09	-5.68E+00
5.64E+09	-5.46E+00

Frequency[Hz]	S_{21} [dB]
5.64E+09	-5.28E+00
5.65E+09	-5.14E+00
5.65E+09	-5.00E+00
5.66E+09	-4.91E+00
5.66E+09	-4.91E+00
5.66E+09	-4.90E+00
5.67E+09	-4.86E+00
5.67E+09	-4.74E+00
5.68E+09	-4.56E+00
5.68E+09	-4.32E+00
5.69E+09	-4.03E+00
5.69E+09	-3.74E+00
5.70E+09	-3.44E+00
5.70E+09	-3.28E+00
5.71E+09	-3.18E+00
5.71E+09	-3.07E+00
5.72E+09	-2.97E+00
5.72E+09	-2.89E+00
5.73E+09	-2.84E+00
5.73E+09	-2.77E+00
5.74E+09	-2.67E+00
5.74E+09	-2.56E+00
5.75E+09	-2.50E+00
5.75E+09	-2.48E+00
5.75E+09	-2.47E+00
5.76E+09	-2.45E+00
5.76E+09	-2.50E+00
5.77E+09	-2.56E+00
5.77E+09	-2.55E+00
5.78E+09	-2.53E+00
5.78E+09	-2.52E+00
5.79E+09	-2.46E+00
5.79E+09	-2.33E+00
5.80E+09	-2.26E+00
5.80E+09	-2.32E+00
5.81E+09	-2.53E+00
5.81E+09	-2.79E+00
5.82E+09	-3.09E+00
5.82E+09	-3.30E+00
5.83E+09	-3.40E+00
5.83E+09	-3.41E+00

Frequency[Hz]	S_{21} [dB]
5.84E+09	-3.38E+00
5.84E+09	-3.29E+00
5.84E+09	-3.19E+00
5.85E+09	-3.12E+00
5.85E+09	-3.03E+00
5.86E+09	-3.03E+00
5.86E+09	-3.08E+00
5.87E+09	-3.15E+00
5.87E+09	-3.22E+00
5.88E+09	-3.25E+00
5.88E+09	-3.26E+00
5.89E+09	-3.22E+00
5.89E+09	-3.11E+00
5.90E+09	-2.96E+00
5.90E+09	-2.79E+00
5.91E+09	-2.65E+00
5.91E+09	-2.64E+00
5.92E+09	-2.79E+00
5.92E+09	-3.02E+00
5.93E+09	-3.26E+00
5.93E+09	-3.44E+00
5.93E+09	-3.55E+00
5.94E+09	-3.63E+00
5.94E+09	-3.65E+00
5.95E+09	-3.64E+00
5.95E+09	-3.64E+00
5.96E+09	-3.69E+00
5.96E+09	-3.81E+00
5.97E+09	-3.98E+00
5.97E+09	-4.19E+00
5.98E+09	-4.34E+00
5.98E+09	-4.36E+00
5.99E+09	-4.29E+00
5.99E+09	-4.13E+00
6.00E+09	-4.00E+00
6.00E+09	-3.87E+00
6.01E+09	-3.80E+00
6.01E+09	-3.86E+00
6.02E+09	-4.06E+00
6.02E+09	-4.36E+00
6.02E+09	-4.75E+00

Frequency[Hz]	S_{21} [dB]
6.03E+09	-5.11E+00
6.03E+09	-5.44E+00
6.04E+09	-5.62E+00
6.04E+09	-5.69E+00
6.05E+09	-5.74E+00
6.05E+09	-5.80E+00
6.06E+09	-5.85E+00
6.06E+09	-5.97E+00
6.07E+09	-6.14E+00
6.07E+09	-6.31E+00
6.08E+09	-6.48E+00
6.08E+09	-6.59E+00
6.09E+09	-6.59E+00
6.09E+09	-6.46E+00
6.10E+09	-6.25E+00
6.10E+09	-6.03E+00
6.11E+09	-5.90E+00
6.11E+09	-5.90E+00
6.11E+09	-6.01E+00
6.12E+09	-6.24E+00
6.12E+09	-6.52E+00
6.13E+09	-6.88E+00
6.13E+09	-7.19E+00
6.14E+09	-7.43E+00
6.14E+09	-7.71E+00
6.15E+09	-7.93E+00
6.15E+09	-8.14E+00
6.16E+09	-8.47E+00
6.16E+09	-8.98E+00
6.17E+09	-9.49E+00
6.17E+09	-1.00E+01
6.18E+09	-1.07E+01
6.18E+09	-1.15E+01
6.19E+09	-1.25E+01
6.19E+09	-1.36E+01
6.20E+09	-1.47E+01
6.20E+09	-1.62E+01
6.20E+09	-1.75E+01
6.21E+09	-1.90E+01
6.21E+09	-2.01E+01
6.22E+09	-2.09E+01

Frequency[Hz]	S_{21} [dB]
6.22E+09	-2.10E+01
6.23E+09	-2.08E+01
6.23E+09	-2.05E+01
6.24E+09	-1.99E+01
6.24E+09	-1.96E+01
6.25E+09	-1.92E+01
6.25E+09	-1.88E+01
6.26E+09	-1.80E+01
6.26E+09	-1.72E+01
6.27E+09	-1.65E+01
6.27E+09	-1.57E+01
6.28E+09	-1.50E+01
6.28E+09	-1.41E+01
6.29E+09	-1.34E+01
6.29E+09	-1.27E+01
6.29E+09	-1.19E+01
6.30E+09	-1.12E+01
6.30E+09	-1.06E+01
6.31E+09	-1.01E+01
6.31E+09	-9.58E+00
6.32E+09	-9.08E+00
6.32E+09	-8.65E+00
6.33E+09	-8.28E+00
6.33E+09	-8.02E+00
6.34E+09	-7.81E+00
6.34E+09	-7.63E+00
6.35E+09	-7.47E+00
6.35E+09	-7.17E+00
6.36E+09	-6.79E+00
6.36E+09	-6.36E+00
6.37E+09	-5.89E+00
6.37E+09	-5.43E+00
6.38E+09	-5.01E+00
6.38E+09	-4.69E+00
6.38E+09	-4.45E+00
6.39E+09	-4.30E+00
6.39E+09	-4.14E+00
6.40E+09	-3.93E+00
6.40E+09	-3.64E+00
6.41E+09	-3.29E+00
6.41E+09	-2.95E+00

Frequency[Hz]	S_{21} [dB]
6.42E+09	-2.63E+00
6.42E+09	-2.43E+00
6.43E+09	-2.35E+00
6.43E+09	-2.36E+00
6.44E+09	-2.46E+00
6.44E+09	-2.60E+00
6.45E+09	-2.69E+00
6.45E+09	-2.71E+00
6.46E+09	-2.68E+00
6.46E+09	-2.58E+00
6.47E+09	-2.44E+00
6.47E+09	-2.30E+00
6.47E+09	-2.18E+00
6.48E+09	-2.09E+00
6.48E+09	-1.96E+00
6.49E+09	-1.82E+00
6.49E+09	-1.68E+00
6.50E+09	-1.59E+00
6.50E+09	-1.47E+00
6.51E+09	-1.35E+00
6.51E+09	-1.18E+00
6.52E+09	-1.06E+00
6.52E+09	-9.70E-01
6.53E+09	-9.09E-01
6.53E+09	-9.12E-01
6.54E+09	-9.64E-01
6.54E+09	-1.10E+00
6.55E+09	-1.25E+00
6.55E+09	-1.40E+00
6.56E+09	-1.51E+00
6.56E+09	-1.55E+00
6.56E+09	-1.53E+00
6.57E+09	-1.50E+00
6.57E+09	-1.48E+00
6.58E+09	-1.42E+00
6.58E+09	-1.41E+00
6.59E+09	-1.42E+00
6.59E+09	-1.44E+00
6.60E+09	-1.49E+00
6.60E+09	-1.57E+00
6.61E+09	-1.55E+00

Frequency[Hz]	S_{21} [dB]
6.61E+09	-1.47E+00
6.62E+09	-1.45E+00
6.62E+09	-1.48E+00
6.63E+09	-1.49E+00
6.63E+09	-1.48E+00
6.64E+09	-1.50E+00
6.64E+09	-1.54E+00
6.65E+09	-1.56E+00
6.65E+09	-1.60E+00
6.65E+09	-1.62E+00
6.66E+09	-1.68E+00
6.66E+09	-1.72E+00
6.67E+09	-1.71E+00
6.67E+09	-1.67E+00
6.68E+09	-1.64E+00
6.68E+09	-1.62E+00
6.69E+09	-1.59E+00
6.69E+09	-1.58E+00
6.70E+09	-1.55E+00
6.70E+09	-1.52E+00
6.71E+09	-1.46E+00
6.71E+09	-1.37E+00
6.72E+09	-1.32E+00
6.72E+09	-1.27E+00
6.73E+09	-1.18E+00
6.73E+09	-1.09E+00
6.74E+09	-1.08E+00
6.74E+09	-1.09E+00
6.74E+09	-1.07E+00
6.75E+09	-9.86E-01
6.75E+09	-9.57E-01
6.76E+09	-9.47E-01
6.76E+09	-9.43E-01
6.77E+09	-8.80E-01
6.77E+09	-8.33E-01
6.78E+09	-8.10E-01
6.78E+09	-7.62E-01
6.79E+09	-7.30E-01
6.79E+09	-6.96E-01
6.80E+09	-7.24E-01
6.80E+09	-7.42E-01

Frequency[Hz]	S_{21} [dB]
6.81E+09	-6.91E-01
6.81E+09	-5.65E-01
6.82E+09	-4.02E-01
6.82E+09	-2.57E-01
6.83E+09	-2.01E-01
6.83E+09	-1.41E-01
6.83E+09	-1.15E-01
6.84E+09	-7.09E-02
6.84E+09	-2.91E-02
6.85E+09	-2.57E-03
6.85E+09	-4.46E-02
6.86E+09	-1.25E-01
6.86E+09	-1.48E-01
6.87E+09	-1.33E-01
6.87E+09	-1.24E-01
6.88E+09	-1.94E-01
6.88E+09	-2.42E-01
6.89E+09	-2.65E-01
6.89E+09	-2.71E-01
6.90E+09	-2.78E-01
6.90E+09	-2.92E-01
6.91E+09	-2.88E-01
6.91E+09	-2.97E-01
6.92E+09	-3.12E-01
6.92E+09	-3.10E-01
6.92E+09	-1.98E-01
6.93E+09	-9.20E-02
6.93E+09	-6.45E-02
6.94E+09	-1.22E-01
6.94E+09	-1.98E-01
6.95E+09	-2.49E-01
6.95E+09	-3.29E-01
6.96E+09	-3.99E-01
6.96E+09	-4.05E-01
6.97E+09	-4.11E-01
6.97E+09	-4.46E-01
6.98E+09	-4.63E-01
6.98E+09	-4.28E-01
6.99E+09	-4.29E-01
6.99E+09	-4.73E-01
7.00E+09	-5.35E-01

Frequency[Hz]	S_{21} [dB]
7.00E+09	-5.49E-01
7.01E+09	-5.19E-01
7.01E+09	-5.73E-01
7.01E+09	-6.17E-01
7.02E+09	-6.41E-01
7.02E+09	-6.48E-01
7.03E+09	-6.45E-01
7.03E+09	-6.82E-01
7.04E+09	-7.03E-01
7.04E+09	-7.07E-01
7.05E+09	-8.02E-01
7.05E+09	-8.65E-01
7.06E+09	-9.34E-01
7.06E+09	-9.37E-01
7.07E+09	-9.26E-01
7.07E+09	-9.21E-01
7.08E+09	-9.25E-01
7.08E+09	-9.26E-01
7.09E+09	-9.22E-01
7.09E+09	-9.29E-01
7.10E+09	-9.53E-01
7.10E+09	-9.89E-01
7.10E+09	-1.06E+00
7.11E+09	-1.17E+00
7.11E+09	-1.28E+00
7.12E+09	-1.37E+00
7.12E+09	-1.43E+00
7.13E+09	-1.42E+00
7.13E+09	-1.40E+00
7.14E+09	-1.37E+00
7.14E+09	-1.35E+00
7.15E+09	-1.33E+00
7.15E+09	-1.31E+00
7.16E+09	-1.30E+00
7.16E+09	-1.27E+00
7.17E+09	-1.25E+00
7.17E+09	-1.14E+00
7.18E+09	-1.04E+00
7.18E+09	-9.05E-01
7.19E+09	-7.85E-01
7.19E+09	-7.03E-01

Frequency[Hz]	S_{21} [dB]
7.19E+09	-6.43E-01
7.20E+09	-6.31E-01
7.20E+09	-6.38E-01
7.21E+09	-6.96E-01
7.21E+09	-7.59E-01
7.22E+09	-7.98E-01
7.22E+09	-8.48E-01
7.23E+09	-8.52E-01
7.23E+09	-8.71E-01
7.24E+09	-8.44E-01
7.24E+09	-7.06E-01
7.25E+09	-5.23E-01
7.25E+09	-4.17E-01
7.26E+09	-3.71E-01
7.26E+09	-3.36E-01
7.27E+09	-2.35E-01
7.27E+09	-1.70E-01
7.28E+09	-9.35E-02
7.28E+09	-5.00E-04
7.28E+09	5.96E-02
7.29E+09	1.64E-01
7.29E+09	2.53E-01
7.30E+09	3.27E-01
7.30E+09	3.71E-01
7.31E+09	3.85E-01
7.31E+09	3.98E-01
7.32E+09	3.82E-01
7.32E+09	4.08E-01
7.33E+09	4.40E-01
7.33E+09	4.74E-01
7.34E+09	5.23E-01
7.34E+09	6.08E-01
7.35E+09	7.05E-01
7.35E+09	8.30E-01
7.36E+09	9.68E-01
7.36E+09	1.07E+00
7.37E+09	1.14E+00
7.37E+09	1.21E+00
7.37E+09	1.30E+00
7.38E+09	1.39E+00
7.38E+09	1.55E+00

Frequency[Hz]	S_{21} [dB]
7.39E+09	1.72E+00
7.39E+09	1.88E+00
7.40E+09	1.93E+00
7.40E+09	1.89E+00
7.41E+09	1.78E+00
7.41E+09	1.62E+00
7.42E+09	1.36E+00
7.42E+09	1.10E+00
7.43E+09	9.21E-01
7.43E+09	7.83E-01
7.44E+09	7.24E-01
7.44E+09	7.95E-01
7.45E+09	8.68E-01
7.45E+09	9.67E-01
7.46E+09	1.13E+00
7.46E+09	1.29E+00
7.46E+09	1.51E+00
7.47E+09	1.71E+00
7.47E+09	1.86E+00
7.48E+09	1.90E+00
7.48E+09	1.91E+00
7.49E+09	2.01E+00
7.49E+09	2.19E+00
7.50E+09	2.27E+00
7.50E+09	2.25E+00
7.51E+09	2.21E+00
7.51E+09	2.39E+00
7.52E+09	3.80E+00
7.52E+09	-5.62E-01
7.53E+09	-5.69E+00
7.53E+09	-3.11E+00
7.54E+09	-2.19E+00
7.54E+09	-1.53E+00
7.55E+09	-1.12E+00
7.55E+09	-7.82E-01
7.55E+09	-5.34E-01
7.56E+09	-2.65E-01
7.56E+09	-2.11E-02
7.57E+09	5.72E-02
7.57E+09	-6.15E-02
7.58E+09	-2.26E-01

Frequency[Hz]	S_{21} [dB]
7.58E+09	-4.33E-01
7.59E+09	-6.57E-01
7.59E+09	-8.34E-01
7.60E+09	-9.39E-01
7.60E+09	-1.04E+00
7.61E+09	-1.14E+00
7.61E+09	-1.21E+00
7.62E+09	-1.30E+00
7.62E+09	-1.37E+00
7.63E+09	-1.45E+00
7.63E+09	-1.58E+00
7.64E+09	-1.74E+00
7.64E+09	-1.94E+00
7.64E+09	-2.10E+00
7.65E+09	-2.18E+00
7.65E+09	-2.21E+00
7.66E+09	-2.16E+00
7.66E+09	-2.06E+00
7.67E+09	-1.96E+00
7.67E+09	-1.85E+00
7.68E+09	-1.75E+00
7.68E+09	-1.66E+00
7.69E+09	-1.55E+00
7.69E+09	-1.48E+00
7.70E+09	-1.39E+00
7.70E+09	-1.33E+00
7.71E+09	-1.29E+00
7.71E+09	-1.33E+00
7.72E+09	-1.41E+00
7.72E+09	-1.55E+00
7.73E+09	-1.71E+00
7.73E+09	-1.82E+00
7.73E+09	-1.90E+00
7.74E+09	-1.99E+00
7.74E+09	-1.99E+00
7.75E+09	-1.96E+00
7.75E+09	-1.82E+00
7.76E+09	-1.60E+00
7.76E+09	-1.40E+00
7.77E+09	-1.22E+00
7.77E+09	-1.04E+00

Frequency[Hz]	S_{21} [dB]
7.78E+09	-7.92E-01
7.78E+09	-5.89E-01
7.79E+09	-4.38E-01
7.79E+09	-2.87E-01
7.80E+09	-1.27E-01
7.80E+09	-7.48E-03
7.81E+09	8.96E-02
7.81E+09	2.10E-01
7.82E+09	3.32E-01
7.82E+09	3.77E-01
7.82E+09	3.50E-01
7.83E+09	3.13E-01
7.83E+09	3.21E-01
7.84E+09	3.44E-01
7.84E+09	4.18E-01
7.85E+09	5.49E-01
7.85E+09	6.93E-01
7.86E+09	8.22E-01
7.86E+09	8.66E-01
7.87E+09	9.94E-01
7.87E+09	1.16E+00
7.88E+09	1.29E+00
7.88E+09	1.35E+00
7.89E+09	1.43E+00
7.89E+09	1.52E+00
7.90E+09	1.61E+00
7.90E+09	1.61E+00
7.91E+09	1.57E+00
7.91E+09	1.51E+00
7.91E+09	1.36E+00
7.92E+09	1.08E+00
7.92E+09	7.86E-01
7.93E+09	5.75E-01
7.93E+09	4.55E-01
7.94E+09	3.26E-01
7.94E+09	2.51E-01
7.95E+09	3.31E-01
7.95E+09	5.35E-01
7.96E+09	7.32E-01
7.96E+09	9.01E-01
7.97E+09	1.11E+00

Frequency[Hz]	S_{21} [dB]
7.97E+09	1.30E+00
7.98E+09	1.33E+00
7.98E+09	1.29E+00
7.99E+09	1.40E+00
7.99E+09	1.50E+00
8.00E+09	1.38E+00
8.00E+09	1.20E+00

2.10 References

Hopkinson, F. and Rittenhouse, D. , "An optical problem, proposed by Mr. Hopkinson, and solved by Mr. Rittenhouse," *Transactions of the American Philosophical Society 2*, pp.201-206, 1786.

D. Ma, X. Pan, X. Jia and M. Wang, "An FDTD Algorithm for Frequency Selective Surfaces Analysis with Excitation of High-power Electromagnetic Wave," *Photonics & Electromagnetics Research Symposium (PIERS)*, Chengdu, China, pp. 1-4, 2024.doi: 10.1109/PIERS62282.2024.10618715.

John L. Volakis. Et,al., "Hybrid Finite Element Methods for Array and FSS Analysis Using Multiresolution Elements and Fast Integral Techniques", *Electromagnetics*, vol.22, pp.297–313, 2002.DOI: 10.1080/0272634029008390 5

Antonio L. P. S. Campos , Robson H. C. Maniçoba , Lincoln M. Araújo , and Adaildo G. d'Assunção, "Analysis of Simple FSS Cascading With Dual Band Response", , *IEEE TRANSACTIONS ON MAGNETICS*, vol. 46, no. 8, AUGUST 2010

A. Yahaghi, A. Fallahi, H. Abiri, M. Shahabadi, C. Hafner and R. Vahldieck, "Analysis of Frequency Selective Surfaces on Periodic Substrates Using Entire Domain Basis Functions," *IEEE Transactions on Antennas and Propagation*, vol. 58, no. 3, pp. 876-886, March 2010.doi: 10.1109/TAP.2009.2039327.

Arup Ray, Manisha Kahar, Partha Pratim Sarkar, "Theoretical Investigation on an Array of Dual Tuned Staggered Dipole Apertures by the Method of Moment and Comparison with Experimental Results", *Microwave Review*, 2012.

Edson R. Schlosser**,** Marcos V. T. Heckler, José R. BergmannJ**,** "Entire-Domain Basis Function with Segmented Edge Condition Applied for Scattering Structures"**,***Microw. Optoelectron. Electromagn. Appl.*, vol.20, no.3,2021.https://doi.org/10.1590/2179-10742021v20i31197

K.Konno, Q Chen, “Efficient Modeling of Two-Dimensional Infinite Periodic Structures and Its Application to Method of Moments.”, *2024 International Applied Computational Electromagnetics Society Symposium (ACES-China)*,2024.https://doi.org/10.1109/ACES-China62474.2024.10699703

Chan-Sun Park et al., "Analysis of Curved Frequency selective surface for radome using characteristic basis function method", *2016 10th European Conference on Antennas and Propagation (EuCAP)*, Davos, Switzerland, pp. 1-4, 2016.doi: 10.1109/EuCAP.2016.7481386.

S. Skokic and Z. Sipus, "Moment Method Analysis of a Spherical FSS in Free Space", *2005 18th International Conference on Applied Electromagnetics and Communications*, pp. 1-4,2005.doi: 10.1109/ICECOM.2005.205025.

R.Mittra, C.H.Chan and T.Cwik, “Techniques for Analyzing Frequency Selective Surface – A Review”, *Proc. IEEE*, vol. 76, no.12, pp. 1593-1615, 1988.

Saptarsika Das, Anirban Bhattacharya, Santanu Mondal, Partha Pratim Sarkar, “Development of Method of Moment Based Programme to Analyze Cross Dipole Frequency Selective Surface and its Verification with Measured Results*”, International Journal of Innovative Technology and Exploring Engineering(IJITEE)*,vol.9 issue-8,pp.1019-1023, 2020.

CHAPTER 3

Planar and Curved FSS: Enhancement of Flatness and Roll -Off Factor of Transmission Characteristic

3.1 Introduction

The development in the field of frequency selective surface (FSS) substantiate its worthiness as polarized filter, electromagnetic compatibility shield, sub reflectors, Radome, satellite dishes etc[1-4]. Radome protects the antenna from environmental hazards without degrading the operational performance of the antenna. In this course, it is not possible to eliminate the interference of electromagnetic signals from nearby devices and it affects the operation of the antenna. The bandpass property of the FSS has been used to develop an FSS based radome which is capable to reduce the electromagnetic interferences [5]. Planar FSS when surmounted on a curved surface of a radome experiences deformation of the FSS elements, which results in the degradation of the shielding and filtering performance of the planar FSS. In satellite antenna systems FSSs are used to reflect or transmit a specific band based on the requirement of the antennas [6,7]. Similar to radome, application of planar FSS in satellite dishes degrades the filtering performance due to dimensional distortion. Hence, to improve the performance of the FSS in view to the application on curved surfaces, originates the necessity of curved FSS.

Curved frequency selective surface has been studied to fulfill the purpose of passing and stopping a band efficiently [8]. It means curved FSS is designed to attain frequency selectivity. The parameters that are put under the microscope for achieving expected frequency selectivity in case of curved FSS are roll-off, flat band and insertion loss. Sharp roll-off make it possible to obtain better frequency selectivity by filtering out undesired frequencies and suppressing frequencies outside the range of passband frequencies. Thus, enhancing the signal quality and the performances of the systems where it is implemented [9]. Low insertion loss validate the passage of substantial part of the incident electromagnetic wave through the FSS, which thereupon ensures strong signal strength at the receiving end of the system [10].Flatness in passband reveals that all the frequencies within the passband

frequency range has been transmitted without any amplification or attenuation [11]. Despite the fact that all the mentioned parameters determine the operational behavior of curved FSS, it is difficult to achieve sharp roll-off, low insertion loss and flat band simultaneously in case of curved FSS. For curved FSS, this attainments are not easy as all the three parameters, ie. Flatness, roll-off, insertion loss, are highly dependable on FSS elements, the lattice and the degree of curvature of the surface.

The simulation of curved FSS cannot be performed considering a unit cell, alike a planar FSS. In planar FSS, a unit cell is simulated with periodic conditions and is then extrapolated for infinite arrays. In case of curved FSS, for a certain incident electromagnetic field, the element currents and scattering from the edges of the curved structure diverges significantly; hence unit cell simulation is impossible and the entire structure of the curved FSS has to be simulated at a time. The time taken for the entire structure simulation of the curved FSS is longer than the unit cell simulation of a planar FSS structure. Researches has been carried out to reduce the simulation time for curved FSS [12]. MOM, FEM etc. are the mathematical techniques used for the purpose [13,14].

The summarization of all the facts state that, the designing of curved FSS is difficult and demanding, which require considerable study. The work presented in the chapter has been published in 'Microwave Journal' [15]. The chapter is dedicated to the study of roll-off, flat passband and other parameters in view of planar and curved FSS. Firstly, a dual layer aperture type planar FSS has been designed with the elements consisting of two concentric annular ring of different radii, to study its roll-off characteristics, insertion loss and passband characteristics. The same planar FSSs are then bend into semi cylindrical form, which is then studied for roll-off, insertion loss etc. The designed FSSs are finally fabricated and experimented for validation purpose.

3.2 Design of the Planar and Curved FSS

The design of planar and curved FSS have been done considering aperture type circular ring elements. Air has been considered as dielectric for both the designing. ANSOFT HFSS software has been employed to design the FSSs.

3.2.1 Design of Planar FSS

A dual layer aperture type planar FSS has been designed with periodicity of 29.7 mm in both vertical and horizontal direction. An array of two concentric annular rings of radius 5.5 mm and 10 mm, and width 3.25 mm and 4 mm respectively have been cut out from an aluminum foil for designing the first layer, the dielectric medium considered for the purpose is air having dielectric constant 1. The unit cell representation of layer 1 of the planar FSS is shown in Fig.3.1.

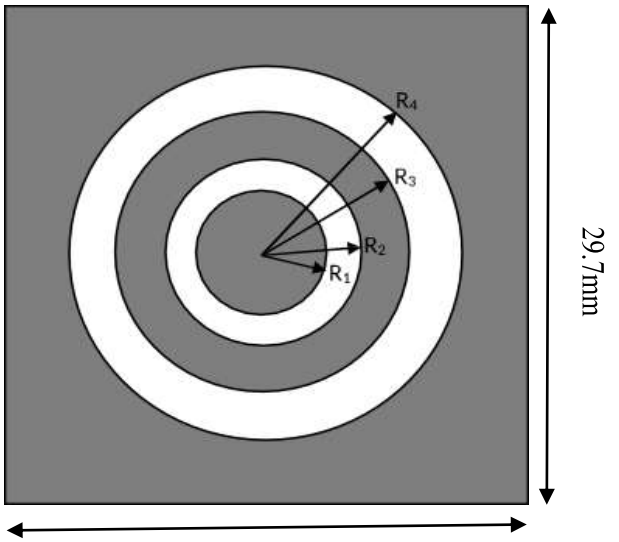

R_1= 5.5 mm, R_2= 8.7 29.7mm = 10 mm, R_4= 14 mm

Fig.3.1. Unit cell of layer-1 of the planar FSS

The second layer consists of array of concentric annular rings cut out from aluminum foil of radius 6 mm and 10 mm, of width 2.25 mm and 4 mm respectively. Air is also considered as dielectric for this layer. The unit cell representation of layer 2 of the planar FSS is shown in Fig. 3.2.The layers of the planar composite FSS are shown in Fig.3.3 and Fig.3.4. 7.6 mm has been optimized as the air gap between the two layers.The entire composite structure has been simulated by HFSS software. The layers of fabricated planar FSS are shown in Fig.3.5. The fabrication has been done by laser cutting machine shown in Fig.3.6.

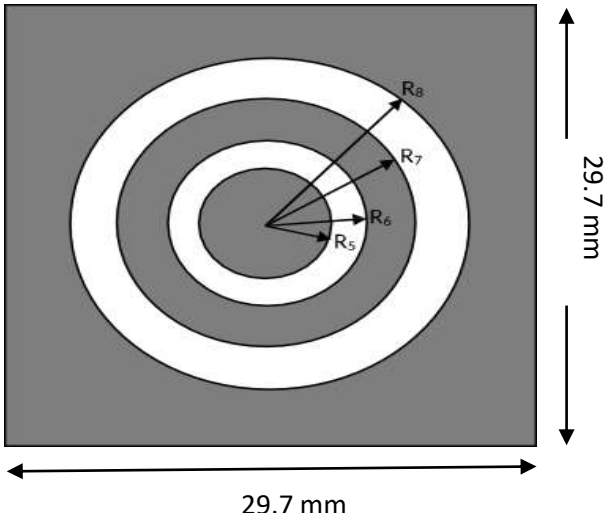

R5=6mm, R6=8.25mm, R7=10mm, R_8= 14 mm

Fig.3.2. Unit cell of layer-2 of the planar FSS

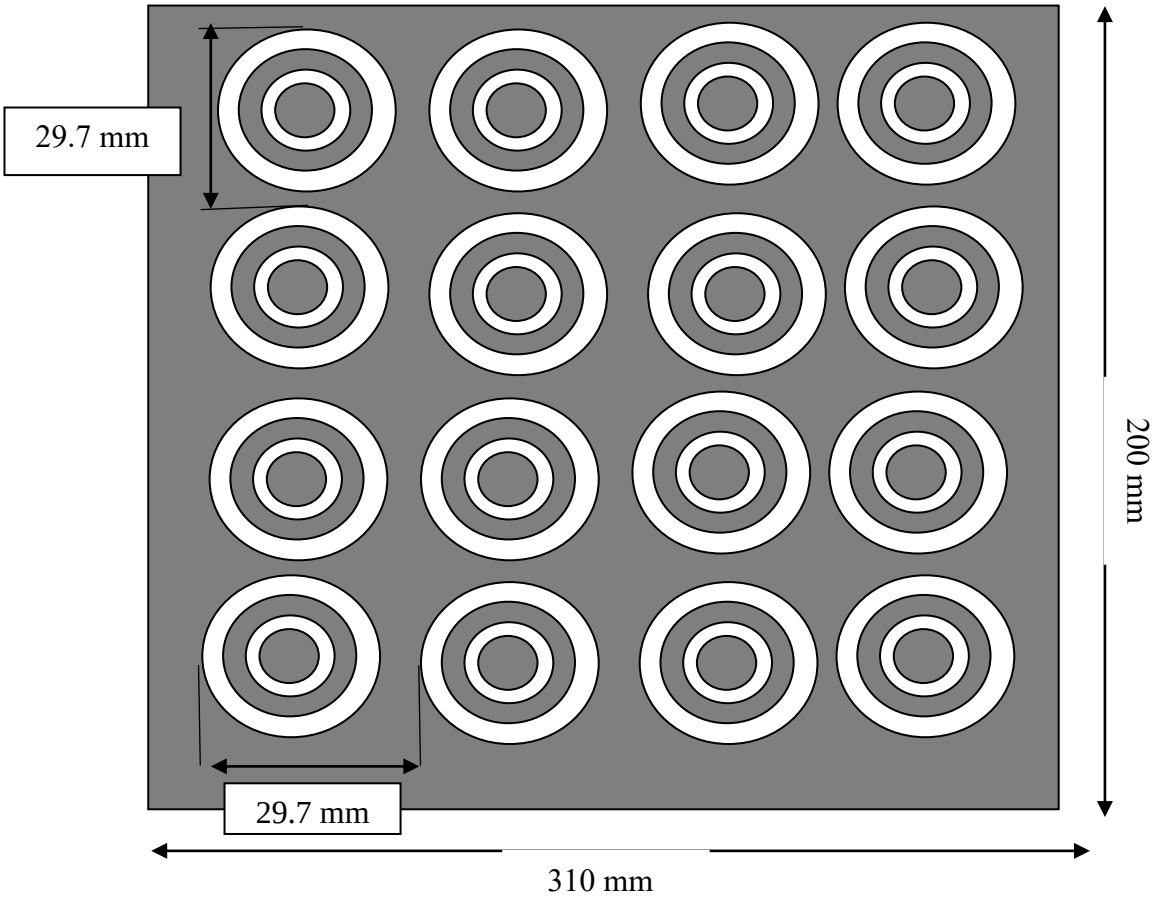

Fig.3.3. Layer-1 of Planar FSS

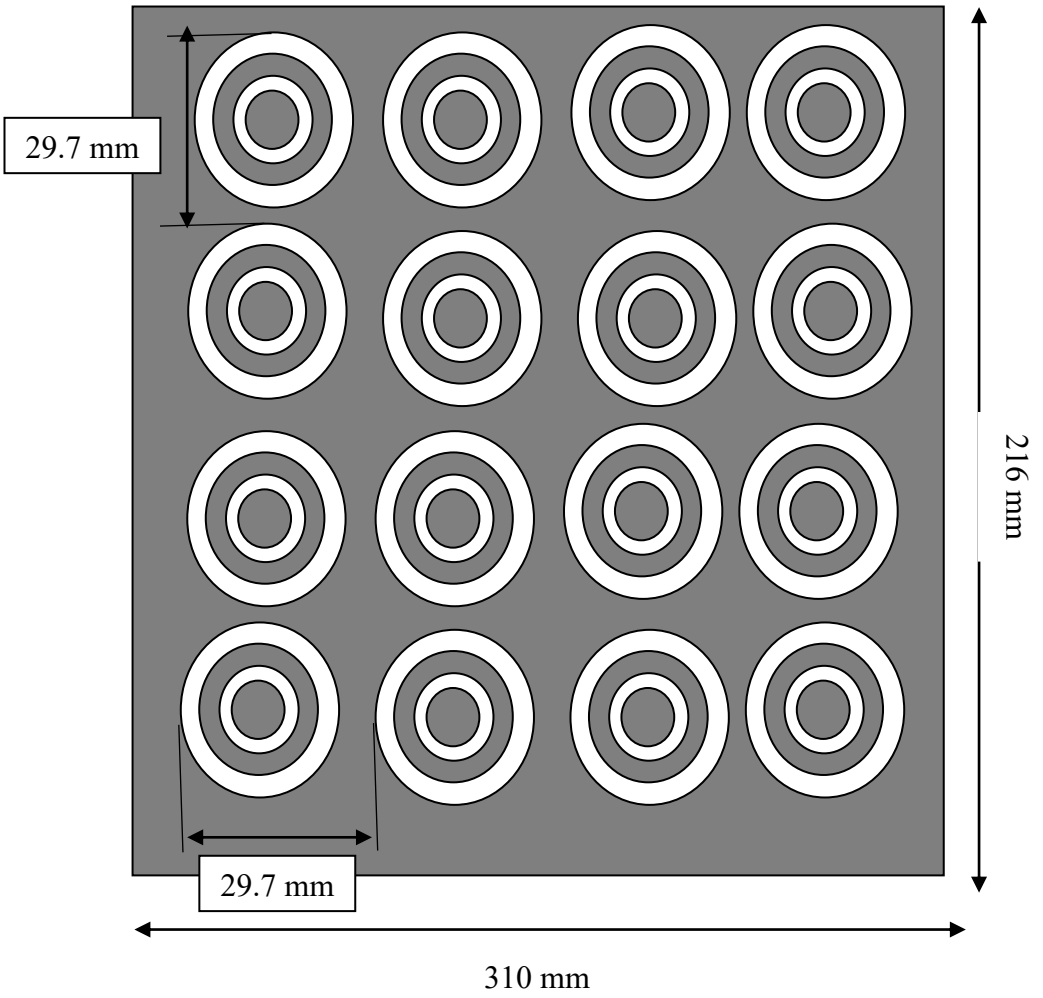

Fig.3.4. Layer-2 of Planar FSS

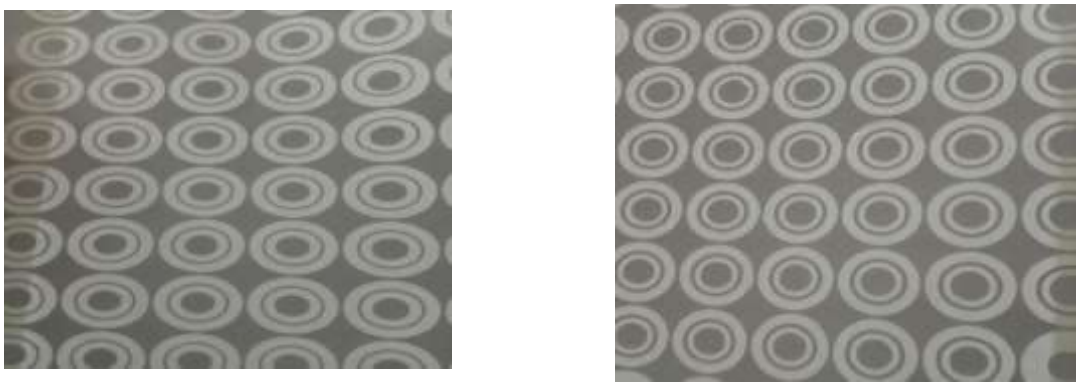

a) Layer-1 b) Layer-2

Fig.3.5. Fabricated Frequency Selective Surfaces

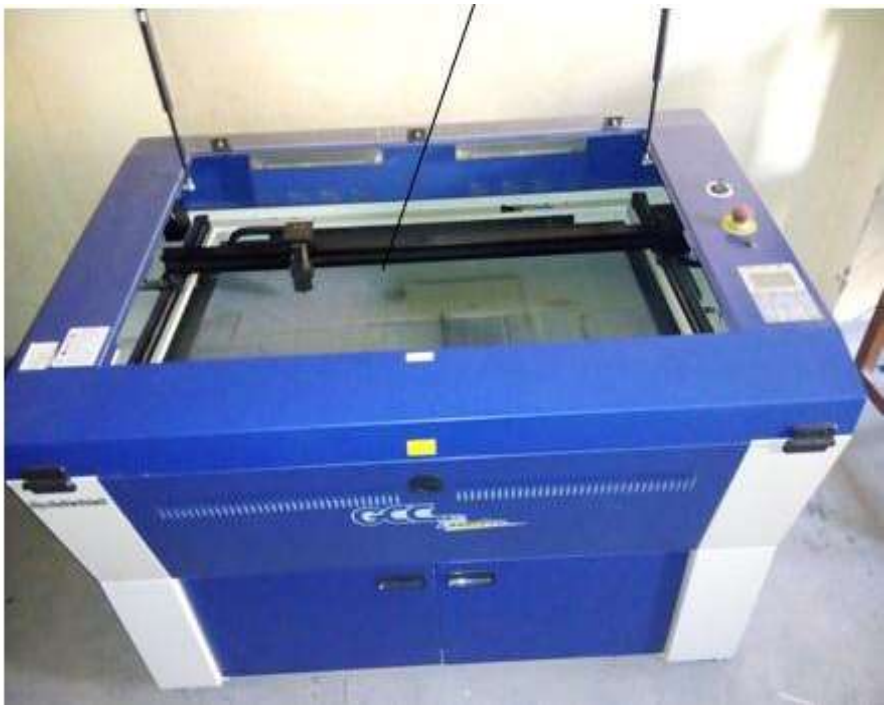

Fig.3.6. Laser cutting machine

The measurement of the fabricated planar FSS has been done by standard microwave test bench. FSS has been placed between a transmitting and a receiving antenna for the purpose of measurement. Vector network analyzer (VNA) is the microwave source that is feeding microwave signal to the transmitting antenna. The power received in the receiving antenna is detected by the power sensor and power meter of the VNA. Fig.3.7 depicts the setup of the experiment performed with the planar FSS.

Fig.3.7. Measurement set up of planar FSS

3.2.2 Design of Curved FSS

The dimension of the elements of layer 1 and layer 2, considered to design the dual layer aperture type curved FSS, is kept same to that of the dimension of elements of layer 1 and layer 2 respectively for dual layer aperture type planar FSS mentioned in section 3.2.1. The periodicity of the structure in both the plane is 29.7 mm for all the two layers. Semi cylindrical form has been considered to study the dual layer aperture type curved FSS. The radius of layer 1 is kept 100 mm. An air gap of 7.6 mm has been maintained between the two layers of the curved FSS taking in view the optimized air gap between the layers of planar FSS. So, the radius of curvature of layer 2 is set to 107.6 mm. The length of the semi cylinder has to be limited to 310 mm considering the fact that high computational resources should be taken into account. Take account of the fact that unit cell simulation is not possible for curved FSS, the entire composite structure of the curved FSS has been simulated by CAD FEKO simulation software. The entire composite structure of curved FSS from different perspective has been shown in Fig. 3.8.

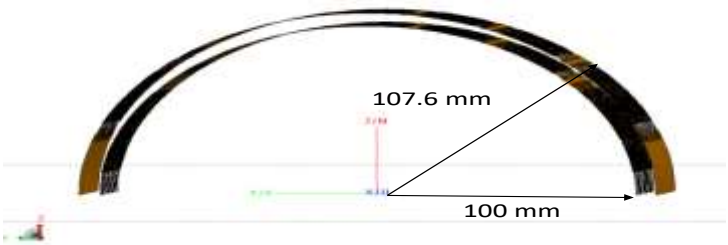

a) Front view of dual layer curved FSS

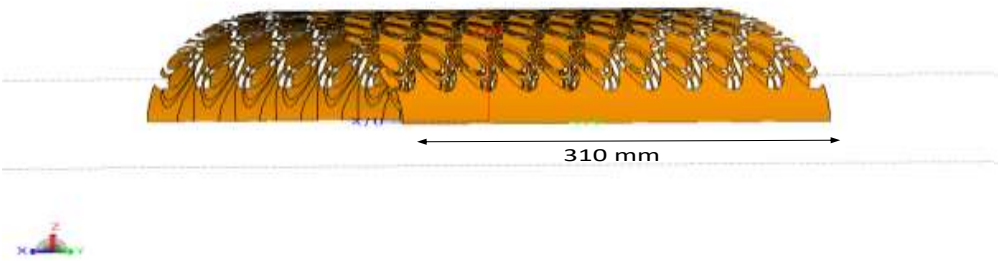

b) Side view of dual layer curved FSS

Fig.3.8. Semi cylindrical FSS structure from different perspectives

The fabricated FSSs presented in Fig.3.5 are bend into semi cylinders to perform the experiment using standard microwave test bench. Polythene foam is used as stand to maintain the stability of the composite curved structure and plastic pin has been used to fix the FSSs. Air whose dielectric constant is 1 has been introduced as dielectric. The experimental set up is shown in Fig.3.9.

Fig.3.9. Measurement set up of dual layer curved FSS

3.3 Results & Discussion

3.3.1 Study of Planar FSS

The air gap between the two layers of the planar FSS has been optimized at first. Table 3.1 depicts the variation in insertion loss and roll-off with increasing air gap between the two layers.

Table 3.1. Parametric study of planar FSS by varying the air gap between the two layers

Air gap between two FSS layers [mm]	Left roll-off [dB/GHz]	Insertion loss [dB]	Right roll-off [dB/GHz]
6	39	0.7	16.67
7.6	45	0.3	73.33
8	49.02	0.9	35.05

The study reported in Table 3.1 depicts that, when the air gap between the two layers have been kept 7.6 mm the insertion loss is minimum ie.0.3 dB. Accordingly, the experimental set up has been done keeping the air gap 7.6 mm between the two layers of planar FSS. The transmission coefficient vs frequency curve of the dual layer planar FSS is shown in Fig.3.10.

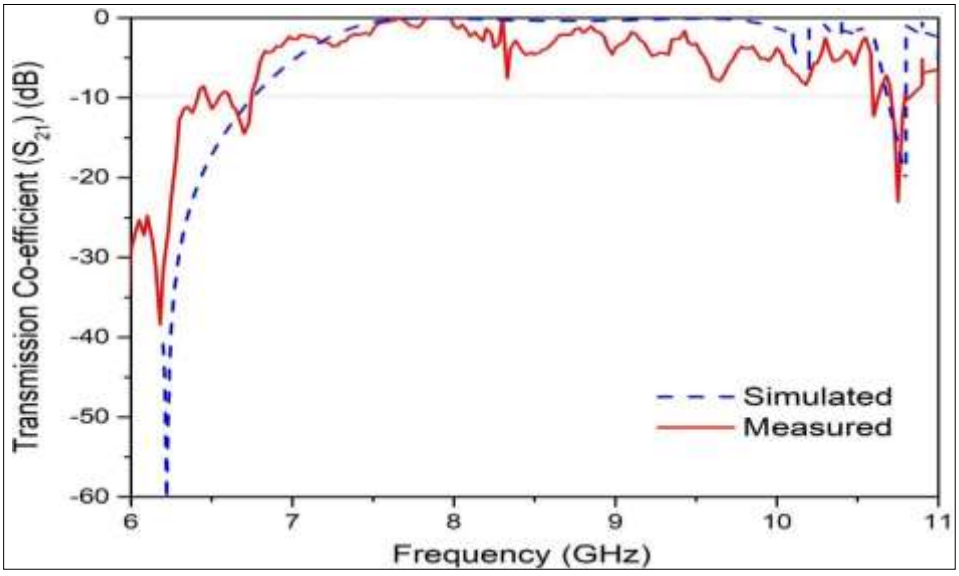

Fig.3.10. Transmission coefficient vs frequency plot of composite planar FSS

The curve shown in Fig.3.10. depicts a good agreement between the simulated and experimentally obtained results of the composite planar structure. In the frequency range of 6.7 GHz to 10.7 GHz the composite planar FSS achieved a good passband characteristics. A wide band of 4 GHz has been obtained with low insertion loss with respect to -10dB. Thus, achieving a percentage bandwidth of 45.96%. The left roll-off attain by the dual layer planar FSS is 45 dB/ GHz and the attainment of right roll-off is 73.33 dB/ GHz. The study of the dual layer aperture type planar FSS presented here shows sharp roll-off, low insertion loss and good passband characteristics.

A comparative study of the designed dual layer aperture type planar FSS with the contemporary work has been executed for the elaborate analysis of the study. An aperture type planar FSS with Archimedian spiral element has been reported for good roll-off [16]. An aperture type planar FSS has been documented with wideband whereas compromising the roll-off [17]. Multiband is achieved with low roll-off for aperture type planar FSS [18]. A steep roll-off and good passband has been achieved by a polarization insensitive aperture type planar FSS [19]. The comparison of the presented work with the documented works is represented in tabular form in Table 3.2.

Table 3.2. Comparison of contemporary works with the presented work for planar FSS

Reference No. Of FSS	-10 dB bandwidth [GHz]	Left roll-off [dB/ GHz]	Right roll-off [dB/ GHz]
16	1.9	9.05	14.20
17	3	4.8	43
18	2.7	7.33	30
19	-	24.54	17.50
Presented work	4	45	73.33

The comparative study establish the fact that the dual layer planar FSS designed and presented in this chapter achieved better -10 dB bandwidth, ie. of 4 GHz, than the presented contemporary works. The sharpest roll-off documented in Table 3.2 among the contemporary works is 24.54 dB/ GHz. The presented work attain much better

left roll-off of 45 dB/ GHz. The sharpest right roll-off documented in contemporary works is 43 dB/ GHz and the presented work achieved 73.33 dB/ GHz right roll-off, which is far better than all the contemporary cases referred here. The beauty of the designed dual layer planar FSS presented here is, it attains low insertion loss of 0.3 dB with wide passband of 4 GHz, without compromising the roll-off parameter in both the edges. The presented planar composite FSS can efficiently transmit the electromagnetic signal and reduce the electromagnetic interference while transition from passband to stopband as well.

The designed dual layer planar FSS efficiently attains low insertion loss, sharp roll-off at both the edges and flat band very easily. All these parameters cannot be attained easily for a curved structure as for each element surface current and scattering from the edges diverges significantly.

3.3.2 Study of Curved FSS

The experimental result of curved composite FSS has been depicted in Fig.3.11.

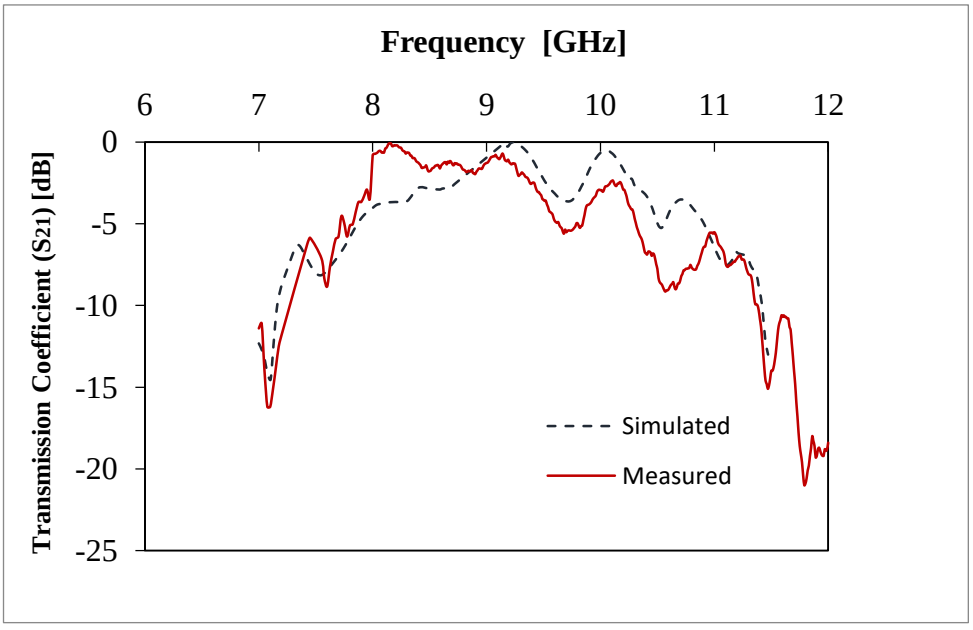

Fig.3.11. Transmission coefficient vs frequency plot of composite curved FSS

The aperture type cascaded curved FSS manifests fine agreement between the simulated and experimentally obtained results. The aperture type composite curved structure attains a wide passband of 4.2 GHz, ie. 45.16% fractional bandwidth has

been achieved by the composite curved structure for an air gap of 7.6 mm between the two layers. The right edge of the curve shown in Fig.3.11 attains a roll-off of 16.66 dB/ GHz and the left edge attains a roll-off of 32.09 dB/ GHz. The designed and presented curved FSS exhibit sharp roll-off characteristics at both the edges with a wide passband and low insertion loss. The study of the curved composite FSS establish its proficiency in frequency selectivity and electromagnetic interference and noise eliminator. As a consequence, the presented dual layer curved FSS demonstrate its competency with the conformal structures like radome, sub reflectors etc.

The dual layer curved FSS presented in this section has been compared with the similar works by the other researchers for embellishing its efficacy. In the frequency range of 8 GHz to 10 GHz, the properties of aperture type curved FSS has been investigated with tripole shaped elements [20]. A poor roll-off has been demonstrated by a spherical dome shaped FSS whereas the conformal structure achieved a wideband [21]. A single layer hemispherical FSS has been reported with roughly equal roll-off in both the edges of the transmission curve [22]. The comparison of the designed dual layer curved FSS with its contemporary work has been represented in tabular form in Table 3.3.

Table 3.3. Comparison of contemporary works with the presented work for curved FSS

Parameter	Ref. [20]	Ref. [21]	Ref. [22]	Presented FSS
% Bandwidth	32.55	23.74	-	45.16
Left roll-off [dB/ GHz]	8.5	4.37	8.98	16.66
Right roll-off [dB/ GHz]	10	2.5	9.93	32.09

From the comparison table it can be stated that the percentage bandwidth achieved by the designed dual layer curved FSS is better than all other documented works. The left roll-off attained by the designed conformal FSS is considerably better than the same attained by all other FSSs. Significantly better right roll-off has been exhibited by the designed curved composite FSS in compare to the attainments of the

contemporary works. The comparative study featured the importance of the designed dual layer curved FSS as passband conformal spatial filter which is capable to reduce the interference of electromagnetic waves and from nearby systems, and ensures accurate recipient of the transmitted signal competently.

3.4 Conclusion

A dual layer aperture type planar FSS and a dual layer semi cylindrical aperture type curved FSS have been studied in this chapter which exhibit sharp roll-off, flat pass band and low insertion loss. The sharpest roll-off achieved by the planar composite FSS is 73.33 dB/ GHz. The fractional bandwidth attained by the structure is 45.96%. It exhibits a low insertion loss of 0.3 dB. The simulated result agreed satisfactorily with the experimental result. All the parameters studied through the chapter reflects better performance than the existing works. The highest roll-off achieved by the semi cylindrical curved composite structure is 32 dB/ GHz. It exhibits 45.16% fractional bandwidth with low insertion loss. The simulated and experimental results are in good agreement. The dual layer semi cylindrical curved FSS also manifest superior behavioral performance in compare to its contemporary works. It is notable that the bending of the planar FSS into semi cylindrical form exhibits insignificant fractional bandwidth alteration. This novel feature puts forward the designed FSSs from the present state of art. The designed and presented planar FSS and the curved FSS have proved their worthiness as passband spatial filter in X and Ku band, which can efficiently reduce electromagnetic interference and noise without deteriorating the signal strength. The curved FSS fulfills the purpose of transmission of frequency in the range of 7.5 GHz to 11 GHz, where planar FSS cannot be pertained, and is compatible with any conformal structure. The presented works set forth applications in radome system, satellite communication systems, wireless devices and electronic warfare systems.

3.5 Experimental datasheet of the fabricated planar and curved FSS

Table 3.4 Datasheet of planar FSS

Frequency [Hz]	S21[dB]
5.00E+09	-2.22E+01
5.03E+09	-2.55E+01
5.05E+09	-2.75E+01
5.08E+09	-3.52E+01
5.10E+09	-3.89E+01
5.13E+09	-3.52E+01
5.15E+09	-3.58E+01
5.18E+09	-4.09E+01
5.20E+09	-2.89E+01
5.23E+09	-2.67E+01
5.25E+09	-2.53E+01
5.28E+09	-2.72E+01
5.30E+09	-2.48E+01
5.33E+09	-2.76E+01
5.35E+09	-3.06E+01
5.38E+09	-3.84E+01
5.40E+09	-3.16E+01
5.43E+09	-2.67E+01
5.45E+09	-2.27E+01
5.48E+09	-1.72E+01
5.50E+09	-1.27E+01
5.53E+09	-1.14E+01
5.55E+09	-1.11E+01
5.58E+09	-1.19E+01
5.60E+09	-1.09E+01
5.63E+09	-8.83E+00
5.65E+09	-8.55E+00
5.68E+09	-1.03E+01
5.70E+09	-1.14E+01
5.73E+09	-1.06E+01
5.75E+09	-9.76E+00
5.78E+09	-9.22E+00
5.80E+09	-9.40E+00
5.83E+09	-1.11E+01
5.85E+09	-1.15E+01
5.88E+09	-1.32E+01
5.90E+09	-1.45E+01

Frequency [Hz]	S21[dB]
5.93E+09	-1.32E+01
5.95E+09	-9.21E+00
5.98E+09	-7.53E+00
6.00E+09	-5.42E+00
6.03E+09	-4.13E+00
6.05E+09	-4.37E+00
6.08E+09	-4.15E+00
6.10E+09	-3.56E+00
6.13E+09	-3.56E+00
6.15E+09	-3.13E+00
6.18E+09	-2.31E+00
6.20E+09	-2.66E+00
6.23E+09	-2.66E+00
6.25E+09	-2.16E+00
6.28E+09	-2.21E+00
6.30E+09	-2.36E+00
6.33E+09	-2.34E+00
6.35E+09	-2.57E+00
6.38E+09	-3.09E+00
6.40E+09	-2.95E+00
6.43E+09	-3.20E+00
6.45E+09	-3.55E+00
6.48E+09	-3.47E+00
6.50E+09	-2.98E+00
6.53E+09	-2.94E+00
6.55E+09	-2.37E+00
6.58E+09	-2.03E+00
6.60E+09	-2.11E+00
6.63E+09	-2.05E+00
6.65E+09	-1.86E+00
6.68E+09	-2.10E+00
6.70E+09	-1.39E+00
6.73E+09	-6.65E-01
6.75E+09	-6.29E-01
6.78E+09	-4.47E-01
6.80E+09	-4.72E-01
6.83E+09	-2.81E-01
6.85E+09	-4.69E-02
6.88E+09	1.76E-01
6.90E+09	-4.70E-01
6.93E+09	-9.64E-01

Frequency [Hz]	S21[dB]
6.95E+09	-9.94E-01
6.98E+09	-1.17E+00
7.00E+09	-7.51E-01
7.03E+09	-1.32E-02
7.05E+09	3.12E-01
7.08E+09	6.99E-01
7.10E+09	8.27E-01
7.13E+09	3.13E-01
7.15E+09	1.37E-01
7.18E+09	3.12E-02
7.20E+09	-9.66E-01
7.23E+09	-1.31E+00
7.25E+09	-8.46E-01
7.28E+09	-1.62E+00
7.30E+09	-2.31E+00
7.33E+09	-1.79E+00
7.35E+09	-2.35E+00
7.38E+09	-2.91E+00
7.40E+09	-1.33E+00
7.43E+09	-1.93E+00
7.45E+09	-3.73E+00
7.48E+09	-3.14E+00
7.50E+09	-2.79E-02
7.53E+09	-7.59E+00
7.55E+09	-3.93E+00
7.58E+09	-2.79E+00
7.60E+09	-3.42E+00
7.63E+09	-4.36E+00
7.65E+09	-4.61E+00
7.68E+09	-4.33E+00
7.70E+09	-4.58E+00
7.73E+09	-4.35E+00
7.75E+09	-4.05E+00
7.78E+09	-3.81E+00
7.80E+09	-3.37E+00
7.83E+09	-2.77E+00
7.85E+09	-2.19E+00
7.88E+09	-2.07E+00
7.90E+09	-2.15E+00
7.93E+09	-2.03E+00
7.95E+09	-1.38E+00

Frequency [Hz]	S21[dB]
7.98E+09	-1.27E+00
8.00E+09	-1.86E+00
8.03E+09	-1.44E+00
8.05E+09	-1.06E+00
8.08E+09	-1.74E+00
8.10E+09	-1.78E+00
8.13E+09	-2.34E+00
8.15E+09	-3.62E+00
8.18E+09	-4.59E+00
8.20E+09	-3.72E+00
8.23E+09	-3.29E+00
8.25E+09	-3.16E+00
8.28E+09	-2.51E+00
8.30E+09	-1.76E+00
8.33E+09	-2.07E+00
8.35E+09	-2.71E+00
8.38E+09	-3.10E+00
8.40E+09	-3.89E+00
8.43E+09	-4.79E+00
8.45E+09	-4.64E+00
8.48E+09	-4.34E+00
8.50E+09	-4.42E+00
8.53E+09	-4.58E+00
8.55E+09	-2.72E+00
8.58E+09	-2.63E+00
8.60E+09	-2.59E+00
8.63E+09	-1.64E+00
8.65E+09	-3.10E+00
8.68E+09	-3.39E+00
8.70E+09	-3.25E+00
8.73E+09	-4.42E+00
8.75E+09	-4.90E+00
8.78E+09	-6.05E+00
8.80E+09	-7.48E+00
8.83E+09	-7.76E+00
8.85E+09	-7.87E+00
8.88E+09	-6.80E+00
8.90E+09	-5.88E+00
8.93E+09	-5.14E+00
8.95E+09	-4.31E+00
8.98E+09	-3.61E+00

Frequency [Hz]	S21[dB]
9.00E+09	-3.78E+00
9.03E+09	-3.85E+00
9.05E+09	-3.56E+00
9.08E+09	-4.56E+00
9.10E+09	-5.15E+00
9.13E+09	-5.07E+00
9.15E+09	-5.36E+00
9.18E+09	-4.66E+00
9.20E+09	-3.79E+00
9.23E+09	-4.49E+00
9.25E+09	-5.86E+00
9.28E+09	-6.12E+00
9.30E+09	-6.79E+00
9.33E+09	-7.21E+00
9.35E+09	-7.87E+00
9.38E+09	-8.36E+00
9.40E+09	-7.52E+00
9.43E+09	-5.73E+00
9.45E+09	-5.68E+00
9.48E+09	-4.23E+00
9.50E+09	-2.52E+00
9.53E+09	-4.46E+00
9.55E+09	-5.49E+00
9.58E+09	-5.23E+00
9.60E+09	-4.98E+00
9.63E+09	-4.10E+00
9.65E+09	-4.42E+00
9.68E+09	-5.88E+00
9.70E+09	-4.66E+00
9.73E+09	-2.87E+00
9.75E+09	-2.46E+00
9.78E+09	-4.38E+00
9.80E+09	-1.23E+01
9.83E+09	-9.95E+00
9.85E+09	-8.47E+00
9.88E+09	-7.22E+00
9.90E+09	-8.58E+00
9.93E+09	-1.38E+01
9.95E+09	-2.30E+01
9.98E+09	-1.21E+01
1.00E+10	-9.00E+00

Frequency [Hz]	S21[dB]
1.00E+10	-1.04E+01
1.01E+10	-8.42E+00
1.01E+10	-5.17E+00
1.01E+10	-6.48E+00
1.01E+10	-6.90E+00
1.02E+10	-6.47E+00
1.02E+10	-8.61E+00
1.02E+10	-9.69E+00
1.02E+10	-1.08E+01
1.03E+10	-1.15E+01
1.03E+10	-1.16E+01
1.03E+10	-1.35E+01
1.03E+10	-1.48E+01
1.04E+10	-1.54E+01
1.04E+10	-1.35E+01
1.04E+10	-1.32E+01
1.04E+10	-1.19E+01
1.05E+10	-1.13E+01
1.05E+10	-1.21E+01
1.05E+10	-1.34E+01
1.05E+10	-1.25E+01
1.06E+10	-1.11E+01
1.06E+10	-1.04E+01
1.06E+10	-1.09E+01
1.06E+10	-1.25E+01
1.07E+10	-1.34E+01
1.07E+10	-1.32E+01
1.07E+10	-1.43E+01
1.07E+10	-1.28E+01
1.08E+10	-1.08E+01
1.08E+10	-1.12E+01
1.08E+10	-1.21E+01
1.08E+10	-1.12E+01
1.09E+10	-1.17E+01
1.09E+10	-1.27E+01
1.09E+10	-1.41E+01
1.09E+10	-1.74E+01
1.10E+10	-1.85E+01
1.10E+10	-1.66E+01
1.10E+10	-1.63E+01
1.10E+10	-1.55E+01

Frequency [Hz]	S21[dB]
1.11E+10	-1.34E+01
1.11E+10	-1.22E+01
1.11E+10	-1.29E+01
1.11E+10	-1.46E+01
1.12E+10	-1.51E+01
1.12E+10	-1.50E+01
1.12E+10	-1.51E+01
1.12E+10	-1.45E+01
1.13E+10	-1.49E+01
1.13E+10	-1.44E+01
1.13E+10	-1.28E+01
1.13E+10	-1.19E+01
1.14E+10	-1.23E+01
1.14E+10	-1.38E+01
1.14E+10	-1.63E+01
1.14E+10	-1.78E+01
1.15E+10	-1.97E+01
1.15E+10	-2.10E+01
1.15E+10	-2.06E+01
1.15E+10	-2.09E+01
1.16E+10	-2.09E+01
1.16E+10	-1.70E+01
1.16E+10	-1.54E+01
1.16E+10	-1.58E+01
1.17E+10	-1.64E+01
1.17E+10	-1.62E+01
1.17E+10	-1.54E+01
1.17E+10	-1.50E+01
1.18E+10	-1.51E+01
1.18E+10	-1.68E+01
1.18E+10	-1.81E+01
1.18E+10	-1.86E+01
1.19E+10	-1.70E+01
1.19E+10	-1.65E+01
1.19E+10	-1.42E+01
1.19E+10	-1.38E+01
1.20E+10	-1.45E+01
1.20E+10	-1.31E+01
1.20E+10	-1.44E+01
1.20E+10	-1.69E+01
1.21E+10	-2.11E+01

Frequency [Hz]	S21[dB]
1.21E+10	-2.29E+01
1.21E+10	-2.12E+01
1.21E+10	-1.93E+01
1.22E+10	-1.80E+01
1.22E+10	-1.85E+01
1.22E+10	-1.93E+01
1.22E+10	-1.86E+01
1.23E+10	-1.88E+01
1.23E+10	-1.85E+01
1.23E+10	-1.91E+01
1.23E+10	-1.78E+01
1.24E+10	-1.72E+01
1.24E+10	-1.76E+01
1.24E+10	-1.92E+01
1.24E+10	-2.17E+01
1.25E+10	-2.44E+01
1.25E+10	-2.47E+01
1.25E+10	-2.35E+01
1.25E+10	-2.45E+01
1.26E+10	-3.22E+01
1.26E+10	-2.57E+01
1.26E+10	-2.45E+01
1.26E+10	-2.41E+01
1.27E+10	-2.10E+01
1.27E+10	-1.89E+01
1.27E+10	-1.73E+01
1.27E+10	-1.73E+01
1.28E+10	-1.68E+01
1.28E+10	-1.63E+01
1.28E+10	-1.79E+01
1.28E+10	-1.83E+01
1.29E+10	-1.91E+01
1.29E+10	-2.19E+01
1.29E+10	-2.26E+01
1.29E+10	-2.51E+01
1.30E+10	-2.61E+01
1.30E+10	-2.51E+01
1.30E+10	-2.41E+01
1.30E+10	-2.25E+01
1.31E+10	-2.10E+01
1.31E+10	-2.25E+01

Frequency [Hz]	S21[dB]
1.31E+10	-2.53E+01
1.31E+10	-2.57E+01
1.32E+10	-2.75E+01
1.32E+10	-2.45E+01
1.32E+10	-1.99E+01
1.32E+10	-1.99E+01
1.33E+10	-1.97E+01

Table 3.5 Datasheet of curved FSS

Frequency [GHz]	S_{21} [dB]
7	-11.4
7.025	-11.1
7.05	-14
7.075	-16.2
7.1	-16.2
7.125	-15.1
7.15	-13.8
7.175	-12.5
7.2	-11.8
7.425	-6.25
7.45	-5.85
7.55	-7.11
7.575	-8.34
7.6	-8.84
7.625	-7.62
7.65	-6.71
7.675	-5.92
7.7	-5.78
7.725	-4.53
7.75	-4.96
7.775	-5.78
7.8	-5.1
7.825	-5.02
7.85	-4.3
7.875	-3.67
7.9	-3.66
7.925	-3.29
7.95	-2.9
7.975	-3.47

Frequency [GHz]	S_{21} [dB]
8	-0.801
8.01	-0.714
8.02	-0.717
8.03	-0.685
8.04	-0.645
8.05	-0.571
8.06	-0.528
8.07	-0.549
8.08	-0.642
8.09	-0.626
8.1	-0.633
8.11	-0.395
8.12	-0.352
8.13	-0.227
8.14	-0.0948
8.15	-0.0693
8.16	-0.0745
8.17	-0.237
8.18	-0.24
8.19	-0.184
8.2	-0.205
8.21	-0.191
8.22	-0.219
8.23	-0.307
8.24	-0.325
8.25	-0.351
8.26	-0.485
8.27	-0.541
8.28	-0.573
8.29	-0.699
8.3	-0.633
8.31	-0.64
8.32	-0.663
8.33	-0.808
8.34	-0.828
8.35	-0.969
8.36	-0.969
8.37	-1
8.38	-1.14
8.39	-1.21
8.4	-1.25

Frequency [GHz]	S_{21} [dB]
8.41	-1.33
8.42	-1.41
8.43	-1.57
8.44	-1.57
8.45	-1.54
8.46	-1.52
8.47	-1.42
8.48	-1.65
8.49	-1.79
8.5	-1.77
8.51	-1.74
8.52	-1.62
8.53	-1.58
8.54	-1.53
8.55	-1.44
8.56	-1.43
8.57	-1.39
8.58	-1.45
8.59	-1.61
8.6	-1.45
8.61	-1.36
8.62	-1.29
8.63	-1.23
8.64	-1.23
8.65	-1.36
8.66	-1.19
8.67	-1.27
8.68	-1.15
8.69	-1.23
8.7	-1.35
8.71	-1.42
8.72	-1.28
8.73	-1.34
8.74	-1.3
8.75	-1.38
8.76	-1.38
8.77	-1.42
8.78	-1.53
8.79	-1.66
8.8	-1.69
8.81	-1.73

Frequency [GHz]	S_{21} [dB]
8.82	-1.82
8.83	-1.82
8.84	-1.75
8.85	-1.77
8.86	-1.78
8.87	-1.71
8.88	-1.88
8.89	-1.91
8.9	-1.96
8.91	-1.82
8.92	-1.73
8.93	-1.62
8.94	-1.61
8.95	-1.63
8.96	-1.63
8.97	-1.48
8.98	-1.36
8.99	-1.31
9	-1.27
9.01	-1.25
9.02	-1.15
9.03	-1.03
9.04	-0.915
9.05	-0.902
9.06	-0.858
9.07	-0.864
9.08	-0.773
9.09	-0.915
9.1	-0.967
9.11	-1.04
9.12	-0.958
9.13	-0.819
9.14	-0.691
9.15	-0.843
9.16	-1.08
9.17	-1.14
9.18	-1.17
9.19	-1.07
9.2	-1.23
9.21	-1.31
9.22	-1.36

Frequency [GHz]	S_{21} [dB]
9.23	-1.29
9.24	-1.31
9.25	-1.32
9.26	-1.57
9.27	-1.84
9.28	-2.06
9.29	-2.01
9.3	-1.95
9.31	-1.85
9.32	-1.92
9.33	-1.99
9.34	-2.11
9.35	-2.15
9.36	-2.19
9.37	-2.32
9.38	-2.49
9.39	-2.56
9.4	-2.5
9.41	-2.47
9.42	-2.51
9.43	-2.75
9.44	-2.94
9.45	-3.05
9.46	-3.06
9.47	-3.18
9.48	-3.25
9.49	-3.48
9.5	-3.52
9.51	-3.6
9.52	-3.58
9.53	-3.81
9.54	-3.97
9.55	-4.22
9.56	-4.28
9.57	-4.34
9.58	-4.43
9.59	-4.68
9.6	-4.83
9.61	-4.9
9.62	-4.94
9.63	-4.89

Frequency [GHz]	S_{21} [dB]
9.64	-5.09
9.65	-5.2
9.66	-5.27
9.67	-5.48
9.68	-5.6
9.69	-5.35
9.7	-5.51
9.71	-5.44
9.72	-5.4
9.73	-5.41
9.74	-5.42
9.75	-5.39
9.76	-5.33
9.77	-5.24
9.78	-5.15
9.79	-4.96
9.8	-4.97
9.81	-5.13
9.82	-5.25
9.83	-5.14
9.84	-5.1
9.85	-4.77
9.86	-4.46
9.87	-4.09
9.88	-3.88
9.89	-3.84
9.9	-3.81
9.91	-3.75
9.92	-3.66
9.93	-3.52
9.94	-3.42
9.95	-3.35
9.96	-3.26
9.97	-3.04
9.98	-2.94
9.99	-2.91
10	-2.94
10.01	-2.94
10.02	-3.04
10.03	-2.94
10.04	-2.73

Frequency [GHz]	S_{21} [dB]
10.05	-2.7
10.06	-2.68
10.07	-2.62
10.08	-2.55
10.09	-2.43
10.1	-2.37
10.11	-2.35
10.12	-2.52
10.13	-2.65
10.14	-2.68
10.15	-2.54
10.16	-2.54
10.17	-2.44
10.18	-2.5
10.19	-2.69
10.2	-2.9
10.21	-2.92
10.22	-3.11
10.23	-3.33
10.24	-3.66
10.25	-3.86
10.26	-3.97
10.27	-4.1
10.28	-4.12
10.29	-4.32
10.3	-4.66
10.31	-4.93
10.32	-5.21
10.33	-5.41
10.34	-5.63
10.35	-5.78
10.36	-5.9
10.37	-6.12
10.38	-6.43
10.39	-6.74
10.4	-6.81
10.41	-6.88
10.42	-6.7
10.43	-6.7
10.44	-6.76
10.45	-6.96

Frequency [GHz]	S_{21} [dB]
10.46	-6.81
10.47	-6.87
10.48	-7.13
10.49	-7.48
10.5	-7.76
10.51	-8.32
10.52	-8.56
10.53	-8.65
10.54	-8.73
10.55	-8.89
10.56	-9.05
10.57	-9.15
10.58	-9.07
10.59	-9.07
10.6	-8.99
10.61	-8.85
10.62	-8.73
10.63	-8.67
10.64	-8.57
10.65	-8.86
10.66	-9.01
10.67	-8.89
10.68	-8.66
10.69	-8.65
10.7	-8.48
10.71	-8.2
10.72	-8.07
10.73	-7.85
10.74	-7.83
10.75	-7.75
10.76	-7.75
10.77	-7.72
10.78	-7.7
10.79	-7.51
10.8	-7.66
10.81	-7.75
10.82	-7.8
10.83	-7.81
10.84	-7.78
10.85	-7.58
10.86	-7.45

Frequency [GHz]	S_{21} [dB]
10.87	-7.25
10.88	-6.99
10.89	-6.76
10.9	-6.52
10.91	-6.4
10.92	-6.39
10.93	-6.09
10.94	-5.87
10.95	-5.68
10.96	-5.54
10.97	-5.56
10.98	-5.53
10.99	-5.6
11	-5.51
11.01	-5.62
11.02	-5.8
11.03	-6.11
11.04	-6.28
11.05	-6.36
11.06	-6.45
11.07	-6.57
11.08	-6.7
11.09	-6.99
11.1	-7.44
11.11	-7.6
11.12	-7.63
11.13	-7.53
11.14	-7.53
11.15	-7.47
11.16	-7.4
11.17	-7.32
11.18	-7.32
11.19	-7.2
11.2	-7.12
11.21	-7
11.22	-6.98
11.23	-6.94
11.24	-7.18
11.25	-7.18
11.26	-7.2
11.27	-7.4

Frequency [GHz]	S_{21} [dB]
11.28	-7.7
11.29	-7.91
11.3	-8.08
11.31	-8.12
11.32	-8.16
11.33	-8.42
11.34	-8.95
11.35	-9.54
11.36	-9.92
11.37	-9.93
11.38	-10
11.39	-10.3
11.4	-10.8
11.41	-11.3
11.42	-12.1
11.43	-13
11.44	-13.9
11.45	-14.6
11.46	-14.8
11.47	-15.1
11.48	-14.9
11.49	-14.5
11.5	-14
11.51	-14
11.52	-13.8
11.53	-13.4
11.54	-12.9
11.55	-12.2
11.56	-11.5
11.57	-11.1
11.58	-10.9
11.59	-10.6
11.6	-10.7
11.61	-10.6
11.62	-10.7
11.63	-10.7
11.64	-10.8
11.65	-10.8
11.66	-11.3
11.67	-11.5
11.68	-12.3

Frequency [GHz]	S_{21} [dB]
11.69	-13.1
11.7	-14
11.71	-14.8
11.72	-15.9
11.73	-16.8
11.74	-17.8
11.75	-18.6
11.76	-19.1
11.77	-19.6
11.78	-20.4
11.79	-21
11.8	-20.9
11.81	-20.6
11.82	-20.1
11.83	-19.8
11.84	-19.2
11.85	-18.7
11.86	-18
11.87	-18.3
11.88	-18.6
11.89	-19.3
11.9	-19.2
11.91	-18.8
11.92	-18.7
11.93	-18.9
11.94	-19.1
11.95	-19.2
11.96	-19.2
11.97	-18.8
11.98	-18.9
11.99	-18.8
12	-18.4

3.6 References

N. M. Littman, S. G. O'keefe, A. Galehdar, H. G. Espinosa and D. V. Thiel, "Ultra-Thin Broadband Transmission FSS for Linear Polarization Rotation," *IEEE Access*, vol. 9, pp. 127335-127342, 2021.doi: 10.1109/ACCESS.2021.3106959.

Harikrishna Paika and Kambham Premchandb, "A dual-band FSS-based electromagnetic shield for 5G and 6G applications", *INTERNATIONAL JOURNAL OF ELECTRONICS LETTERS*,vol.12,pp.317-329,2024.https://doi.org/10.1080/21681724.2023.2267208

M. F. Palvig and M. Zhou, "Design of a Modulated FSS Subreflector for a Dual-Reflector System," *2021 15th European Conference on Antennas and Propagation (EuCAP)*, Dusseldorf, Germany, pp. 1-5, , 2021.doi: 10.23919/EuCAP51087.2021.9411345.

R. A. Pandhare, C. Dhote and F. L. Lohar, "Design of Octagonal FSS Based Radome Wall for Broadband Airborne Application," *2021 2nd International Conference on Range Technology (ICORT)*, Chandipur, Balasore, India, pp. 1-5, 2021.doi: 10.1109/ICORT52730.2021.9582022.

N. Liu, X. Sheng, C. Zhang and D. Guo, "Design and Synthesis of Band-Pass Frequency Selective Surface With Wideband Rejection and Fast Roll-Off Characteristics for Radome Applications," *IEEE Transactions on Antennas and Propagation*, vol. 68, no. 4, pp. 2975-2983, April 2020.doi: 10.1109/TAP.2019.2955665.

G. Venkatesh, M. Thottappan and S. P. Singh, "Highly Angularly Stable Dual-Band Stop FSS for Blocking Satellite Downlink Frequencies, *" IEEE Transactions on Electromagnetic Compatibility*, vol. 64, no. 6, pp. 2055-2059, Dec. 2022.doi: 10.1109/TEMC.2022.3200212.

G. Sen, M. Midya and S. Ghosh, "Design of a band pass FSS with a sharp transition response based on SIW technology for satellite application," *2021 5th International Conference on Electronics, Materials Engineering & Nano-Technology (IEMENTech)*, Kolkata, India, pp. 1-3, 2021.doi: 10.1109/IEMENTech53263.2021.9614742

Zhaoran Chen , Xiangyu Li , Junjie Hu , Xiayuan Yao, “Dual-band flexible FSS conformal to elliptic cylindrical surface”, *IET Microwave, Antennas & Propagation,* vol.19, issue-1,2025.DOI: 10.1049/mia2.12548

Yanfei Ren, Zhenghu Xi, Qinqin Liu, Jiayi Gong, Zhiwei Sun,Boyu Sima, “A Wide Passband Frequency-Selective Surface with a Sharp Roll-Off Band Using the Filtering Antenna-Filtering Antenna Method”, *Materials,* vol.17, 2024.10.3390/ma17246131

B. Wang, Q. Zhang, J. X. Tian and W. W. Men, "A Wide Bandpass FSS with High Selectivity and Low Insertion Loss," *2023 International Conference on Microwave and Millimeter Wave Technology (ICMMT),* Qingdao, China, pp. 1-3, 2023.doi:10.1109/ICMMT58241.2023.10276980.

Z. Zhao et al., "Bandpass FSS With Zeros Adjustable Quasi-Elliptic Response," *IEEE Antennas and Wireless Propagation Letters,* vol. 18, no. 6, pp. 1184-1188, June 2019.doi: 10.1109/LAWP.2019.2911908.

Zvonimir Sipus and Marko Bosiljevac, “Improving the Convergence of Double Series Summation Encountered in the Analysis of Curved Frequency Selective Surfaces”,*EuCAP-2011*, pp.2716-2719,2011.

Chan-Sun Park et al., "Analysis of Curved Frequency selective surface for radome using characteristic basis function method," *2016 10th European Conference on Antennas and Propagation (EuCAP*), Davos, Switzerland , pp. 1-4, 2016.doi: 10.1109/EuCAP.2016.7481386.

P. H. B. Cavalcanti Filho, J. A. I. Araujo, M. R. T. de Oliveira, M. T. de Melo, A. G. Neto and I. B. G. Coutinho, "A New Design of Sierpinski Curve Fractal FSS for S-band Interference Protection Applications," *2019 SBMO/IEEE MTT-S International Microwave and Optoelectronics Conference (IMOC),* Aveiro, Portugal, pp. 1-3, 2019.doi: 10.1109/IMOC43827.2019.9317417.

Saptarsika Das, et al. "Design of Dual-Layer Curved Cylindrical FSS with Sharp Roll-Off and Flat Bandpass Property." *Microwave Journal* , vol.67, no.4,2024.

S.Peddakrishna, T.Khan, B.K.Kanaujia, et al., “Study of Pass Band Resonance Characteristics of Aperture Type FSS”, AEU International Journal of Electronics and Communications,vol.83, pp.479-483, 2018.

S.Balta, M.Kartal, “A Novel Double-layer Low-profile Multiband Frequency Selective Sur- face for 4G Mobile Communication System” ,ACES Journal,vol.37, no.4, 2022.

Gao shan, Chun Yan Cleo, Hong Bin Pu et al., “A Tri-Band Second Order Frequency Selective Surface Designing and Analysis”,E3S Web Conference (EILCD)2021,275,2021.

W.Wu, X.Liu, K.Cui et a1. “An Ultrathin and Polarization-Insensitive Frequency Selective Surface at Ka-Band”, IEEE Antennas and Wireless Propagation Letter,vol. 17, no.1, 2018.

P.Samaddar,S.Sarkar, P.P.Sarkar et al., “Bandpass planar and hemispherical FSS coipris- ing of tripole element”, Journal Of Physical Sciences,vol.18, pp.14-18, 2014.

H.F.Avarez, D.A.Cadman, A.Gou1as et al., “3D Conformal Bandpass Millimeter-Wave Frequency Selective Surface with Improved Fields of View” ,Scientific Reports,vol.11,no.1, 2021.

N.Begam, S.Saha, P.Sammadar et a1., “Design of a Broadband Hemispherical Frequency Selective Surface with Incident Angle Independent Transmission Characteristics and High Roll-Off”, Internntional Journal of Electronics Engineering Research,vol.9,no.1, pp.9-13, 2017.

CHAPTER 4

Design of a Reduced Size Frequency Selective Surface

4.1 Introduction

Frequency Selective Surface (FSS) replaced the electronic filter in wireless systems and is also known as spatial filter. It is classified as patch type or aperture type FSS based on its filtering property, like bandstop and bandpass respectively [1]. The development in communication and wireless technologies requisite multifunctional handheld devices. In these devices frequency selective surface plays an important role. Bandstop FSS reduces the noise in a communication system by separating the unwanted signals [2]. FSS integrated with antenna enhances the gain and directivity of the antenna [3]. Multiple closely spaced bands produced by a single FSS eliminates the need of multiple single band FSS and is utilitarian for its multifunctionality, which in lieu reduces the size and weight of the handheld device. Summarization of the above facts put on view that the FSS has to be of small size to amalgamate with the modern wireless communication portable devices.

Reduction of the size of FSS is challenging at low frequency, as the size of the unit cell of the FSS increases with lowering of frequency. Different methods have been documented in the literature to reduce the size of the FSS.Introducing slit and slot on the patch type element of the FSS unit cell increased the current path which is responsible for lowering the frequency without altering the net size of the FSS unit cell [4]. Reduction in thickness of the substrate cut down the size of the element of the FSS [5]. Compact FSS has been documented adapting the element designing methods like convoluted method and fractal method [6,7].Square patch elements with rectangular slot and circular slot reduce the size of the FSS by 90% to 91% [8,9]. The circular slots introduced on the double square patches result into dual band. 94% compactness has been achieved by loading back to back slot on a metallic patch and slot loaded square patch [10]. A pi shaped modified square patch has been documented with 96.48% reduction in the size of the FSS [11]. Multiple band is the key requirement to accomplish multifunctionality in compact FSS. Combination of elements of multi periodicity result into multiple bands [12]. Multiband is the

consequence of combination of multiple layers to design the FSS composite structure [13]. Loop elements are incorporated to attain multiband FSS [9,14,15]. It is very difficult to attain multiband without compromising the dimension of the FSS structure. The chronicles put forward the actuality, that, the study of frequency selective surface demands the designing of multiband compact FSS.

The aim of this chapter is to design a multiband compact FSS considering conventional method of incorporating slits and slots on a patch of the FSS element and considering simple elemental structure. In the first place, circular and square patch elements are modified to obtain multiband and compactness [16]. These structures have been studied by simulation. Finally, a modified square patch loaded with slits and slots has been fabricated and experimented to validate the achieved compactness by simulation at very low frequency of 1.72 GHz [17].

4.2 Design of FSSs

A circular shaped patch type FSS has been modified incorporating circular slots and swastika shaped slot. The periodicity considered for the case is 20 mm X 20 mm. The designed FSS has been studied by simulation only. A square patch of periodicity 12 mm X 12 mm has been modified by introducing square loop slots and is simulated to study the size reduction thus achieved. The substrate thickness considered for both the cases is 1.6 mm. An FSS has been designed incorporating slits and slots on a square patch of periodicity 23 mm X 23 mm. The substrate thickness considered here is 0.8 mm. The designed FSS is fabricated and measured to validate the result obtained by simulation. Copper is used as patch and FR-4 epoxy is used as substrate for all the cases. The measurement of the FSS has been done by standard microwave test bench.

4.2.1 Modification of circular type patch element to reduce the size of the FSS

A single layer FSS structure has been reconfigured from a circular patch of radius 9.8 mm imprinted on an FR4-epoxy substrate of thickness 1.6 mm. The periodicity in each of the structure is 20 mm X 20 mm. The unit cell of the reference circular patch is shown in Fig. 4.1.

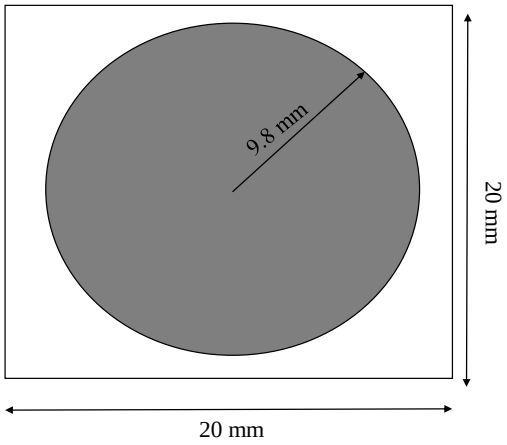

Fig 4.1. Unit cell of reference circular patch FSS

Two circular slots of 0.1 mm each have been introduced at the distance of 7.9 mm and 9.1 mm respectively from the center of the circle. A cross dipole slot has been introduced in the middle of the circle of radius 7.9 mm as shown in Fig.4.2.

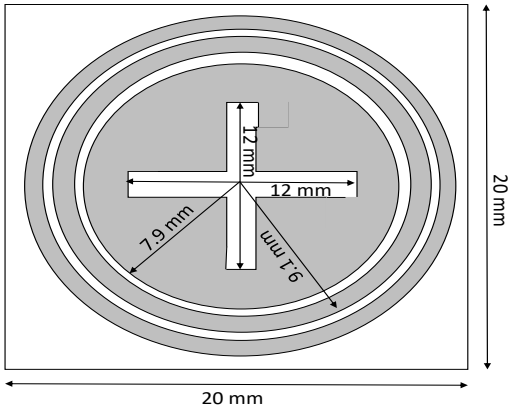

Fig.4.2. Intermediate step of circular and cross dipole slots loaded patch for the modification of circular patch

The cross dipole slot is further modified by introducing four square slots of dimension 2 mm X 2 mm forming a Swastika shaped slot. The final modified

circular shaped patch has been depicted in Fig.4.3. The design and simulation of all the structures have been done by using ANSYS HFSS software based on MOM numerical method.

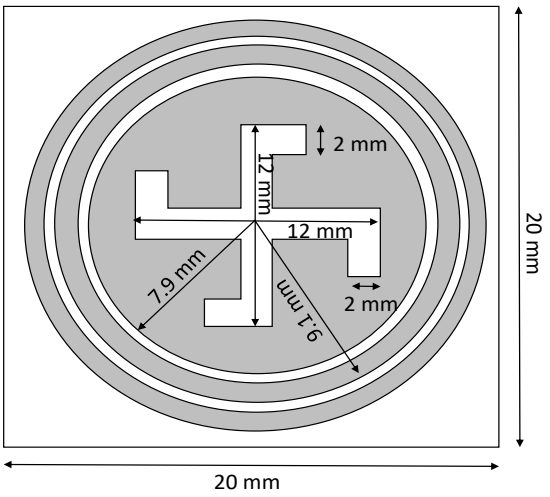

Fig.4.3. Final modified circular patch

4.2.2 Modification of square type patch element with loop type slots to reduce the size of the FSS

A square patch of 11 mm X 11 mm has been considered as reference patch. The reference patch is embedded on FR4 epoxy substrate of thickness 1.6 mm. 12 mm periodicity has been considered in both horizontal and vertical directions of two dimension. Fig. 4.4 shows the unit cell of the reference patch. The reference square patch has been modified as shown in Fig. 4.5.The modified square loop structures introduced two stopbands in the frequency range of 2 GHz to 9 GHz. The inner modified structure is responsible to attain upper band and the lower band has been obtained by the modified outer square loop of 0.5 mm. The structure is further modified by incorporating an inner square loop of 0.5 mm as shown in Fig.4.6. The modified structure accomplished three bands where the introduction of the inner square loop is accountable for the stop band in the frequency range of 12 GHz to 19 GHz. The dimensions of the final modified structure are presented in Table 4.1.

These structures are designed and simulated by using ANSYS HFSS software based on MOM numerical method.

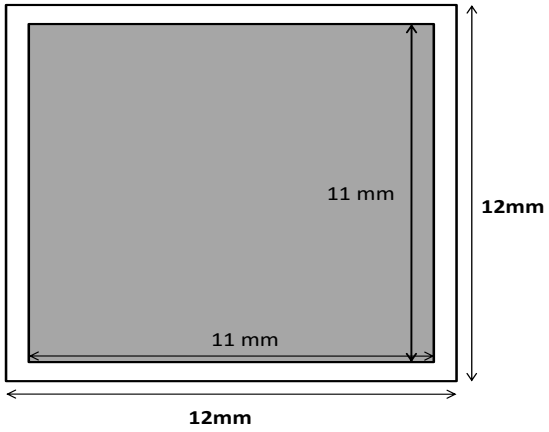

Fig 4.4. Unit cell of reference square patch FSS

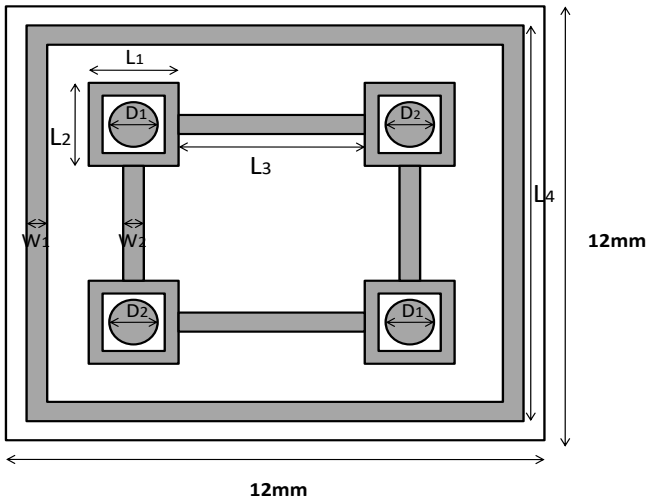

Fig 4.5. Unit cell of modified square patch FSS (1st step)

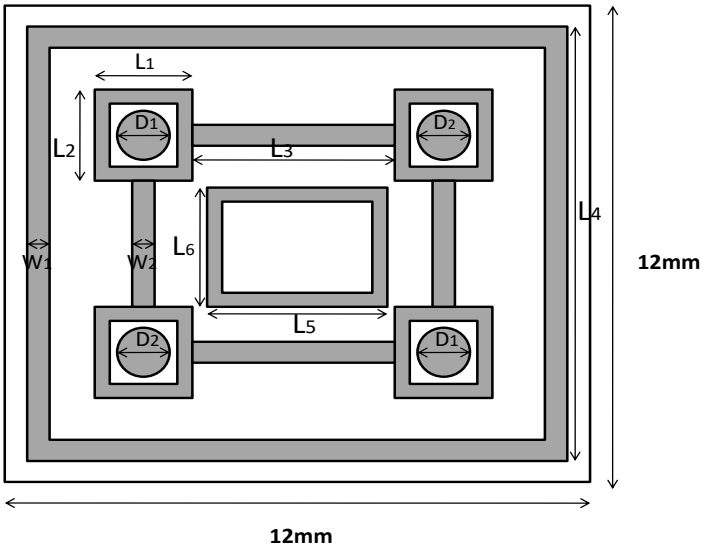

Fig 4.6. Unit cell of final modified square patch FSS

Table 4.1. Dimensions of finally modified square patch FSS

Parameters	Dimensions in (mm)
L_1	3
L_2	3
L_3	4
L_4	11
L_5	3.5
L_6	3.5
W_1	0.5
W_2	0.5
D_1	0.7
D_2	0.6

4.2.3 Modification of square type patch element with rectangular slots and slits to reduce the size of the FSS

A square patch of dimension 16 mm X 16 mm is considered as reference patch as shown in Fig.4.7. The square patch is imprinted on FR4- epoxy substrate of thickness 0.8 mm. The structure has the periodicity of 23 mm X 23 mm.

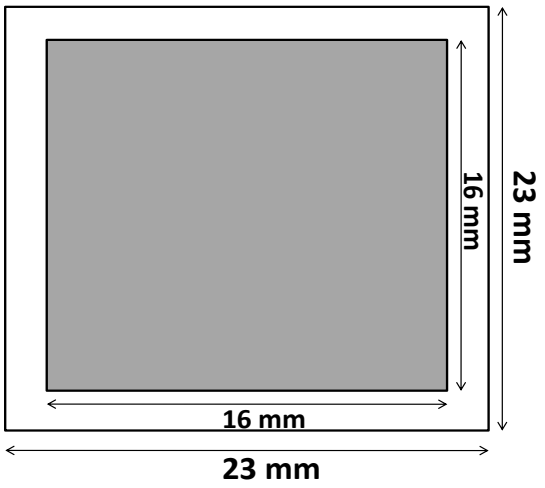

Fig 4.7. Unit cell of reference square patch FSS

Slots and slits are gradually introduced in the patch to increase the current path which in lieu lowers the operating frequency resulting into the reduction of the size of the FSS. Two intermediate steps of modification is shown in Fig 4.8 and Fig.4.9. A series of modified states has been observed by introducing slots and slits, and varying the length and width of the slots and slits. These modification steps finally put forward the optimized modified square patch loaded with slots and slits that exhibits the lowest resonant frequency. Fig 4.10 depicts the unit cell of optimized modified square patch. Table 4.2 documented the dimension of slots and slits of the final modified square patch. The design and simulation of the FSS structures have been done by ANSYS HFSS software based on MOM numerical method. The designed structure has been fabricated for validation purpose. The fabricated FSS has

been shown in Fig.4.11. The measurement of the fabricated FSS has been performed by the standard microwave test bench depicted in Fig.4.12.

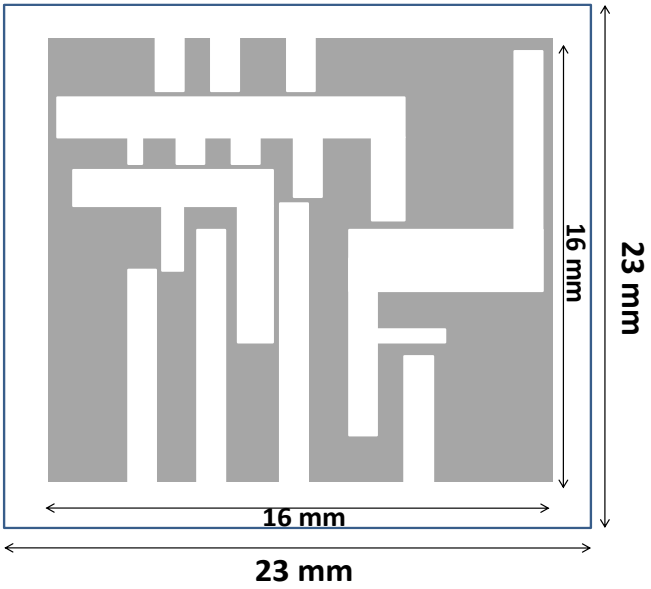

Fig.4.8. An intermediate step of modification of the square patch unit cell loaded with slits and slots

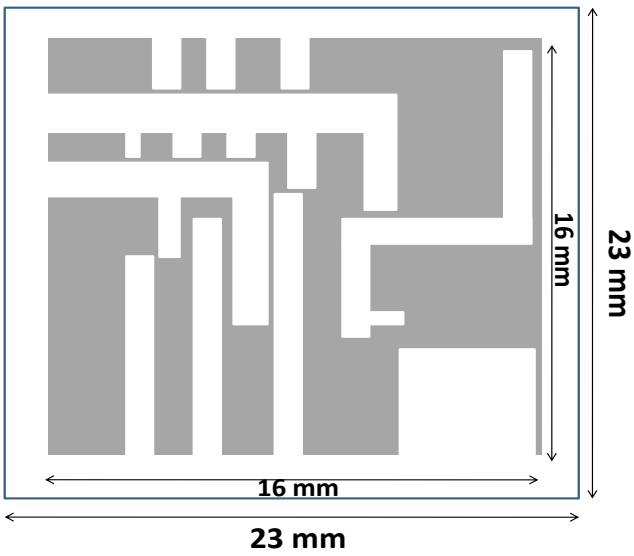

Fig 4.9. Second intermediate step of modification of the square patch unit cell loaded with slits and slots

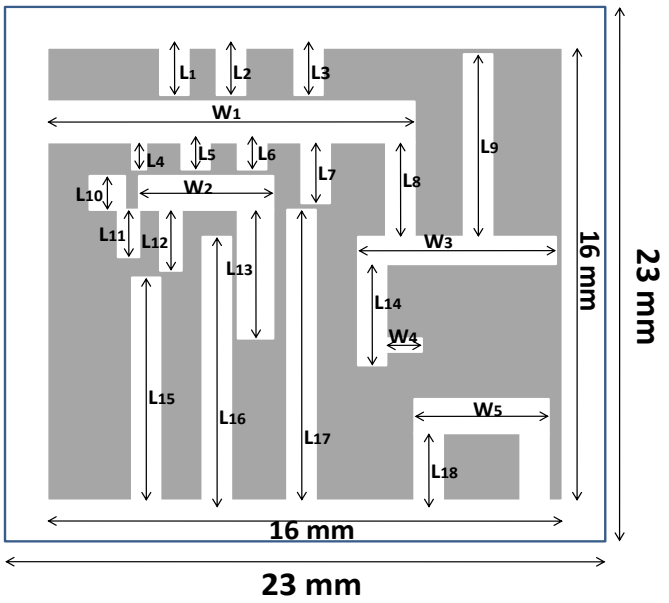

Fig. 4.10. Final and optimized modification of square patch unit cell loaded with slits and slots

Table 4.2.Dimensions of slits and slots of the final modified square patch

Variable	Size (mm)	Variable	Size (mm)	Variable	Size (mm)
L_1	2	L_{10}	1	W_1	12
L_2	2	L_{11}	2	W_2	4
L_3	2	L_{12}	2.5	W_3	6
L_4	1	L_{13}	4	W_4	1
L_5	1	L_{14}	3	W_5	4
L_6	1	L_{15}	7		
L_7	2	L_{16}	8		
L_8	3	L_{17}	10		
L_9	7	L_{18}	3		

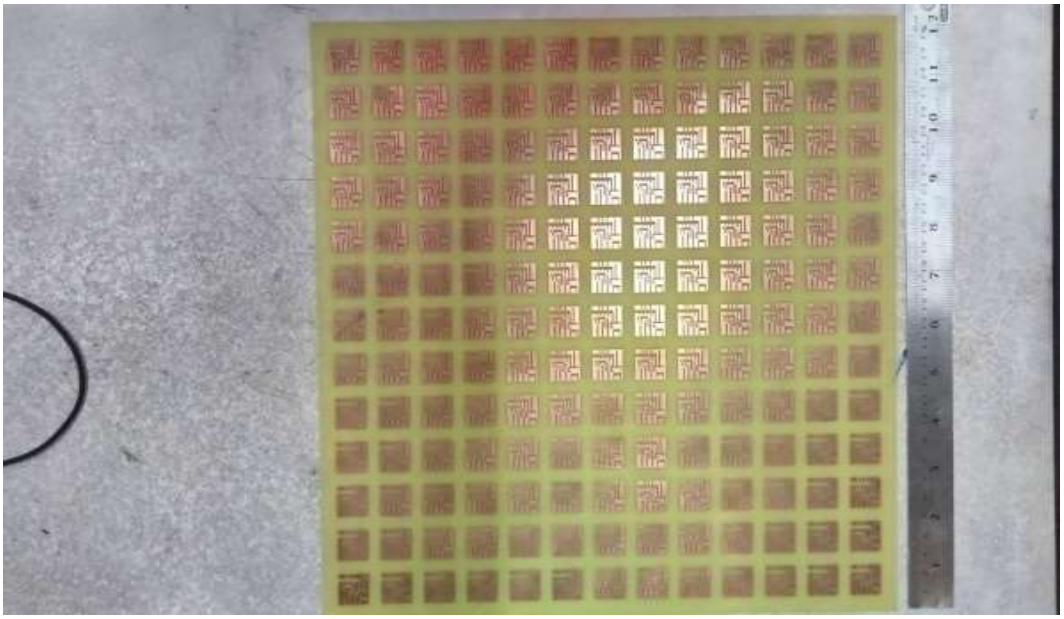

Fig. 4.11. Fabricated square patch FSS loaded with slits and slots

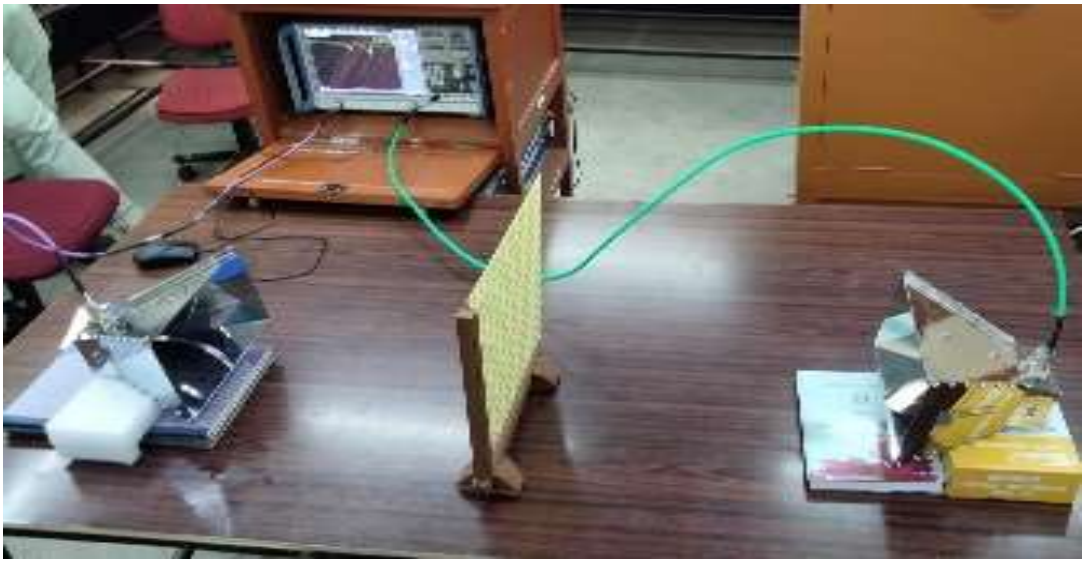

Fig. 4.12. Measurement set up of the fabricated FSS

4.3 Results & Discussion

All the modified circular patch, square patches are designed and simulated by using ANSYS HFSS software. The fabricated FSS has been measured by the standard microwave test bench. The transmission characteristics of all the simulated structures and the fabricated one have been produced in this section. Comparative study of the

presented works have been done with the works of the cutting edge. The compactness calculation have been done for all the designed FSS.

4.3.1 Study of compactness of modified circular patch type element

The transmission characteristics of reference circular patch has been shown in Fig. 4.13. The structure resonated at 9.36 GHz.

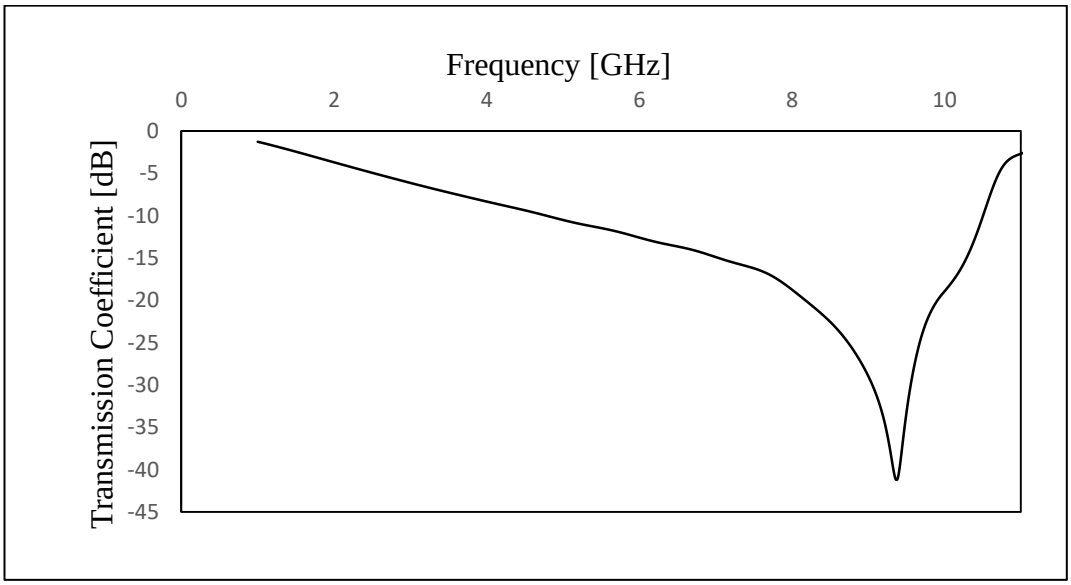

Fig.4.13. Transmission characteristics of reference circular patch FSS by simulation

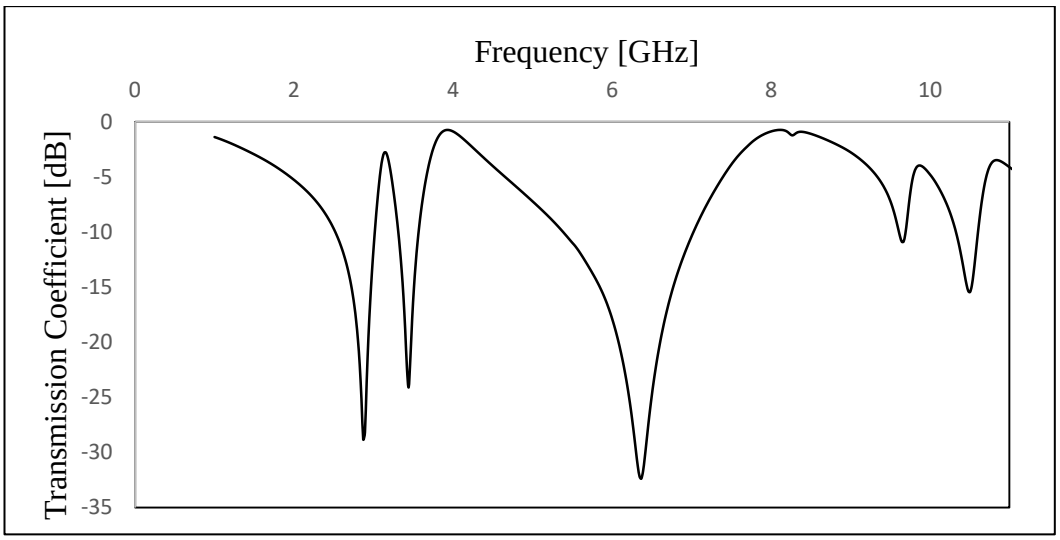

Fig.4.14. Simulated transmission characteristics of intermediate step of circular and cross dipole slots loaded patch for the modification of circular patch FSS

The structure exhibits four prominent stopband. The lowest resonant frequency attained by the structure is 2.87 GHz. The circular patch has been further modified by Swastika slot to obtain better compactness. The transmission characteristics of finally modified circular patch is shown in Fig.4.15.

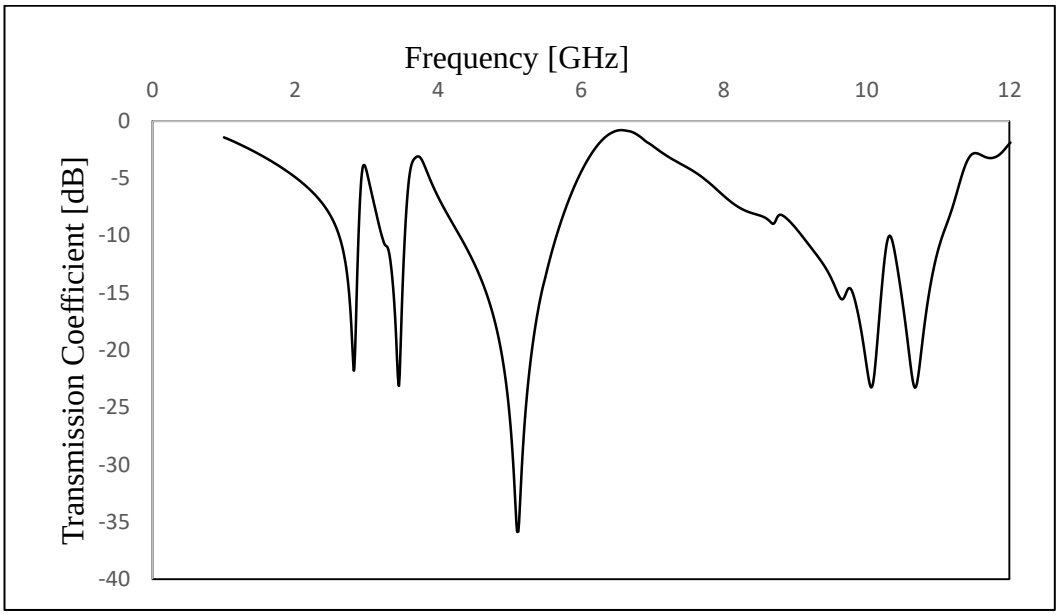

Fig.4.15. Transmission Characteristics of finally modified circular patch FSS

The lowest resonant frequency accomplished by the final modified circular patch FSS is 2.82 GHz. Four stop bands in the frequency range of 2.6 GHz to 2.9 GHz, 3.2 GHz to 3.55 GHz, 4.3 GHz to 5.65 GHz, and by staggering effect 9.08 GHz to11.05 GHz. The bandwidth of first, second, third and fourth operating bands are 30 MHz, 35 MHz, 1.35 GHz and 1.97 GHz respectively.

A relation is exist between the dimension of the patch and the resonant wavelength of the FSS. Wavelength of the FSS is equal to the electrical length of the perimeter of the patch element [18]. The resonating frequency is inversely proportional to the effective current path length. The detail calculation of the reduction of size of the FSS has been furnished in section 4.3.1.1.

\

4.3.1.1 Calculation of size reduction of the final modified circular patch type FSS

The circular patch FSS of radius 9.8 mm, having no slots and slits resonates at 9.36 GHz.

The resonant frequency lowered to 2.82 GHz while incorporating circular slots and Swastika sign slot.

The required dimension (circumference) to design of a circular patch without slots and slits that will resonate at 2.82 GHz will be

$$\frac{2 \text{ X } 3.14 \text{ X } 9.8 \text{ X } 9.36}{2.82} \text{ mm} = 204.27 \text{ mm}$$

So, its radius will be $\frac{204.27}{2 \text{ X } 3.14}$ mm = 32.53 mm

Corresponding area of the patch will be (3.14 X 32.53 X 32.53) mm^2 = 3322.75 mm^2

The modification of the circular patch is responsible for lowering the frequency to 2.82 GHz from the patch dimension (area) of 301.57 mm^2 instead of 3322.75 mm^2.

So, the size reduction obtained by modification is

$$\frac{3322.75-301.57}{3322.75} \text{ X } 100 = 90.92 \text{ \%}$$

Thus, 90.92 % compactness has been achieved by simulation of the designed circular patch by incorporating circular slots and Swastika shape slot.

4.3.2 Study of compactness of modified square patch type element with loop type slot

The transmission characteristics of the square patch of dimension 11 mm X 11 mm depicted in Fig. 4.4 is shown in Fig.4.16. The structure resonated at 19.37 GHz. The transmission characteristics of the first modification of the square patch is shown in Fig.4.17. The modified structure attains dual band in the frequency range of 2.5 GHz to 11 GHz and the lowest resonant frequency achieved by the modified structure is 3.45 GHz. Introduction of inner square loop to the first modified structure shown in

Fig.4.5 further lowers the resonant frequency to 3.41 GHz. The transmission characteristics of the finally modified square loop shown in Fig.4.6 is shown in Fig.4.18. The structure finally attains a triple stop band with resonating frequency at 3.41 GHz, 7.20 GHz and by staggering effect at 16.33 GHz and 17.55 GHz. The outer square loop is responsible for the attainment of low frequency band of 520 MHz of fractional bandwidth of 15.24%. The modified middle loop structure is responsible for achieving the mid frequency band of 3.24 GHz of fractional bandwidth of 45%. A higher frequency band of 2.49 GHz having fractional bandwidth of 15.18 % has been achieved by the modification of the square patch introducing the inner square loop of 0.5 mm.

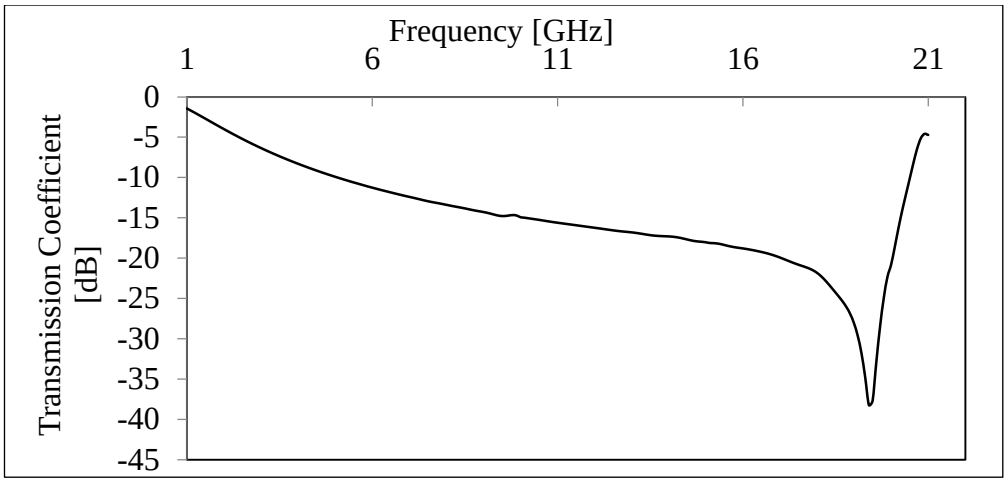

Fig.4.16. Transmission characteristics of reference square patch FSS by simulation

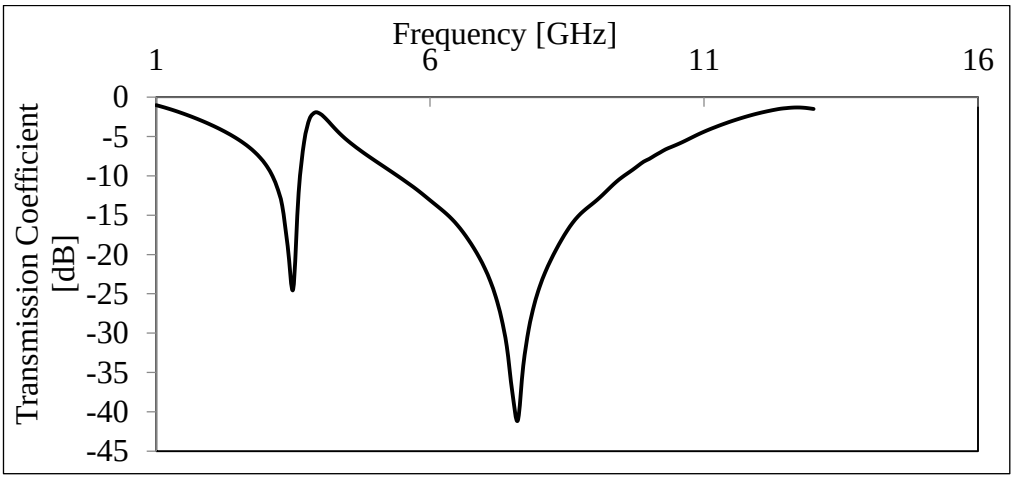

Fig.4.17. Transmission characteristics of the first modified square patch FSS by simulation

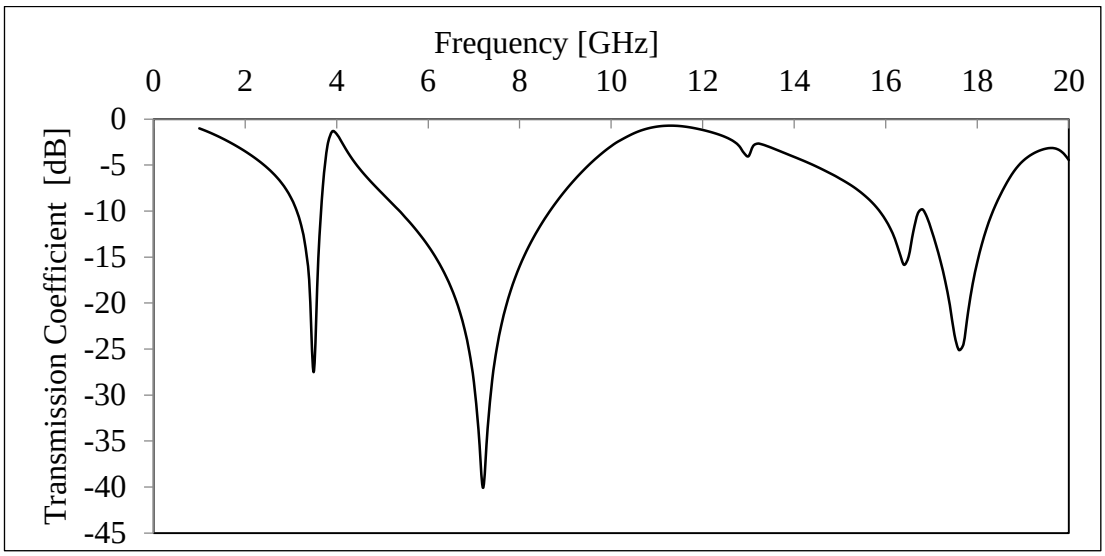

Fig.4.18. Transmission characteristics of finally modified square patch FSS by simulation

4.3.2.1 Calculation of size reduction of the final modified square patch type FSS

The reference square patch of Fig. 4.4 resonates at 19.37 GHz.

Modification of the square patch lowers the resonant frequency to 3.41 GHz.

The perimeter of the square patch that should be needed to resonate at 3.41 GHz will be

$\frac{4 \text{ X } 11 \text{ X } 19.37}{3.41}$ mm = 249.94 mm

Therefore, the side of the square patch will be $\frac{249.94}{4}$ mm = 62.48 mm

Corresponding area of the square patch will be (62.48 X 62.48) mm^2 = 3903.75 mm^2

The modification of the square patch lowers the resonant frequency to 3.41 GHz considering the reference square patch area of 121 mm^2 instead of 3903.75 mm^2

So, the compactness achieved by the modification of the square patch is

$\frac{3903.75-121}{3903.75}$X 100 = 96.90 %

Hence, the modification of the square patch reduces the size of the FSS up to 96.90% by simulation.Table 4.3 gives the detail information of the improvement attained with each modification of the square patch.

Table 4.3. Overview of all the simulated results

FSS Design	Resonating Frequency [GHz]			Number of Band	Size Reduction
	Band 1	Band 2	Band 3		
Fig.4.4	19.37			1	
Fig.4.5	3.45	7.54		2	96.82%
Fig.4.6	3.41	7.20	16.33 17.55	3	96.90%

4.3.2.2 Comparative study of the designed square patch with the contemporary works

The comparison of the designed square patch has been done with the works of the present state of art which is documented in Table 4.4.

Table 4.4. Comparison of the designed square patch with the related works

Reference No.	Resonant Frequency [GHz]			Number of Stop Band
	Low Frequency	Mid Frequency	High Frequency	
[14]	1.92 & 3.50	5.64		03
[9]	3.37	8.10		02
[15]	4.00		10.60 & 14.30	03
Designed Square Patch	3.41	7.20	16.33,17.55	03

The study depicts that for most of the cases the compactness have been accomplished with three bands either in low and mid frequency range or in low and high frequency

range. The designed square patch achieved compactness with three bands in low, mid and high frequency range. The designed FSS efficiently fulfil the purpose of spatial filter in C, X and Ku frequency band and proved its multifunctionality characteristics. The dimension and the periodicity of the designed square patch FSS is smaller than all of its contemporary works. The reduction of the size of the FSS with triple band has been done considering simple elemental structure which are easy to simulate and study.

4.3.3 Study of compactness of modified square patch type element with rectangular slot and slits

A parametric study has been carried out by changing the periodicity of the rectangular slot and slit loaded square patch FSS to optimise the periodicity of the structure.

4.3.3.1 Effect of periodicity P on compactness of the FSS

The study of compactness by varying periodicity has been documented in Table 4.5.

Table 4.5. Study of compactness by changing the periodicity

Periodicity [mm]	Resonance Frequency [GHz]	Transmission Coefficient [dB]	Bandwidth [GHz]
19	1.75	-12.90	0.11
	7.52	-19.38	1.14
	10.35	-13.62	2.14
	11.23	-21.17	
	11.57	-20.49	
21	1.79	-11.82	0.07
	7.49	-16.02	0.6
	10.24	-11.91	1.51
	11.04	-20.32	
23	1.72	-13.49	0.04
	7.44	-13.07	0.61
	9.73	-18.28	1.87
	10.71	-28.62	
25	1.84	-10.65	0.02
	7.34	-15.55	0.47
	9.83	-16.15	0.37
	10.47	-32.92	0.97
27	7.03	-16.07	0.35
	9.58	-31.49	0.84

It has been observed from the table 4.5 that the higher order resonant frequency decreases as we increase the periodicity from 19mm to 27mm, whereas lower order resonant frequency is minimum for the periodicity of 23mm and vanishes for 27mm. The staggering effect vanishes at high frequency with increase in periodicity and leads to the decrease of total bandwidth. It is also observed that the best compactness has been achieved for the periodicity of 23 mm. Thus, the optimised periodicity depicted by the study is 23 mm. The graphical representation of the study has been furnished on Fig.4.19 to understand the study in a better way.

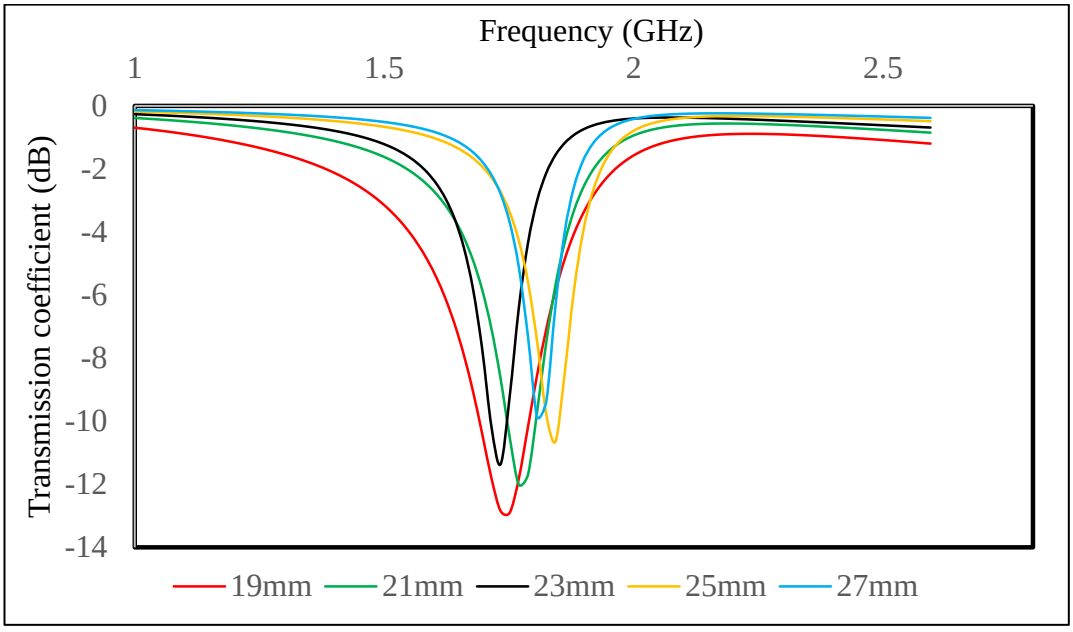

Fig.4.19. Transmission characteristics by changing the periodicity of rectangular slots and slits loaded square patch FSS structure

The optimised periodicity obtained from the study where the FSS structure resonates at 1.72 GHz is 23 mm. Hence the fabrication of the designed FSS has been done for the optimised periodicity of 23 mm, for the validation purpose.

4.3.3.2 Study of the transmission characteristic of rectangular slots and slits loaded square patch FSS

The transmission characteristics of the square shaped reference patch is shown in Fig.4.20. The structure resonate at 10. 80 GHz. The transmission characteristics of the first intermediate modification of the square patch by introducing slots and slits

given in Fig.4.8 is shown in Fig.4.21. The simulation of the structure results in to dual band in the frequency range of 5GHz to 10 GHz. The lowest resonant frequency attained in this stage of modification is 6.47 GHz.

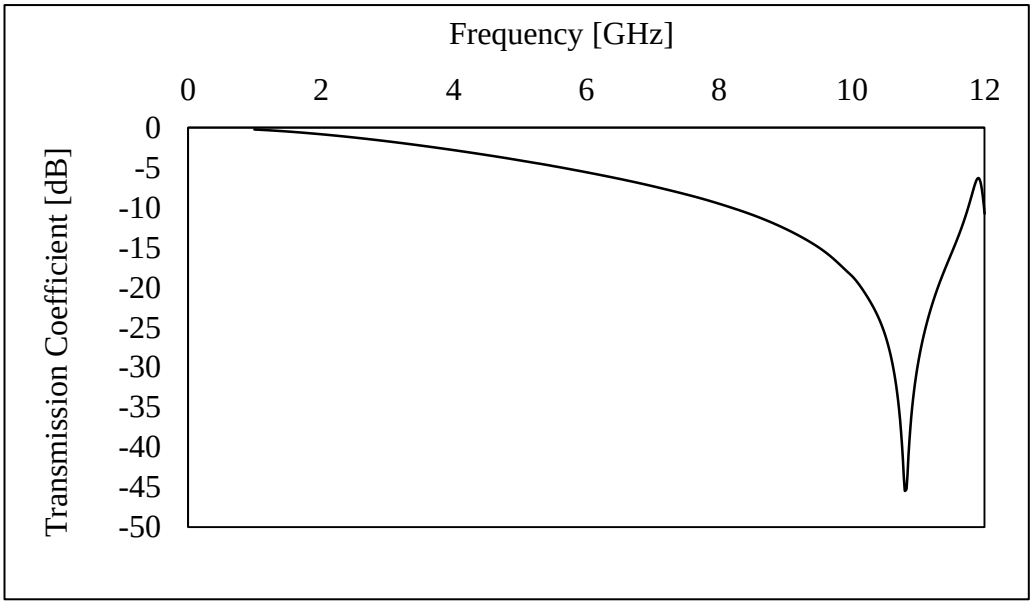

Fig.4.20. Transmission characteristics of reference square patch

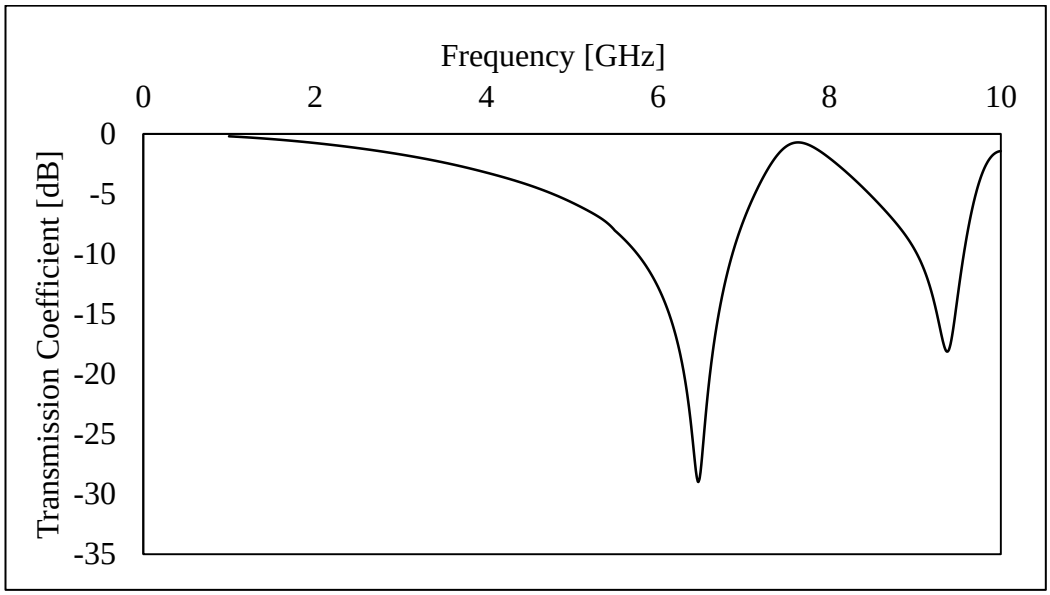

Fig.4.21. Transmission characteristics of an intermediate step of modification of the square patch loaded with slits and slots

The modified square patch of Fig 4.8 is further modified by incorporating slots and slits to lower the resonant frequency. The transmission characteristics of the second modified stage has been furnished in Fig.4.22. The modified structure attains dual band in the frequency range of 2.9 GHz to 4.8 GHz. The lowest resonant frequency achieved in this stage is 2.99 GHz. The final modification of the square patch results into three stop band in the frequency range of 1.6 GHz to 11 GHz. The simulated and measured results of the finally modified slits and slots loaded square patch has been furnished in Fig.4.23. The percentage bandwidth attained by the three bands are 5.05%, 17.28% and 9.56% in the frequency range of 1.6 GHz to 2 GHz, 6 GHz to 8 GHz and 9 GHz to 11 GHz respectively. The measured result validates the simulated result to a good agreement. The lowest frequency attained by the structure by simulation is 1.72 GHz and by measurement it is 1.78 GHz. Fig.4.23 reveals that the finally modified square patch leads to multiple band with compactness.

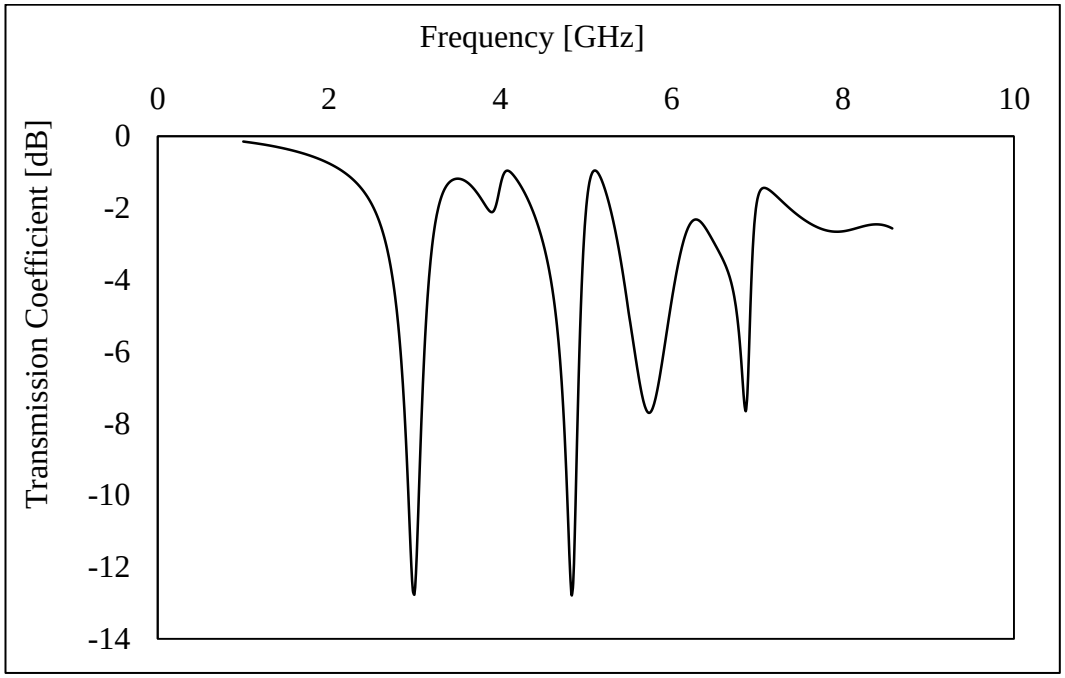

Fig.4.22. Transmission characteristics of second intermediate step of modification of the square patch loaded with slits and slots

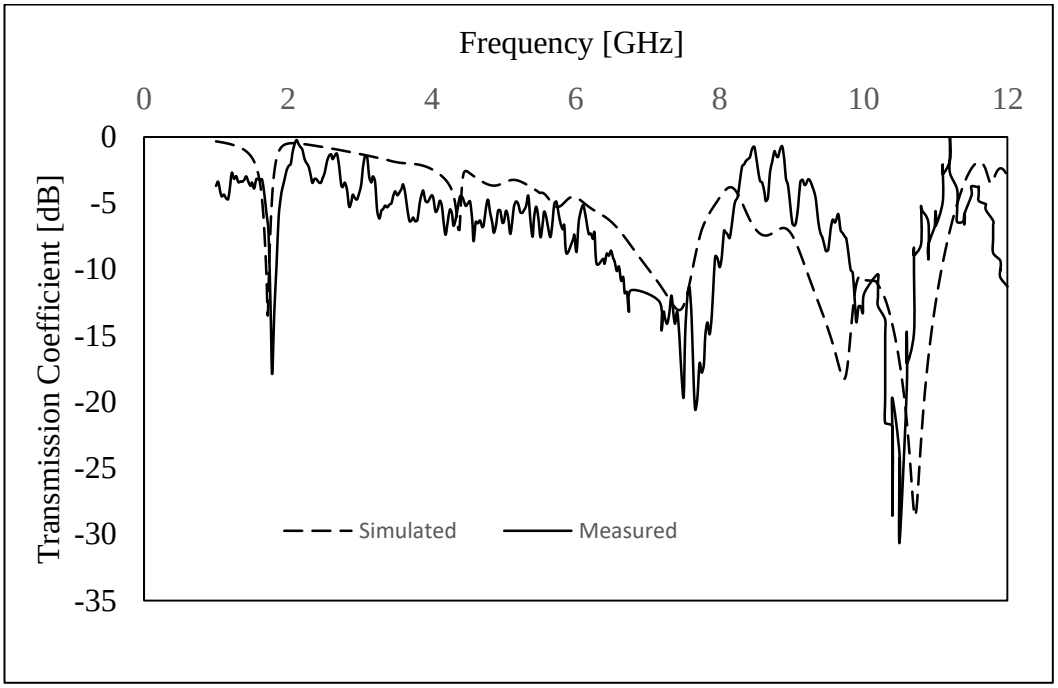

Fig.4.23. Transmission characteristics of finally modified square patch loaded with slits and slots

4.3.3.3 Calculation of size reduction of the final modified rectangular slits and slots loaded square patch type FSS

The reference square patch of Fig. 4.7 resonates at 10.80 GHz.

By measurement it has been found that modification of the square patch lowers the resonant frequency to 1.78 GHz.

The perimeter of the square patch that should be needed to resonate at 1.78 GHz will be

$$\frac{4 \text{ X } 16 \text{ X } 10.80}{1.78} \text{ mm} = 388.314 \text{ mm}$$

Therefore, the side of the square patch will be $\frac{388.314}{4}$ mm = 97.07 mm

Corresponding area of the square patch will be (97.07 X 97.07) mm^2 = 9422.58 mm^2

The modification of the square patch lowers the resonant frequency to 1.78 GHz considering the reference square patch area of 256 mm^2 instead of 9422.58 mm^2

So, the compactness achieved by the modification of the square patch is

$$\frac{9422.58-256}{9422.58} \text{X } 100 = 97.28\ \%$$

Hence, the modification of the square patch reduces the size of the FSS up to 97.28%.

Table 4.6 gives the detail information of the improvement attained with each modification of the square patch.

Table 4.6. Overview of all the stages of modification of the square patch

FSS Design	Resonating Frequency [GHz]			Number of Band	Size Reduction
	Band 1	Band 2	Band 3		
Fig.4.7	10.80			1	
Fig.4.8	6.47	9.37		2	64.10%
Fig.4.9	2.99	4.83		2	92.33%
Fig.4.10	1.78	7.50, 7.66	10.40,10.50	3	97.28 %

4.3.3.4 Comparative study of the designed square patch with the contemporary works

The comparison of the designed and fabricated square patch FSS has been done with respect to reduction of size of the FSS. The comparative study has been presented in Table 4.7.

Table 4.7. Comparison of the designed square patch with the related works

Ref. No. Of FSS	Lowest Resonance Frequency [GHz]	Reduction in size
[8]	3.54	90%
[9]	3.37	91%
[10]	5.10	94%
[11]	2.25	96.48%
Designed FSS	1.78	97.28%

Table 4.7 exhibit the fact that the best compactness has been achieved by the designed and fabricated FSS presented in this section. It can be easily integrated with the handheld devices.

4.4 Conclusion

The modification of the circular patch reduce the size of the FSS to 90.92 %. The structure attains three closely spaced stop band in C and S band of microwave frequency spectrum and a fourth band in X band of the microwave frequency spectrum. The designed circular patch type FSS proves its worthiness as multifunctional compact FSS and fulfil the purpose of spatial bandstop filter in 5G networks, Wi-fi systems, long distance radio communication systems, satellite and broadband space communication systems. The modified square patch with loop type slots reduce the size of the FSS to 96.90 %. The structure is competent to shield microwave frequency in C, S and Ku band of microwave frequency spectrum and can be integrated with radio and satellite communication systems. The designed and fabricated rectangular slit and slot loaded square patch FSS reduces the size of the FSS to 97.28%. The structure exhibits bandstop property in L, C and X band and proves its competency with military and GPS systems to satellite communication systems. The study documented in this chapter considered a vast frequency range of microwave spectrum from 1.6 GHz to 18 GHz. The reduction of the size of the FSS is appreciable for all the cases. All the designed compact FSS have a significant role in practical applications. Compact FSS is responsible to manufacture a compact handheld device. The compactness of the composite structure (Antenna + FSS) depends on the compactness of the FSS. Compact FSS superintend the gain

enhancement of an antenna. Compact FSS satisfied the requirement of minuscule multifunctional spatial filter in household to modern medical applications.

4.5 Experimental datasheet of the fabricated modified square patch using slots and slits

Table 4.8 Data of the fabricated modified square patch FSS

Frequency [GHz]	S_{21} [dB]
1	-0.3274
1.018	-0.34234
1.036	-0.3579
1.054	-0.37416
1.072	-0.39119
1.09	-0.40905
1.108	-0.42782
1.126	-0.4476
1.144	-0.46848
1.162	-0.49056
1.18	-0.51398
1.198	-0.53888
1.216	-0.56542
1.234	-0.59381
1.252	-0.62425
1.27	-0.65703
1.288	-0.69245
1.306	-0.73089
1.324	-0.7728
1.342	-0.81872
1.36	-0.8693
1.378	-0.92538
1.396	-0.98793
1.414	-1.05822
1.432	-1.13784
1.45	-1.22879
1.468	-1.3337
1.486	-1.45598
1.504	-1.60019
1.522	-1.77247
1.54	-1.98127
1.558	-2.2384
1.576	-2.56073

Frequency [GHz]	S_{21} [dB]
1.594	-2.97278
1.612	-3.5109
1.63	-4.22971
1.648	-5.21102
1.666	-6.57054
1.684	-8.42383
1.702	-10.5822
1.72	-13.4835
1.738	-9.64964
1.756	-7.07556
1.774	-5.03787
1.792	-3.60932
1.81	-2.63569
1.828	-1.97347
1.846	-1.51948
1.864	-1.20461
1.882	-0.98358
1.9	-0.82676
1.918	-0.71463
1.936	-0.63413
1.954	-0.57639
1.972	-0.53531
1.99	-0.50659
2.008	-0.48717
2.026	-0.47484
2.044	-0.46797
2.062	-0.46536
2.08	-0.46612
2.098	-0.46954
2.116	-0.47512
2.134	-0.48243
2.152	-0.49116
2.17	-0.50107
2.188	-0.51195
2.206	-0.52365
2.224	-0.53605
2.242	-0.54904
2.26	-0.56253
2.278	-0.57647
2.296	-0.59079
2.314	-0.60545

Frequency [GHz]	S_{21} [dB]
2.332	-0.62041
2.35	-0.63564
2.368	-0.65111
2.386	-0.66679
2.404	-0.68267
2.422	-0.69873
2.44	-0.71495
2.458	-0.73132
2.476	-0.74783
2.494	-0.76448
2.512	-0.78124
2.53	-0.79813
2.548	-0.81513
2.566	-0.83224
2.584	-0.84946
2.602	-0.86679
2.62	-0.88423
2.638	-0.90178
2.656	-0.91944
2.674	-0.93722
2.692	-0.95512
2.71	-0.97315
2.728	-0.99131
2.746	-1.00961
2.764	-1.02804
2.782	-1.04662
2.8	-1.06535
2.818	-1.08422
2.836	-1.10325
2.854	-1.12243
2.872	-1.14175
2.89	-1.16123
2.908	-1.18084
2.926	-1.2006
2.944	-1.22048
2.962	-1.24048
2.98	-1.2606
2.998	-1.28083
3.016	-1.30115
3.034	-1.32156
3.052	-1.34205

Frequency [GHz]	S_{21} [dB]
3.07	-1.36262
3.088	-1.38326
3.106	-1.40399
3.124	-1.42479
3.142	-1.4457
3.16	-1.46672
3.178	-1.48788
3.196	-1.50922
3.214	-1.53077
3.232	-1.55261
3.25	-1.57478
3.268	-1.58683
3.286	-1.60345
3.304	-1.62378
3.322	-1.647
3.34	-1.67232
3.358	-1.69898
3.376	-1.72631
3.394	-1.75368
3.412	-1.78056
3.43	-1.80649
3.448	-1.83112
3.466	-1.85416
3.484	-1.87541
3.502	-1.89477
3.52	-1.91218
3.538	-1.92767
3.556	-1.94133
3.574	-1.95329
3.592	-1.96376
3.61	-1.97296
3.628	-1.98115
3.646	-1.98863
3.664	-1.99572
3.682	-2.00275
3.7	-2.01004
3.718	-2.01796
3.736	-2.02683
3.754	-2.03699
3.772	-2.04877
3.79	-2.06246

Frequency [GHz]	S_{21} [dB]
3.808	-2.07836
3.826	-2.09674
3.844	-2.11782
3.862	-2.14181
3.88	-2.1689
3.898	-2.19923
3.916	-2.23292
3.934	-2.27007
3.952	-2.31073
3.97	-2.35497
3.988	-2.40282
4.006	-2.45431
4.024	-2.50947
4.042	-2.56837
4.06	-2.63111
4.078	-2.69786
4.096	-2.76885
4.114	-2.84448
4.132	-2.92532
4.15	-3.01218
4.168	-3.10626
4.186	-3.20929
4.204	-3.32376
4.222	-3.45334
4.24	-3.60352
4.258	-3.78274
4.276	-4.00436
4.294	-4.29022
4.312	-4.67696
4.33	-5.22499
4.348	-6.01186
4.366	-6.95539
4.384	-7.00605
4.402	-5.18632
4.42	-3.53918
4.438	-2.82335
4.456	-2.59923
4.474	-2.56648
4.492	-2.60447
4.51	-2.66798
4.528	-2.73971

Frequency [GHz]	S_{21} [dB]
4.546	-2.81299
4.564	-2.88531
4.582	-2.95585
4.6	-3.02443
4.618	-3.09112
4.636	-3.15598
4.654	-3.21899
4.672	-3.28005
4.69	-3.33888
4.708	-3.39508
4.726	-3.44811
4.744	-3.49732
4.762	-3.54196
4.78	-3.58121
4.798	-3.61425
4.816	-3.64026
4.834	-3.65852
4.852	-3.66842
4.87	-3.66957
4.888	-3.66185
4.906	-3.64543
4.924	-3.62083
4.942	-3.58894
4.96	-3.55102
4.978	-3.50865
4.996	-3.46368
5.014	-3.41812
5.032	-3.37407
5.05	-3.33355
5.068	-3.29841
5.086	-3.27022
5.104	-3.25017
5.122	-3.23905
5.14	-3.2372
5.158	-3.24459
5.176	-3.2608
5.194	-3.28514
5.212	-3.31674
5.23	-3.35458
5.248	-3.39763
5.266	-3.44488

Frequency [GHz]	S_{21} [dB]
5.284	-3.49539
5.302	-3.54838
5.32	-3.60317
5.338	-3.65931
5.356	-3.71649
5.374	-3.77457
5.392	-3.83359
5.41	-3.89373
5.428	-3.95531
5.446	-4.01876
5.464	-4.08457
5.482	-4.1533
5.5	-4.22555
5.518	-4.20222
5.536	-4.2138
5.554	-4.25933
5.572	-4.33571
5.59	-4.43789
5.608	-4.55911
5.626	-4.69143
5.644	-4.82631
5.662	-4.95523
5.68	-5.07024
5.698	-5.16453
5.716	-5.23278
5.734	-5.27153
5.752	-5.27936
5.77	-5.25698
5.788	-5.20714
5.806	-5.13446
5.824	-5.04501
5.842	-4.94586
5.86	-4.84447
5.878	-4.74806
5.896	-4.66302
5.914	-4.59444
5.932	-4.54577
5.95	-4.51872
5.968	-4.51338
5.986	-4.52846
6.004	-4.56167

Frequency [GHz]	S_{21} [dB]
6.022	-4.61009
6.04	-4.67056
6.058	-4.73992
6.076	-4.81526
6.094	-4.89404
6.112	-4.97412
6.13	-5.05382
6.148	-5.1319
6.166	-5.20748
6.184	-5.28005
6.202	-5.34937
6.22	-5.41549
6.238	-5.47863
6.256	-5.5392
6.274	-5.59774
6.292	-5.65486
6.31	-5.71127
6.328	-5.76771
6.346	-5.82493
6.364	-5.88366
6.382	-5.94463
6.4	-6.00849
6.418	-6.07583
6.436	-6.14716
6.454	-6.22291
6.472	-6.30339
6.49	-6.38881
6.508	-6.47929
6.526	-6.57482
6.544	-6.67531
6.562	-6.78058
6.58	-6.89039
6.598	-7.00441
6.616	-7.12228
6.634	-7.24359
6.652	-7.36793
6.67	-7.49487
6.688	-7.62398
6.706	-7.75484
6.724	-7.88706
6.742	-8.02027

Frequency [GHz]	S_{21} [dB]
6.76	-8.15415
6.778	-8.28838
6.796	-8.42273
6.814	-8.55695
6.832	-8.69089
6.85	-8.8244
6.868	-8.95739
6.886	-9.0898
6.904	-9.2216
6.922	-9.35281
6.94	-9.48348
6.958	-9.61369
6.976	-9.74354
6.994	-9.87318
7.012	-10.0028
7.03	-10.1325
7.048	-10.2626
7.066	-10.3933
7.084	-10.5249
7.102	-10.6576
7.12	-10.7918
7.138	-10.9276
7.156	-11.0654
7.174	-11.2056
7.192	-11.3481
7.21	-11.4933
7.228	-11.6412
7.246	-11.7916
7.264	-11.9442
7.282	-12.0982
7.3	-12.2525
7.318	-12.4054
7.336	-12.5541
7.354	-12.6952
7.372	-12.8238
7.39	-12.9337
7.408	-13.0172
7.426	-13.0653
7.444	-13.0684
7.462	-13.0169
7.48	-12.9026

Frequency [GHz]	S_{21} [dB]
7.498	-12.7202
7.516	-12.4686
7.534	-12.151
7.552	-11.7753
7.57	-11.3528
7.588	-10.8965
7.606	-10.4199
7.624	-9.93553
7.642	-9.45445
7.66	-8.98569
7.678	-8.5363
7.696	-8.11155
7.714	-7.71522
7.732	-7.34989
7.75	-7.01722
7.768	-6.75595
7.786	-6.51766
7.804	-6.30048
7.822	-6.10195
7.84	-5.91915
7.858	-5.749
7.876	-5.58839
7.894	-5.43445
7.912	-5.2847
7.93	-5.1372
7.948	-4.99061
7.966	-4.84433
7.984	-4.6985
8.002	-4.55408
8.02	-4.4128
8.038	-4.27719
8.056	-4.15046
8.074	-4.03642
8.092	-3.93924
8.11	-3.86323
8.128	-3.81252
8.146	-3.79067
8.164	-3.80037
8.182	-3.8431
8.2	-3.919
8.218	-4.02681

Frequency [GHz]	S_{21} [dB]
8.236	-4.16399
8.254	-4.32695
8.272	-4.51135
8.29	-4.71246
8.308	-4.92544
8.326	-5.14561
8.344	-5.3686
8.362	-5.5905
8.38	-5.80788
8.398	-6.01783
8.416	-6.21789
8.434	-6.40608
8.452	-6.58081
8.47	-6.74081
8.488	-6.88515
8.506	-7.01315
8.524	-7.12436
8.542	-7.21855
8.56	-7.29567
8.578	-7.35585
8.596	-7.39937
8.614	-7.42671
8.632	-7.43851
8.65	-7.4356
8.668	-7.41901
8.686	-7.39001
8.704	-7.35008
8.722	-7.30098
8.74	-7.24474
8.758	-7.18368
8.776	-7.12042
8.794	-7.05785
8.812	-6.9991
8.83	-6.9475
8.848	-6.90646
8.866	-6.87938
8.884	-6.86949
8.902	-6.87969
8.92	-6.91242
8.938	-6.96946
8.956	-7.05189

Frequency [GHz]	S_{21} [dB]
8.974	-7.15997
8.992	-7.2932
9.01	-7.45036
9.028	-7.62964
9.046	-7.82875
9.064	-8.04516
9.082	-8.27619
9.1	-8.51915
9.118	-8.7715
9.136	-9.03091
9.154	-9.29529
9.172	-9.56285
9.19	-9.83211
9.208	-10.1019
9.226	-10.3712
9.244	-10.6394
9.262	-10.9062
9.28	-11.1712
9.298	-11.4345
9.316	-11.6962
9.334	-11.9566
9.352	-12.2161
9.37	-12.4752
9.388	-12.7346
9.406	-12.995
9.424	-13.2573
9.442	-13.5223
9.46	-13.7912
9.478	-14.065
9.496	-14.345
9.514	-14.6324
9.532	-14.9288
9.55	-15.2356
9.568	-15.5542
9.586	-15.8857
9.604	-16.2306
9.622	-16.5883
9.64	-16.9554
9.658	-17.3243
9.676	-17.6791
9.694	-17.9915

Frequency [GHz]	S_{21} [dB]
9.712	-18.2148
9.73	-18.2824
9.748	-18.1175
9.766	-17.6619
9.784	-16.9124
9.802	-15.9347
9.82	-14.84
9.838	-13.7476
9.856	-12.7564
9.874	-11.9325
9.892	-11.3064
9.91	-10.8774
9.928	-10.6241
9.946	-10.5163
9.964	-10.5239
9.982	-10.6224
10	-10.7938
10.16667	-10.8811
10.185	-11.0309
10.20333	-11.1834
10.22167	-11.3444
10.24	-11.5196
10.25833	-11.7137
10.27667	-11.9313
10.295	-12.1754
10.31333	-12.4484
10.33167	-12.7518
10.35	-13.0862
10.36833	-13.4519
10.38667	-13.8489
10.405	-14.2772
10.42333	-14.7372
10.44167	-15.2299
10.46	-15.7572
10.47833	-16.3218
10.49667	-16.9278
10.515	-17.5806
10.53333	-18.2873
10.55167	-19.0569
10.57	-19.9006
10.58833	-20.8318

Frequency [GHz]	S_{21} [dB]
10.60667	-21.8655
10.625	-23.0166
10.64333	-24.2923
10.66167	-25.6727
10.68	-27.0606
10.69833	-28.1922
10.71667	-28.6234
10.735	-28.076
10.75333	-26.7981
10.77167	-25.2393
10.79	-23.6785
10.80833	-22.222
10.82667	-20.8934
10.845	-19.687
10.86333	-18.5885
10.88167	-17.583
10.9	-16.6568
10.91833	-15.7985
10.93667	-14.9985
10.955	-14.2488
10.97333	-13.5429
10.99167	-12.8753
11.01	-12.2416
11.02833	-11.6382
11.04667	-11.0618
11.065	-10.5101
11.08333	-9.98092
11.10167	-9.47257
11.12	-8.98365
11.13833	-8.51302
11.15667	-8.05974
11.175	-7.62302
11.19333	-7.20224
11.21167	-6.79686
11.23	-6.40646
11.24833	-6.03069
11.26667	-5.66928
11.285	-5.32207
11.30333	-4.98894
11.32167	-4.66989
11.34	-4.36502

Frequency [GHz]	S_{21} [dB]
11.35833	-4.07452
11.37667	-3.79872
11.395	-3.53805
11.41333	-3.29304
11.43167	-3.06437
11.45	-2.85276
11.46833	-2.65906
11.48667	-2.48416
11.505	-2.32905
11.52333	-2.19481
11.54167	-2.08265
11.56	-1.99406
11.57833	-1.93094
11.59667	-1.8959
11.615	-1.89264
11.63333	-1.92652
11.65167	-2.00504
11.67	-2.13807
11.68833	-2.33636
11.70667	-2.60545
11.725	-2.93034
11.74333	-3.2519
11.76167	-3.46372
11.78	-3.47689
11.79833	-3.30613
11.81667	-3.04905
11.835	-2.79681
11.85333	-2.59553
11.87167	-2.45812
11.89	-2.38303
11.90833	-2.36483
11.92667	-2.39827
11.945	-2.47917
11.96333	-2.60433
11.98167	-2.77101
12	-2.97658

4.6 References

V Krushna Kanth, and S Raghavan, “Ultrathin wideband slot and patch FSS elements with sharp band edge characteristics”, *International Journal of Electronics*, vol.107,no.9,pp.1365–1385,2020. https://doi.org/10.1080/00207217.2020.1726493

D. D, S. Paik, B. S. Raghav and J. Rahul Babu, "An FSS Based Dual-band Bandstop Filter for Minimizing Interference in C Band Satellite Downlink Communication",*2023 4th International Conference for Emerging Technology (INCET*), Belgaum, India, pp. 1-4, 2023doi: 10.1109/INCET57972.2023.10170412.

S.Maity, T.Tewary, S.Mukherjee, A.Roy, P.P.Sarkar, S.Bhunia,“Wideband hybrid microstrip patch antenna and gain improvement using frequency selective surface”,*International Journal of Communication Systems*, vol. 35, no.14,2022. https://doi.org/10.1002/dac.5268

Pablo B. C. Medeiros, Valdemir P. Silva Neto, Adaildo G. D'Assunção,“A compact and stable design of FSS with radial slit circular elements using an iterative method”,*Microwave and Optical Technology Letters*, vol.57,no.3,2015.https://doi.org/10.1002/mop.28942

Khalil,T., Riaz,M.A., Shahid,H., Khan, M.J., Amin, Y,“Compact Frequency Selective Surface for X-band Shielding”,*International Journal of Innovation in Science and Technology*,vol.3, no.4, pp.140-152, 2021.

Catton, G.D., Espinosa, H.G., Dewani, A.A., keefe, S.G.O.,“Miniature Convoluted FSS for Gain Enhancement of a Multiband Antenna”,*IEEE Access*, vol.9, 36898,2021.

Seyfollah Khajevandi , Homayoon Oraizi , Amrollah Amini, Mohammad Poordaraee,“Design of miniaturised-element FSS based on 2.5-dimensional closed-loop Hilbert fractal”, *IET Microwaves, Antennas & Propagation*, 2019. https://doi.org/10.1155/2015/614780

R Bhattacharyya, P D Sinha, P P Sarkar, “A Compact Frequency Selective Surface with Multi Frequency Operation*”, International Journal of Electronics and Communication Engineering*, vol.9, no.1, 2016.

S Saha, S Chatterjee, R Basak,“Miniaturized Dual Band Frequency Selective Surface Suitable for C and S Band in Satellite Communication”,*International Journal of Advanced Research in Electronics and Communication Engineering*, vol.7, no.2, pp. 98-100,2018.

A Chatterjee, D Sharma, D Chandra, P.P.Sarkar,“Theoretical and Experimental Investigation on a Slot Loaded Compact Multi-band FSS”, *Astronomy*,2012.

S Mondal, S Nandi, T Mondal, S Singh, P.P.Sarkar,“Studies on Compact Multiple Resonant FSS by Cutting Different Novel Shaped Slits Within Rectangular Shaped Patch”,*5th International Conference on Computers and Devices for Communication (CODEC)*,2012.

L. Mingyun, H. Minjie, W. Zhe, “Design of Multi-band Frequency Selective Surface Using Multi Periodicity Combined Elements”, *Journal of Systems Engineering and Electronics*, vol.20, no. 4, pp.675-680, 2009.

Z. Yao, S. Xiao, Y. Li and B. -Z. Wang, "On the Design of Wideband Absorber Based on Multilayer and Multiresonant FSS Array”,*IEEE Antennas and Wireless Propagation Letters*, vol. 20, no. 3, pp. 284-288, March 2021.

doi: 10.1109/LAWP.2020.3046010.

A. Ghosh, A. Banerjee, S. Das, “Design of Compact Polarisation Insensitive Triple Bandstop FSS with High Stability under Oblique Incidence.”, *Radioengineering*, 2019.

M. Bilal, N.Saleem, A. Quddus, A.Ali, A.Rehman, S.Z.Jan, M. F. Shafique, “ A Compact Tri- Band EM- Shield for 5G/X/Ku-Band Indoor Wireless Applications.”, *Wireless Personal Communications*, vol.130, no.4, pp.3027-3045,2023

S.Das, R.C.Tiwari, L.L.K.Singh, P.P.Sarkar, “Design of a Compact Triband Frequency Selective Surface”, *International Conference on Recent Innovation in Science, Computing and Communication (RISCC 2024)*,2024.

S.Das, R.C.Tiwari, L.L.K.Singh, P.P.Sarkar, “Design of Compact Frequency Selective Surface Comprising of Slot and Slit Loaded Square Patch Elements.” *TANZ Research Journal*, vol.11, no.3,2025.

T.K. Wu, ―Frequency Selective Surface and Grid Array‖, Jhon Wiley & Sons.Inc., Nework,1995, ch 1, pp 5-6, ISBN 0-471-31189-8.

CHAPTER 5

Design of a Frequency Selective Surface as Absorber

5.1 Introduction

The development of technology forced the entire world to live amidst the microwave frequency spectrum. Although the development of microwave systems were boon to the society, whereas the extensive usage of microwave devices in daily life to the fortification of the defense systems put forward the requirement of the suppression of the electromagnetic signals. In radar systems, heretofore the detected unwanted frequencies were reflected in other directions, whereas the chances of detection of these reflected frequencies become too high with the development of multistatic radar systems. Hence, unwanted frequencies should be absorbed to improve the stealth capability of the radar systems [1]. Subjection to electromagnetic radiation for long time is not good for living being. Exposure to electromagnetic radiation effectuate to health issues like Alzheimer's, Brain and ear tumour, motor neuron disease etc. [2]. The cardinal cycle disturbance is the cause of exposure to electromagnetic radiation, which affects the normal secretion of Melatonin hormone. The continuous reaction of electromagnetic radiation with the increasing cells adversely influence the developing embryo and thinnen the placenta barrier fluid [3,4]. Electromagnetic radiation interferes in the cultivation of the crops like paddy, wheat etc., and reduces the productions of the crops. The radiation is also responsible to reduce the outturn of the fruit bearing trees from 100% to 5% [5]. A study suggested that the tolerance to the microwave radiation of small creatures is positively correlated with its mass and is the strong reason of declination in bird population [6]. The present state of art in technology indicates to the reality that electromagnetic radiation is unavoidable. At the same time, the utter need of suppression of electromagnetic radiation can be comprehensible in vision of the documented facts. The requisite of electromagnetic wave suppression initiate the study of absorption technology. Frequency Selective Surface (FSS) which has been studied broadly for the purpose of blocking and passing of the electromagnetic signal, are now has to be explored for absorption purpose.

The foundation of absorption technology was proffered during early nineteenth century for military application. The absorption of electromagnetic wave had been done at first by Salisbury screen [7,8]. Thereafter the advancement of absorption technology progressed with Jaumann absorber and Circuit Analog absorber [9, 10]. Later, the application of absorptive material like resistive ink, resistive sheets, and magnetic sheets enhances the absorption capacity [11, 12]. Presently, the absorption technology advances focusing on frequency selective surface [13]. FSS based absorber also depends on magnetic and resistive absorbing materials [14, 15]. Multiresonant FSS absorber has been designed with multiple layers consisting of resistive loaded square loop FSS backed by metallic ground plane [16]. A back to back FSS absorber formed a decoupling structure, where resistive pattern has been imprinted on the dielectric structure backed by electromagnetic reflector structure [17]. It has been observed that the documented studies on FSS absorber either depends on absorptive material or on the ground plane. The total cost of the composite absorber increases as absorbing materials are costlier.

The objective of this chapter is to design and study an FSS absorber without utilizing any absorbing material or ground plane. The blocking property of the conventional frequency selective surface has been utilized in more than one layers to attain the absorption of the electromagnetic signals in desired frequency band. Firstly, a three layer FSS composite absorber has been designed imprinting simple elemental structures, which exhibit multiband absorption [18]. The size of the FSS absorber has been then reduced by proposing a simple elemental design consisting of two layers. The composite FSS absorber depicts enhance multiband absorption [19].

5.2 Design of FSS absorber

Fr4-epoxy has been considered as substrate for both the design presented in this section. A three layer and a two layer FSS absorber have been presented here by exploiting the bandstop property of the conventional FSSs. Square type patch elements has been considered for the purpose and the modification of the square patches have been done according to requisite.

5.2.1 Design of three layer FSS absorber

A three layer FSS absorber has been designed considering Fr4-epoxy as substrate of thickness 1.6 mm for all the three layers. The periodicity of 25 mm has been considered for both the dimensions of the plane for all three layers. A square patch of dimension 24 mm X 24 mm has been considered for the designing of the bottom layer. The square patch is then modified incorporating square slots and slits as shown in Fig.5.1. The middle layer has been designed with two square patches of dimension 6.5 mm and 9.5 mm imprinted on both sides of the substrate. This layer is placed at a distance of 4 mm from the bottom layer. The unit cell representation of top and bottom of the middle layer has been presented separately in Fig.5.2 and Fig.5.3 respectively. Two square patches of dimension 15 mm and 9.4 mm have been embossed on both sides of the substrate to design the upper layer. This layer has been placed at a distance of 3 mm from the middle layer. The unit cell representation of top and bottom of the upper layer have been presented separately in Fig.5.4 and Fig.5.5 respectively. The composite FSS absorber designed in ANSYS HFSS software has been shown in Fig.5.6.

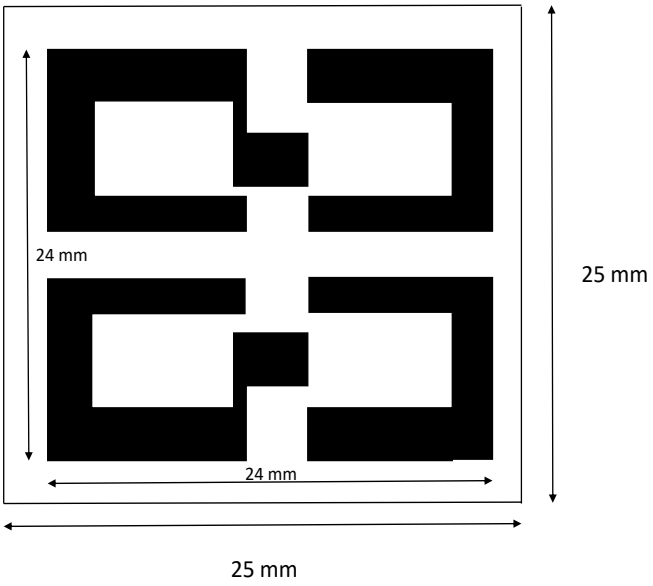

Fig.5.1. Square patch imprinted on top of the substrate representing unit cell of the bottom layer of the FSS absorber

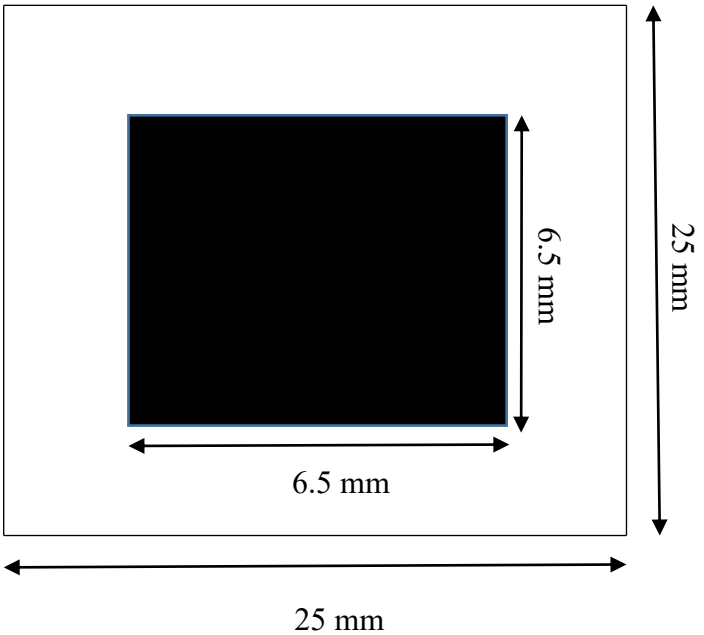

Fig.5.2. Square patch imprinted on top of the substrate representing unit cell of the middle layer of the FSS absorber

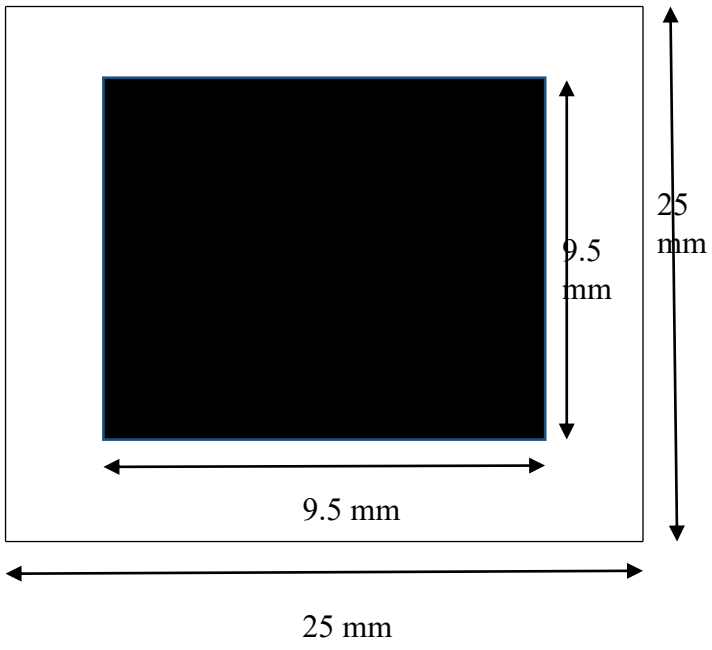

Fig.5.3. Square patch imprinted on bottom of the substrate representing unit cell of the middle layer of the FSS absorber

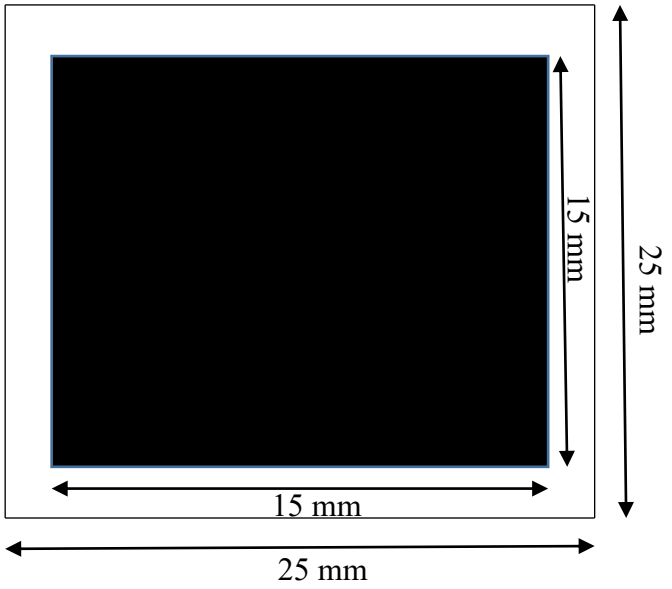

Fig.5.4. Square patch imprinted on top of the substrate representing unit cell of the top layer of the FSS absorber

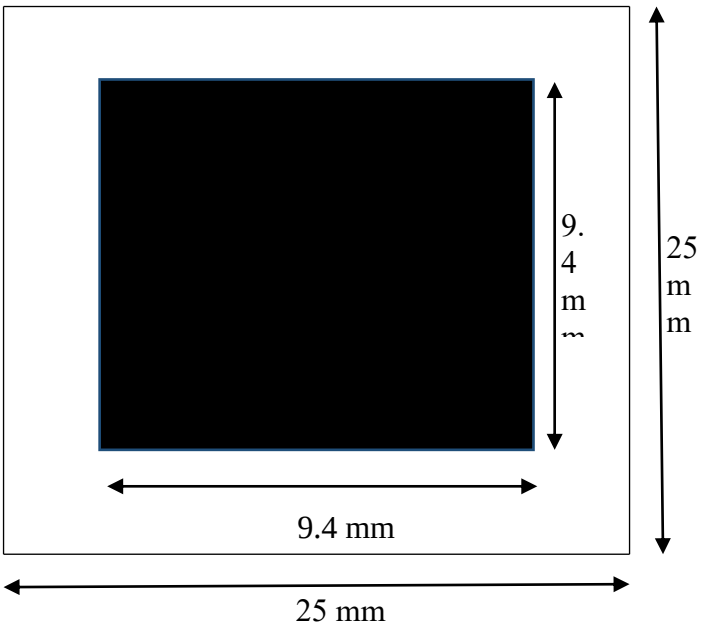

Fig.5.5. Square patch imprinted on bottom of the substrate representing unit cell of the top layer of the FSS absorber

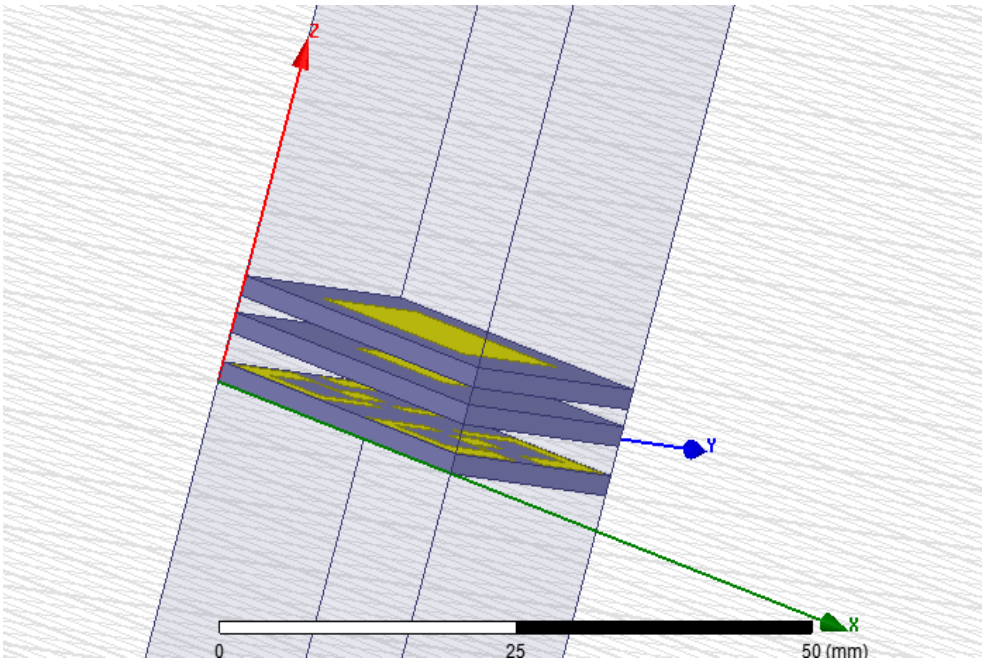

Fig.5.6. Unit cell representation of composite FSS absorber

5.2.2 Design of two layer FSS absorber

A two layer FSS absorber has been designed with periodicity of 22 mm X 22 mm. FR4-epoxy of thickness 1.6 mm and 0.8 mm have been chosen as the substrate for

the lower and upper layer respectively, of the two layer FSS absorber. Fig.5.7 shows the patch imprinted on one side of the substrate that will serve as top layer. The patch comprise of five L shaped patches of width 1.2 mm oriented by 90 degree, enclosed by a square loop patch of width 1 mm. Two slots of dimension 1.2 mm X 1 mm have been inserted in the outer square loop patch. The dimensions considered for the designing of the patch has been shown in Fig.5.7. On the other side of the substrate, a square patch of dimension 21.2 mm has been modified by inserting slots and slits, which will serve as bottom layer. The unit cell representation of the bottom layer is shown in Fig.5.8. This single layer produces a narrow absorption band which will be discussed in the result section. A square patch of dimension 9.7 mm X 9.7 mm has been imprinted on the substrate of thickness 0.8 mm as shown in Fig.5.9. This layer has been added as the superstrate to the bottom layer at a distance of 1 mm from it. The entire composite structure of the two layer FSS absorber designed in ANSYS HFSS software has been depicted in Fig.5.10.

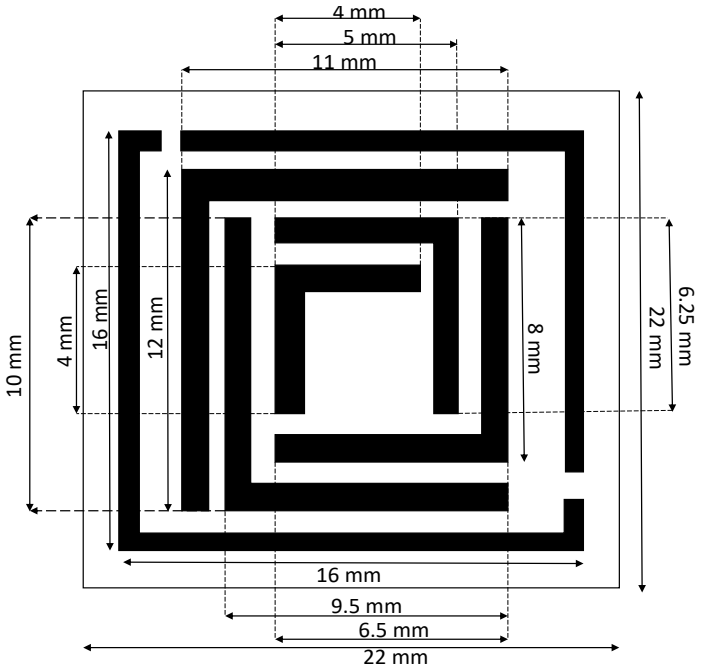

Fig.5.7. Patch imprinted on top of the substrate representing unit cell of the top of the lower layer of the FSS absorber

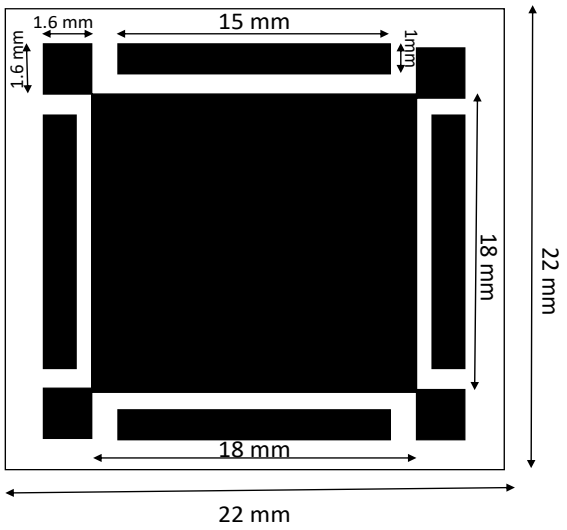

Fig.5.8. Patch imprinted on bottom of the substrate representing unit cell of the bottom of lower layer of the FSS absorber

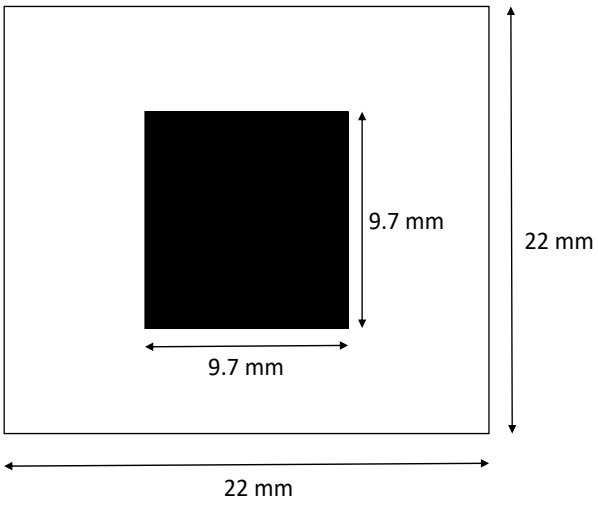

Fig.5.9. Unit cell representation of the superstrate where the square patch is imprinted on the bottom of the substrate

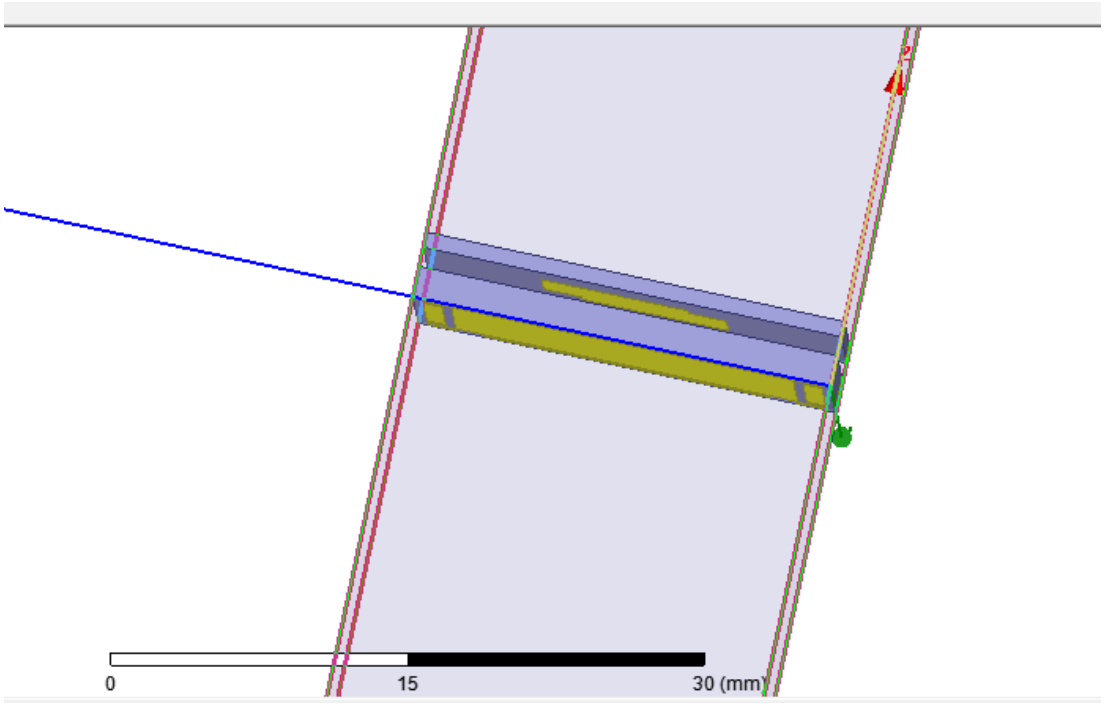

Fig.5.10. Unit cell representation of composite FSS absorber

5.3 Results & Discussion

All the designed structures have been simulated by using ANSYS HFSS software. At first, the transmission and reflection characteristics of all the individual layers have been studied. Henceforth, the study of combination of the layers have been set forth. Absorption coefficients have been determined from the transmission/reflection characteristics curves of the three layer or two layer composite FSS absorber and are plotted against frequency to obtain a clear view of the maximum and minimum absorption capacity of the FSS absorbers.

5.3.1 Study of three layer FSS absorber

The bandstop property of the conventional patch type FSS has been utilised to design the three layer FSS absorber. The transmission/ reflection characteristics of all the individual layers have been furnished in Fig.5.11, Fig.5.12 and Fig.5.13. These three layers are integrated to obtain absorption in microwave frequency. The dimensions of the patches, periodicity of the FSS and thickness of the substrate are the factors responsible for the attainment of absorption peak. The transmission/ reflection characteristics of the composite three layer FSS absorber has been shown in Fig.5.14.

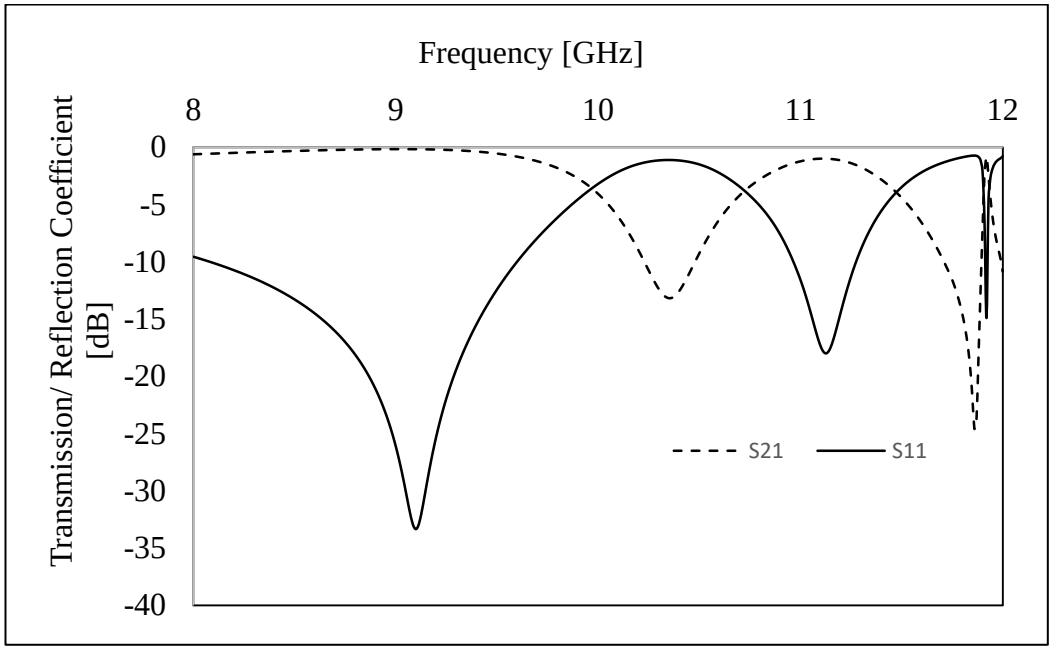

Fig.5.11. Transmission/ Reflection Characteristic of top layer of the three layer FSS absorber by combining Fig.5.4 & Fig.5.5

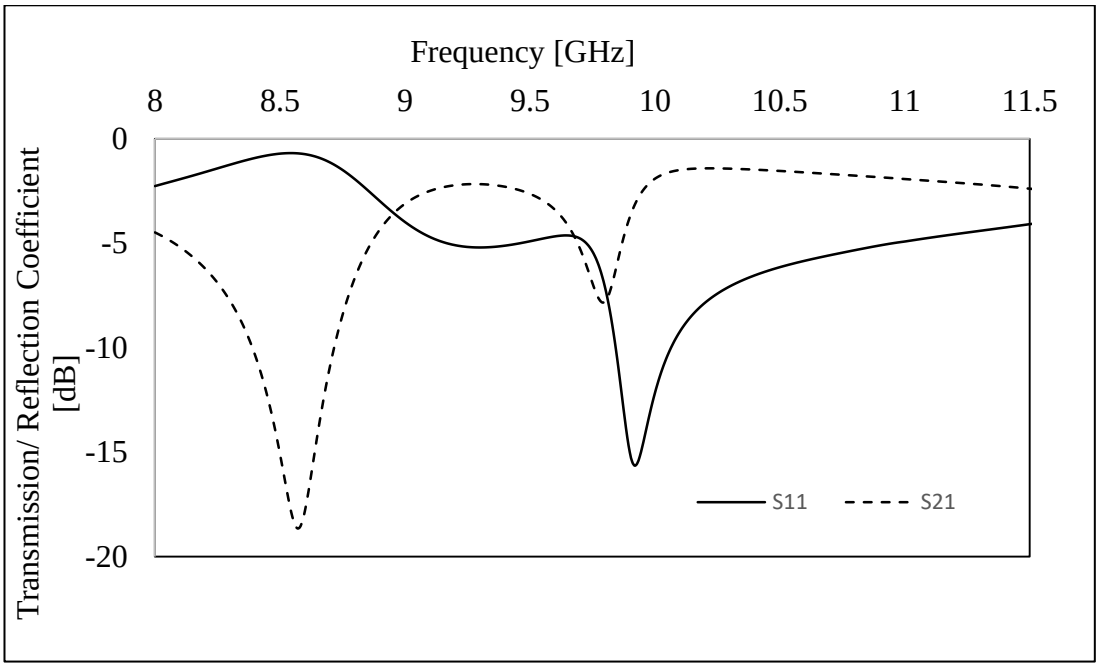

Fig.5.12. Transmission/ Reflection Characteristic of middle layer of the three layer FSS absorber by combining Fig. 5.2 & Fig. 5.3

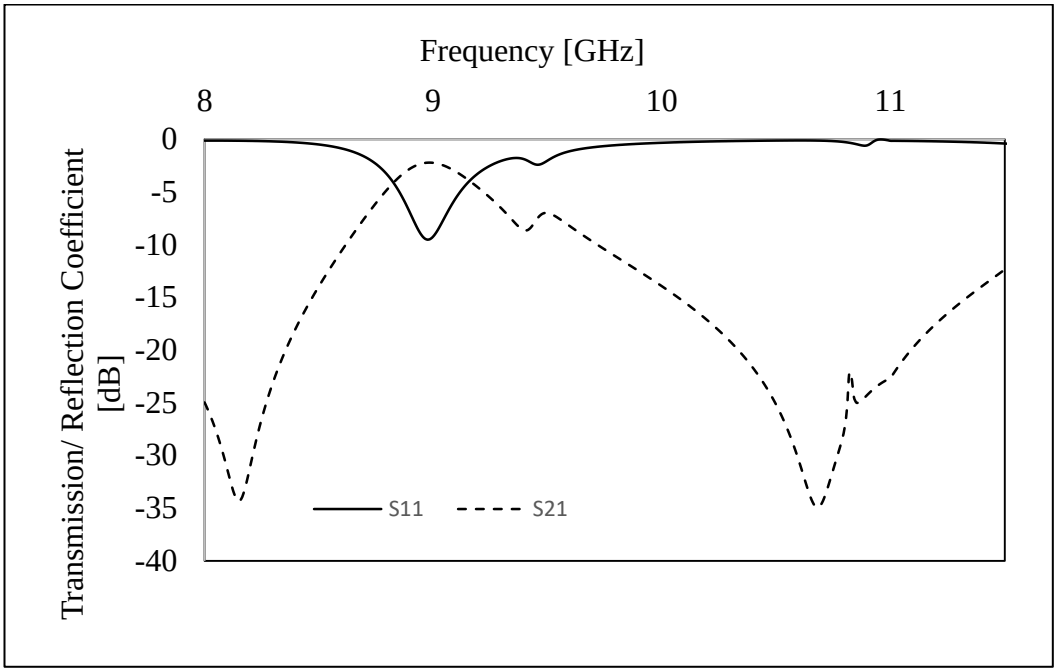

Fig.5.13. Transmission/ Reflection Characteristic of bottom layer of the three layer FSS absorber shown in Fig.5.1

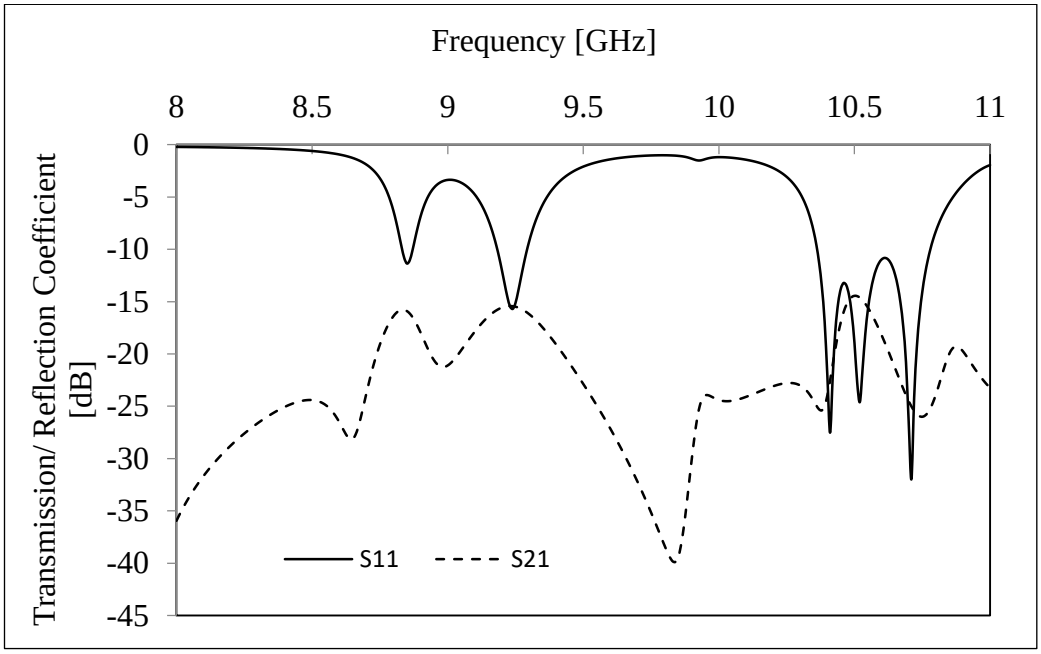

Fig.5.14. Transmission/ Reflection Characteristic of three layer FSS absorber

Fig.5.14 depicts that the three layer FSS absorber attains three absorption band in the frequency range of 8.82 GHz to 8.86 GHz, 9.17 GHz to 9.28 GHz and 10.35 GHz to 10.77 GHz. In all the three layers the bandstop property of the conventional FSS has

been utilised. Proper optimization and selection of the dimension of the elements result into the absorption band of bandwidths 40 MHz, 110 MHz and 420 MHz. The absorption characteristics of the three layer FSS absorber has been shown in Fig.5.15. A maximum of 90% absorption and minimum of 81% absorption have been attained by the composite FSS absorber in the frequency range of 8.82 GHz to 8.86 GHz. In the frequency range of 9.17 GHz to 9.28 GHz the maximum absorption percentage is 94.4% and the minimum absorption percentage is 80%. By staggering effect, the FSS absorber achieved a maximum of 99.62% absorption and minimum of 81% absorption in the frequency range of 10.35 GHz to 10.77 GHz. All the highlighted portion in Fig.5.15 justify the observation documented here. The designed and simulated three layer FSS absorber can be used for stealth and shielding purpose in X-band of the microwave spectrum.

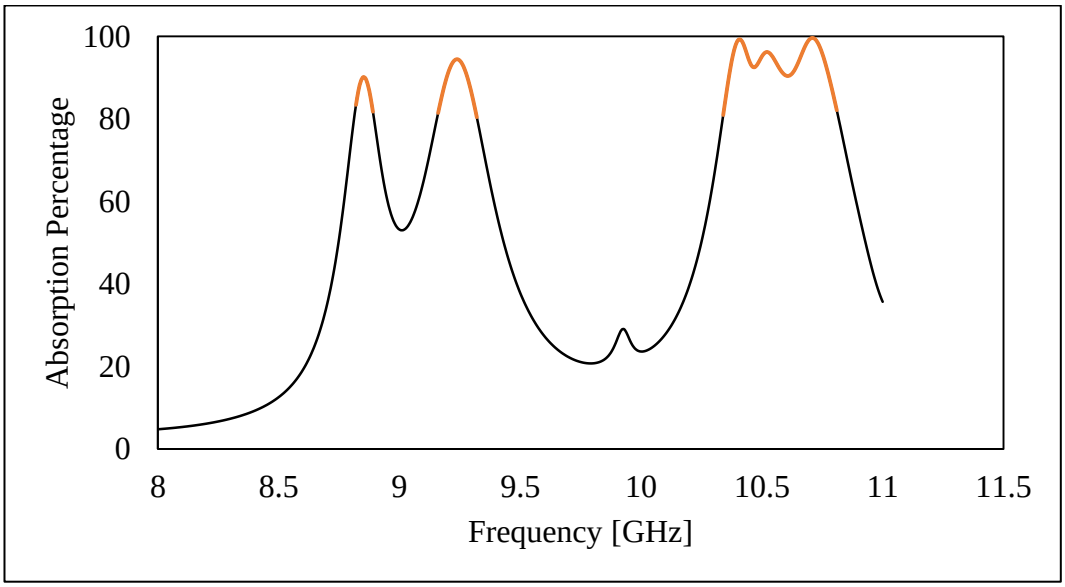

Fig.5.15. Absorption percentage vs frequency plot of three layer FSS absorber

5.3.2 Study of two layer FSS absorber

The transmission / reflection characteristics plot of the unit cell designed in Fig 5.7 and Fig.5.8 have been shown in Fig.5.16 and Fig.5.17 respectively. Embossing the patches shown in Fig 5.7 and Fig.5.8 respectively on top and bottom of a substrate accomplished two narrow absorption band as shown in Fig.5.18. Two absorption band of 50 MHz and 60 MHz have been observed in the plot shown in Fig.5.18, in the frequency range of 4 GHz to 7 GHz. Multiband absorption has been achieved

while a superstrate shown in Fig.5.9 has been included to the single layer FSS absorber mentioned here. The transmission/ reflection characteristics of the final two layer FSS absorber has been shown in Fig.5.19. Three absorption band of 153 MHz, 309 MHz and 240 MHz have been observed in the frequency range 6.530 GHz to 6.683 GHz, 7.418 GHz to 7.727 GHz and 8.896 GHz to 9.138 GHz respectively. Absorption percentage vs frequency of the design and simulated two layer FSS has been presented in Fig.5.20. It has been observed from the plot that, a minimum of 88% and maximum of 97% absorption is attained by the structure in the frequency range of 6.530 GHz to 6.683 GHz. In the frequency range of 7.418 GHz to 7.727 GHz, the minimum percentage of absorption is 89% and the maximum percentage of absorption is 97%. The structure achieved minimum and maximum percentage of absorption of 83% and 95% respectively in the frequency range of 8.896 GHz to 9.136 GHz.The designed two layer absorber is capable to absorb electromagnetic radiation efficiently in upper C and lower X band of microwave spectrum.

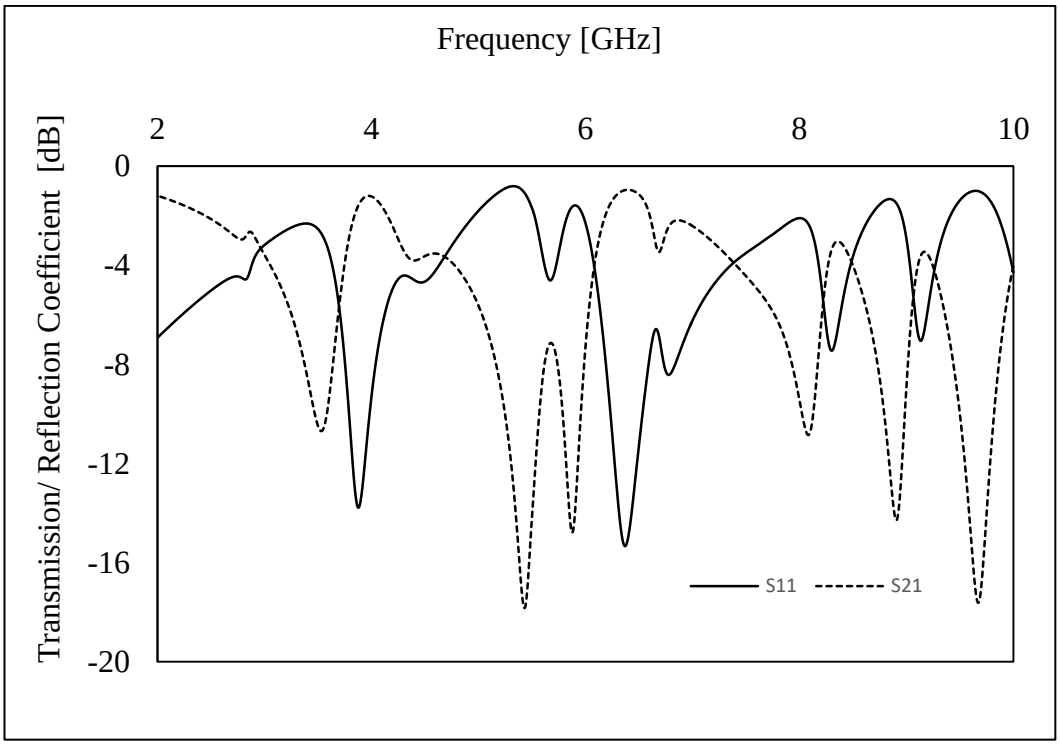

Fig.5.16. Transmission/ Reflection Characteristic of the patch shown in Fig.5.7

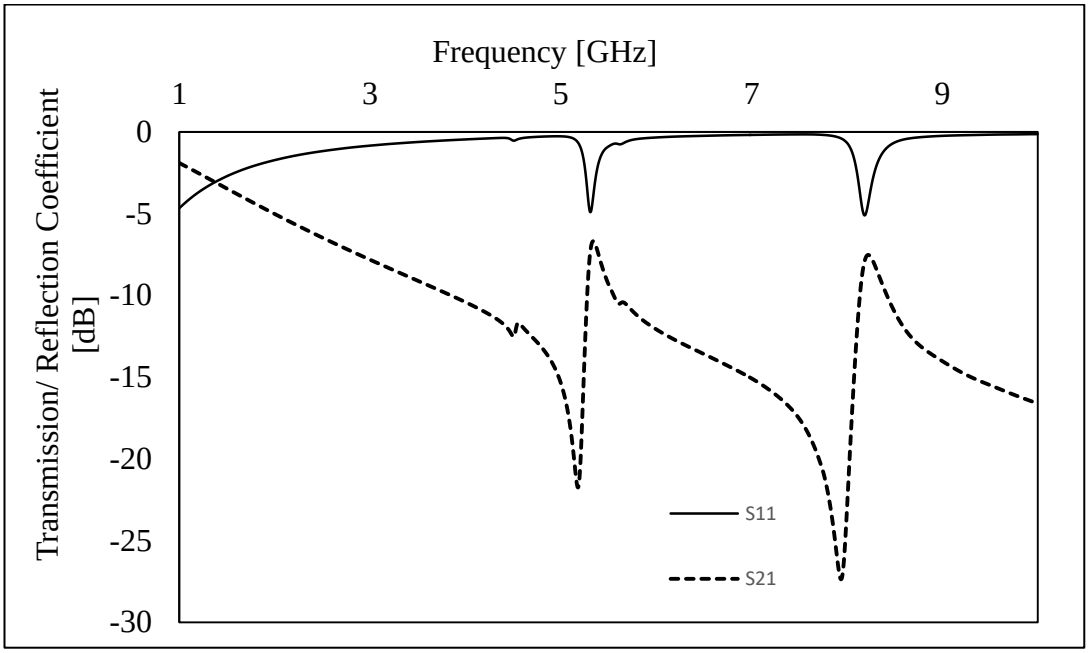

Fig.5.17. Transmission/ Reflection Characteristic of the patch shown in Fig.5.8

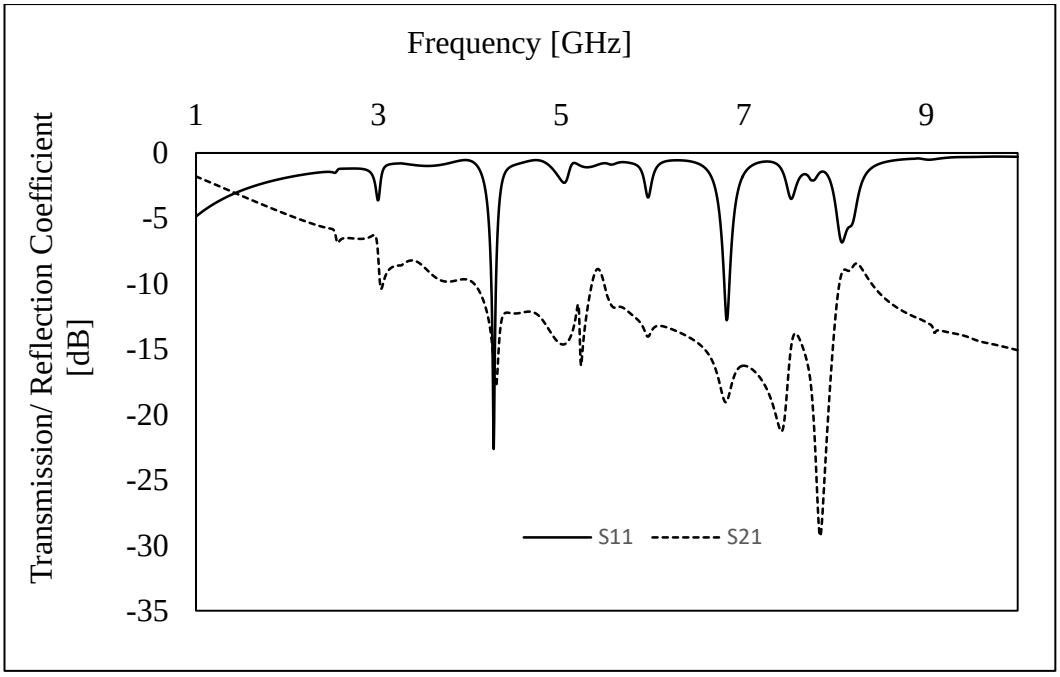

Fig.5.18. Transmission/ Reflection Characteristic of the combination of patches shown in Fig.5.7 & Fig.5.8

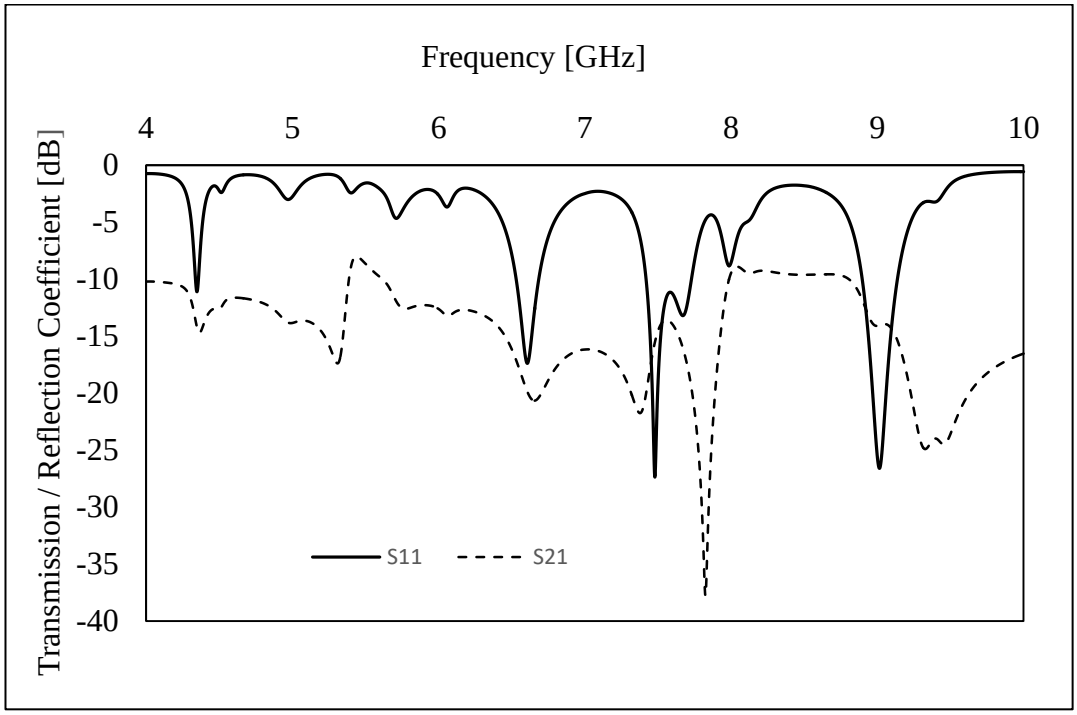

Fig.5.19. Transmission/ Reflection Characteristic of the two layer FSS absorber

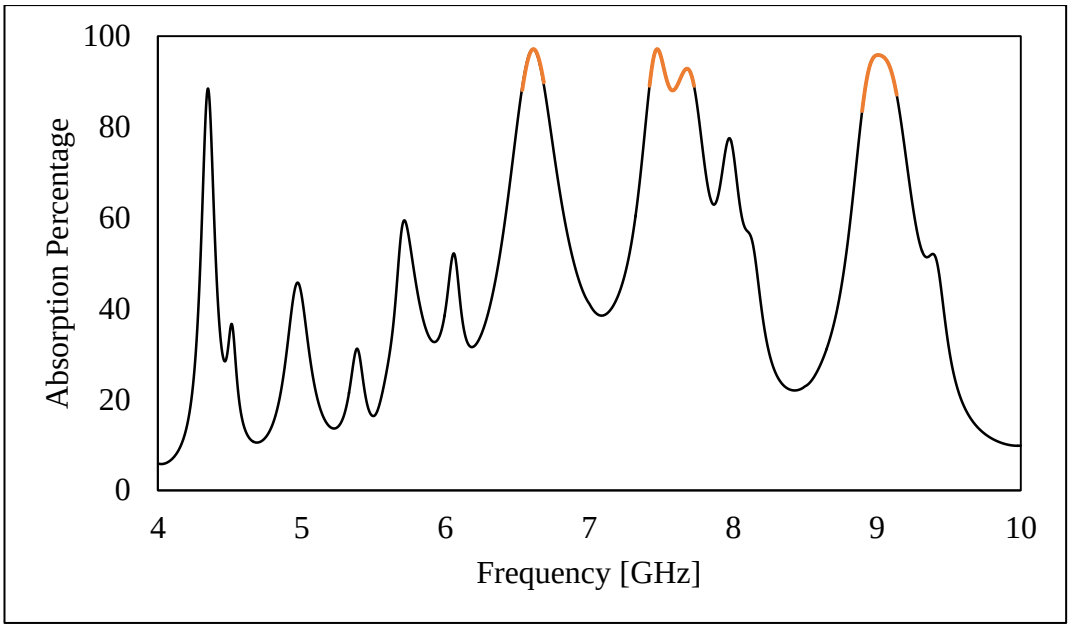

Fig.5.20. Absorption percentage vs frequency plot of the two layer FSS absorber

The detail study of three layer and two layer FSS absorber have been shown in table 5.1.

Table 5.1 Overview of the study of FSS absorber

Type of FSS Absorber	No. of bands	Total Thickness of the FSS [mm]	Maximum Absorption Percentage	Minimum Absorption Percentage
Three layer FSS	03	11.8	99.62%	80%
Two layer FSS	03	3.4	97%	83%

5.4 Conclusion

The FSS absorbers designed and studied here does not use any ground plane or costly absorbing materials, which claims the cost effectiveness of the designed absorber. The study of the FSS absorbers reveal that the absorption capacity of all the attained bands are above 90% , with the maximum of 99.62% for three layer absorber and 97% for two layer absorber. The high absorption capacity of the FSS absorbers can be efficiently utilized for the radiation shielding and absorption purposes. The FSS absorbers are capable to allow the desired frequencies of electromagnetic radiation by FSS' passband nature and absorb the undesired frequencies. Thus, the FSS absorbers studied in this chapter proves their worthiness to hide the Radar systems and can also be used for the purpose of obscuration of defence systems. Concomitantly, the absorbers can be used in window screens of hospitals and residences to reduce the ill effects of electromagnetic radiation. Prolong exposure to electromagnetic radiation results into health hazards, which can be minimized by the absorption of the undesired radiation using FSS absorbers. Conclusively, the study of FSS absorbers presented here are the leading lights manifesting the technological requirement of the time.

5.5 References

T. H. Brandão, H. R. D. Filgueiras, S. A. Cerqueira, J. F. Mologni and A. Bogoni, "FSS-based dual-band cassegrain parabolic antenna for RadarCom applications," *2017 SBMO/IEEE MTT-S International Microwave and Optoelectronics Conference (IMOC)*, Aguas de Lindoia, Brazil, pp. 1-4,2017. doi: 10.1109/IMOC.2017.8121131.

J H Kim, J K Lee, H G Kim, K B Kim, H R Kim, "Possible effects of radiofrequency electromagnetic field exposure on central nerve system", *Biomolecules & Therapeutics,* vol.27,no.3,pp.265-275,2018.

N Kumar, G Kumar, "Biological Effects of Cell Tower Radiation on Human Body", *ISMOT,* 2009.

J. C. Lin, "Human Exposure to RF, Microwave, and Millimeter-Wave Electromagnetic Radiation [Health Effects]," *IEEE Microwave Magazine*, vol. 17, no. 6, pp. 32-36, June 2016.doi: 10.1109/MMM.2016.2538540.

Abdelghafar M. AbuElsaoud, "Effect of Microwave Electromagnetic Radiofrequency on Germination and Seedling Growth Consequences of Six Wheat Triticum aestivum L. Cultivars", *Advances in Environmental Biology,* vol.9,no.24, pp. 270-280, November 2015.

K. K. Dhami, "The electromagnetic radiations and its impacts on bird diversity in India", *International Journal of Avian and Wildlife Biology",*vol.5, no.1, pp.5-7, 2020.DOI:10.15406/ijawb.2020.05.00166

P. G. Lederer, "Modelling of practical Salisbury screen absorbers," *IEE Colloquium on Low Profile Absorbers and Scatterers*, London, UK, pp. 1/1-1/4,1992.

Liming Yuan, Fei Dai, Yonggang Xu and Yuan Zhang, "Study on the millimeter-wave scale absorber based on the Salisbury screen", *Material Research Express,* vol.5,no.3,2018. DOI 10.1088/2053-1591/aab741

Fadil Kuyucuoglu, "A novel approach to the design of multi section ultra-wideband Jaumann absorber", *Optik,* vol.287,2023.

https://doi.org/10.1016/j.ijleo.2023.171152

S. Ghosh, S. Bhattacharyya and K. V. Srivastava, "Design and analysis of a broadband single layer circuit analog absorber," *2016 46th European Microwave Conference (EuMC)*, London, UK, pp. 584-587, 2016.doi:10.1109/EuMC.2016.7824410.

Y. Tayde, M. Saikia, K. V. Srivastava and S. A. Ramakrishna, "Polarization-Insensitive Broadband Multilayered Absorber Using Screen Printed Patterns of Resistive Ink", *IEEE Antennas and Wireless Propagation Letters*, vol. 17, no. 12, pp. 2489-2493, Dec. 2018.doi: 10.1109/LAWP.2018.2879274.

D. Wan, S. Bie, J. Zhou, H. Xu, Y. Xu, J. Jiang, "A Thin and Broadband Microwave Absorber Based on Magnetic Sheet and Resistive FSS.", *Progress in Electromagnetics Research*, vol.56, pp.93-100, 2015.

K. R. Jha, Z. A. P. Jibran and S. K. Sharma, "Absorption Peak Controlled Low-Frequency Wideband Flexible FSS Absorber," *IEEE Transactions on Electromagnetic Compatibility*, vol. 64, no. 4, pp. 975-986, Aug. 2022.doi: 10.1109/TEMC.2022.3159746.

Ning Liu, Jiaxin Li, Xianjun Sheng and Haoran Fu, "An equivalent circuit model based design method for wideband absorber using resistive FSS." *Physica Scripta*, vol. 99,no.9, 2024.

V. Violi, D. Brizi and A. Monorchio, "Ultra-Thin Wide-Band Multilayer FSS-Based Magnetic Absorber," *2024 IEEE International Symposium on Antennas and Propagation and INC/USNC-URSI Radio Science Meeting (AP-S/INC-USNC-URSI)*, Firenze, Italy, pp. 1817-1818, 2024.
doi: 10.1109/AP-S/INC-USNC-URSI52054.2024.10686154.

Z. Yao, S. Xiao, Y. Li and B. -Z. Wang, "On the Design of Wideband Absorber Based on Multilayer and Multiresonant FSS Array," *IEEE Antennas and Wireless Propagation Letters*, vol. 20, no. 3, pp. 284-288, March 2021.doi: 10.1109/LAWP.2020.3046010.

F. Merzaki et al., "A Compact Double-Sided FSS Absorbing Wall for Decoupling 5G Antenna Arrays," *IEEE Transactions on Electromagnetic Compatibility*, vol. 64, no. 2, pp. 303-314, April 2022.doi: 10.1109/TEMC.2021.3129368.

Saptarsika Das, R.C.Tiwari, L.L.K.Singh, P.P.Sarkar, "Design of a Multiband FSS Absorber", *International Conference on Sustainable Technologies (ICST-2024)*,2024.

Saptarsika Das, R.C.Tiwari, L.L.K.Singh, P.P.Sarkar, "Design of Frequency Selective Surface as Multiband Absorber*", Journal of Systems Engineering and Electronics*, vol.35, issue-2, pp.75-81, February 2025.

Chapter 6

Summary and Conclusion

The design, analysis and characterization of different types of frequency selective surfaces and frequency selective absorber have been presented in this research. The FSSs have been designed and studied from L-band to X-band of the microwave spectrum.

In the first instance, a cross dipole FSS has been theoretically formulated using MOM numerical technique and by MATLAB programming. The FSS has been designed in the C-band of the microwave spectrum. The designed FSS has been simulated by using ANSYS ANSOFT software. The designed FSS has been fabricated and experimented exhibit bandstop property. The result obtained by the MATLAB programming shows a good agreement with the experimentally obtained results. Hence establishes the fact that the theoretical formulation has been done by us with ample accuracy and is better than that of the result generated by the software.

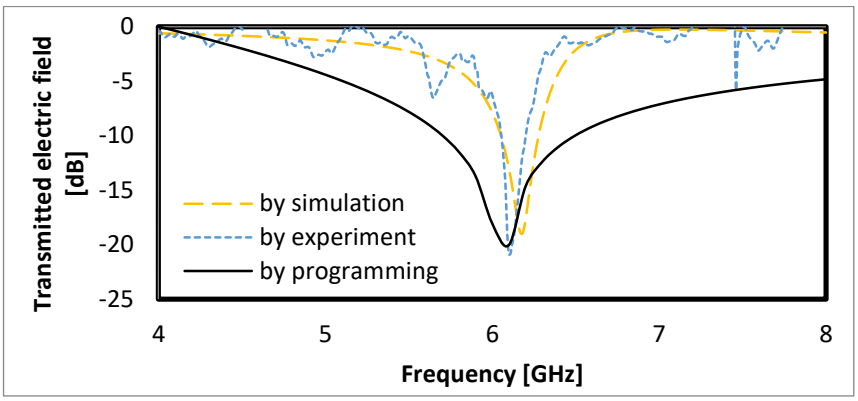

Transmission coefficient vs frequency graph of the cross dipole FSS

The planar and curved FSS have been designed in X and Ku band of the microwave spectrum. Focus have been given to the characterization of insertion loss, roll-off and flat band. The success of the documented design is the fractional bandwidth remain unaltered while transforming the planar FSS into curved FSS. For both the cases, sharp roll-off have been attained on both the edges of the transmission characteristic curve. The insertion loss obtained for planar and curved FSS are low.

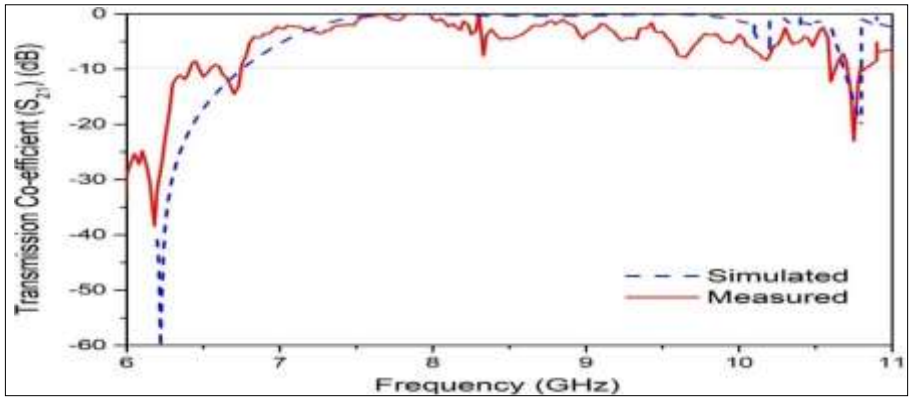

Transmission coefficient vs frequency plot of composite planar FSS

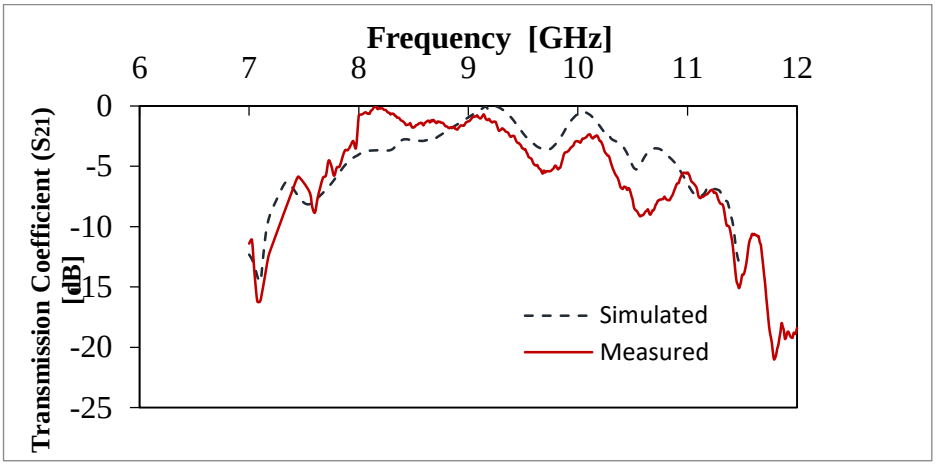

Transmission coefficient vs frequency plot of composite curved FSS

The demand of handheld devices wants compact wireless systems, therefrom the requirement of compact FSS emerges. FSS have been designed and modified with simple elements throughout the documented work. All the structures reported reduction of size above 90%, with highest size reduction of 97.28% experimentally. The compact FSS have been designed in C, L, S, X and Ku band with multiple band of operation. The multiband compact FSSs designed and documented in the chapter fulfil the requirement of multifunctional FSS in microwave spectrum.

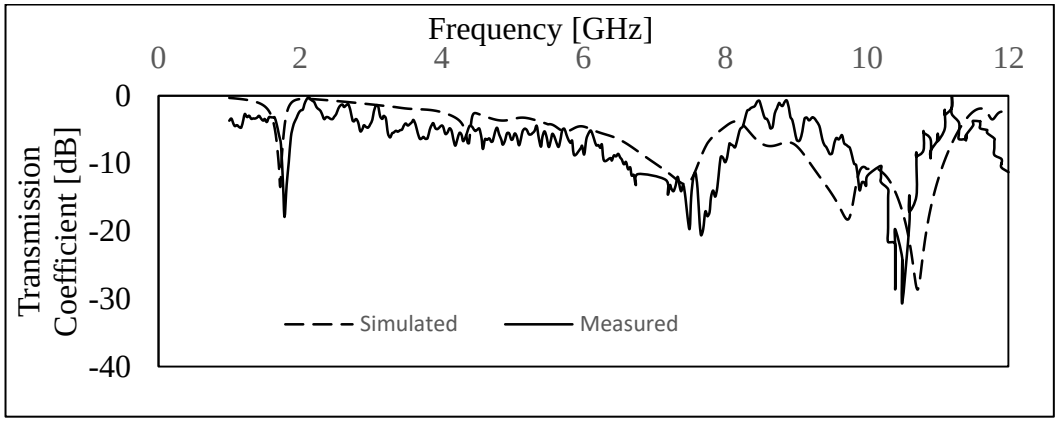

Transmission coefficient vs frequency curve of the FSS prototype that achieved best compactness

The presented FSS absorbers have been designed in the C and X band of the microwave spectrum without using any absorbing material. Both the three layer and two layer FSS absorbers attain absorption percentage above 90% for all the absorption bands. The highest absorption percentage of the three layer FSS is 99.62% and that of two layer is 97%. The documented FSS absorbers are cost effective and can be judiciously integrated with the microwave systems associated with stealth and absorption purposes.

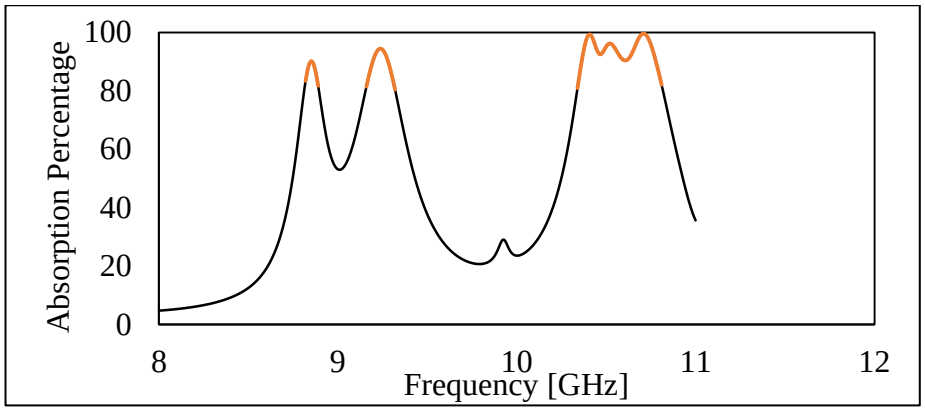

Absorption percentage vs frequency plot of three layer FSS absorber

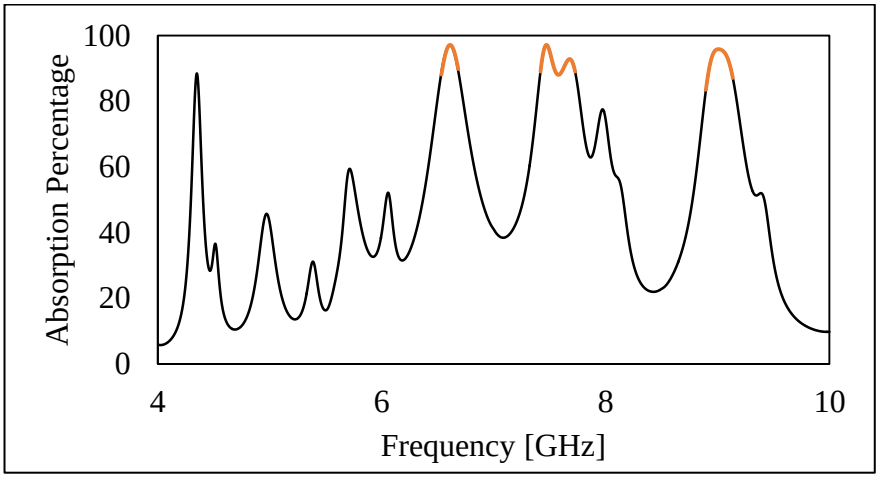

Absorption percentage vs frequency plot of the two layer FSS absorber

The documented FSSs manifest the characteristics of passband or stopband for a fixed range of frequency of operation. In future, we may design tunable FSS where the passband or the stopband will be varied by incorporating PIN or varactor diode with the FSS, where the variation can be controlled by changing the voltage of PIN or varactor diode.

In the documented works, the FSS has been designed either as stopband FSS or as passband FSS. In future, reconfigurable FSS will be designed by us using LDR or by exploiting the on and off state feature of PIN or varactor diode.

In case of FSS absorber, we will also explore the tunable property to change the operating region and the reconfigurable property to use a single FSS as absorber FSS and passband or stopband FSS.

BIO-DATA OF THE CANDIDATE

Name of Candidate	:	Saptarsika Das
Date of Birth	:	02/01/1982
Contact	:	8336993834
Permanent Address	:	Kalianibash North, P.O- Nona Chandan Pukur Kolkata-700122, West Bengal, India.
Married	:	Yes
Educational Details	:	
B.Sc	:	Electronics Honours , Calcutta University (2002), West Bengal, with 69.87%
M.Sc	:	Electronic Science, Calcutta University (2004), West Bengal, with 65.83%
Ph.D Course Work	:	Mizoram University, SGPA of 9.43

LIST OF PUBLICATIONS

Referred Journals

SCI

1. Saptarsika Das, Ramesh Chandra Tiwari, Lourembam Lolit Kumar Singh, Nurnihar Begum, Rahul Mondal, Partha Pratim Sarkar, Durjoy Roy, "Design of Dual Layer Curved Cylindrical FSS with Sharp Roll-Off and Flat Bandpass Property", *Microwave Journal*, vol.67, no.4, 2024.

SCOPUS

1. Saptarsika Das, Anirban Bhattacharya, Santanu Mondal, Partha Pratim Sarkar, "Development of Method of Moment Based Programme to Analyze Cross Dipole Frequency Selective Surface and its Verification with Measured Results*", International Journal of Innovative Technology and Exploring Engineering(IJITEE)*,vol.9 issue-8,pp.1019-1023, 2020.
2. Saptarsika Das, Ramesh Chandra Tiwari, Lourembam Lolit Kumar Singh, Partha Pratim Sarkar, "Design of Frequency Selective Surface as Multiband Absorber", *Journal of Systems Engineering and Electronics*, vol.35, no.2,pp.75-81,2025.
   https://doi.org/10.5281/zenodo.14811874
3. Saptarsika Das, Ramesh Chandra Tiwari, Lourembam Lolit Kumar Singh, Partha Pratim Sarkar, "Design of compact frequency selective surface comprising of slot and slit loaded square patch elements", *TANZ Research Journal*,vol.11, no.3, pp.118-127, 2025.
   DOI:10.6084/doi.25.11.3.TANZ220016

International Conferences

1. Saptarsika Das, Ramesh Chandra Tiwari, Lourembam Lolit Kumar Singh, Partha Pratim Sarkar, "Design of Compact Tri-band Frequency Selective Surface", presented in *1st International Conference on Recent Innovation in*

2. *Science, Communication & Computation 2024*, JIS University, West Bengal, India, pp.87-95, 2024.
3. Saptarsika Das, Ramesh Chandra Tiwari, Lourembam Lolit Kumar Singh, Partha Pratim Sarkar, "Design of a Multiband FSS Absorber" in *First International Conference on Sustainable Technologies (ICST-2024*), Microsystem Design-Integration Lab Bidhan Chandra College, WB, India,12-15th December 2024

Microwave Journal
Frequency Matters.

www.microwavejournal.com/articles/41755-design-of-dual-layer-curved-cylindrical-fss-with-sharp-roll-off-and-flat-bandpass-property

Design of Dual-Layer Curved Cylindrical FSS with Sharp Roll-Off and Flat Bandpass Property

Saptarsika Das, Ramesh Chandra Tiwari and Lourembam Lolit Kumar Singh, Mizoram University, Mizoram, India, Nurnihar Begam, Rahul Mondal and Partha Pratim Sarkar, University of Kalyani, West Bengal, India, and Durjoy Roy Rishi Bankim, Chandra College, Naihati, West Bengal, India
April 12, 2024

The frequency selective surface (FSS) has been the subject of extensive research for the last three decades. An FSS acts like a bandpass or bandstop filter at microwave frequencies. Extensive research has been done on bandwidth enhancement and the decrease of insertion loss, for example, but this work has been done mainly on planar FSSs. Very little work has been done on curved FSSs. The design of a dual-layer curved cylindrical FSS with the sharp roll-off and flat bandpass properties described here can reduce interference and increase channel capacity in a communication system.

The FSS is a spatial filter in the radio frequency range. It comprises a periodic arrangement of identical elements in a 1D or 2D array. Patch and aperture are two fundamental types. A vast amount of research has been done on planar FSSs because a unit cell of an infinite array can be used for the analysis and comprehensive study of the entire structure. The same approach cannot be taken for a curved structure as its extrapolation from a single unit cell is not possible because, for certain incident fields, element currents and scattering from the edges of the curved surface diverge significantly.[1] Hence, the curved FSS is a mathematically complex structure and is difficult to analyze.

While wide bandwidth is the basic requirement for high speed communications, roll-off plays an important role in reducing noise and interference during the transition from the passband to the stopband. Good roll-off has been documented with aperture-type planar FSSs having Archimedean spiral and annular ring elements.[2-4] Wideband and multiband aperture-type planar FSSs have been reported. A flat passband response with high roll-off has been achieved.[5,6]

A bandpass planar FSS with a square slot exhibited 2.7 GHz bandwidth with left and right roll-offs of 7.33 dB/GHz and 30 dB/GHz, respectively.[7] A polarization-insensitive FSS was designed using a square unit cell loaded with two pairs of ring slots and one split-ring slot pair.[8] The structure demonstrated good transmission characteristics within the passband with a steep roll-off. These planar structures are excellent candidates for high performance passband FSSs and can be designed easily. The task of achieving high performance with sharp roll-off, wide bandwidth and low insertion loss, however, is not easy to realize in a curved structure, as the nature of the transmission curve entirely depends on the FSS element, the lattice and the degree of surface curvature.

The properties of curved FSSs have been studied using basic elemental structures like tripoles, circles and others.[9-11] A design with a tripole element,[9] resulted in reduced bandwidth for a curved structure as compared to a planar FSS. A sandwich radome wall investigation was carried out using a double square loop FSS structure.[12]

sciencejournal.org/impact-factor-of-microwave-j.shtml
Microwave Journal
Overview
Impact Factor
0.306
H Index
31
Impact Factor
0.218
Web of Science Group
Google
Scopus
I. Basic Journal Info
Country
United States
Journal ISSN: 1936225
Publisher: Horizon House Publications
History: 1969-1988, 1994-ongoing
Journal Homepage: Link
How to Get Published:
Find out more
Research Categories
Search
USD/INR -0.59%
ENG
16:20

International Journal of Innovative Technology and Exploring Engineering (IJITEE)
ISSN: 2278-3075, Volume-9 Issue-8, June 2020

Development of Method of Moment Based Programme to Analyze Cross Dipole Frequency Selective Surface and its Verification with Measured Results

Saptarsika Das, Anirban Bhattacharya, Santanu Mondal, Partha Pratim Sarkar

Abstract: Theoretical analysis of frequency selective surface comprising of cross dipole elements has been presented in this paper. Algorithm for theoretical analysis based on method of moment has been implemented by MATLAB programming. Theoretical, simulated and experimental results are compared. Simulated result is obtained by ANSOFT designer version 2.2 software. Experimental result is obtained by standard microwave test bench. Good parity in the results is observed. The presented FSS Structure has relevance in the field of mobile and satellite communication.

Keywords : Cross Dipole, Frequency Selective Surface, Method Of Moment

I. INTRODUCTION

An assemble of periodic array of patches on a dielectric substrate or that of apertures within a metallic screen is called Frequency selective surface (FSS). It exhibits frequency filtering properties like the frequency filters in traditional radio frequency (RF) circuits. The patch type and aperture type array resemble band stop and band pass filter respectively, thus realizing its application in spatial microwave and optical filters. Patch type FSS and aperture type FSS are exactly complementary to each other. Patch type FSS is also known as thin screen FSS, which is widely used due to its light weight, low volume, low cost and can be fabricated with conventional printed circuit technology. Relative permittivity of dielectric, distance between two patches, and patch dimensions are some of the primary factors on which the operating frequency of FSS structures depends on [1-2],[4],[7]. Various FSS element shapes include square patch, dipole, circular patch, cross-dipole, Jerusalem cross, ring and many more. Slots and slits can be incorporated on the patch to improve its efficiency [3-4], [6-9]. Thus, for more than four decades, FSS becomes the key interest of researchers and are being used as polarized filters, absorbers, electromagnetic compatibility (EC) shield, sub reflectors, radomes etc [10-14]. FSS is also used as broadband absorber and back scatter transponder [15-18].

Different types of FSS structures are theoretically analyzed by using various methods like- FDTD, FEM, MOM. The formulation of electromagnetic scattering problems for normal incidence by MOM is complicated, whereas due to its perfect accuracy in the frequency domain, it is widely used for analysis. In method of moment (MOM), the characteristic basis functions are used to considerably reduce the matrix size and to converge quickly, hence can electrically solve large problems knowing fewer unknowns [3-6].

A MOM based algorithm is theoretically established in this paper to calculate the scattered electric field of a cross dipole patch type FSS structure and then the transmission coefficient of the structure is determined by MATLAB programming from the scattered electric field. We have simulated the same cross dipole patch type FSS structure by using ANSOFT designer version 2.2 which works on MOM. The programmed and simulated results obtained have been compared with the measured data obtained by experiment. Although this paper only appraises a cross dipole patch type FSS, other type of FSSs may also be analyzed by the same method.

II. DESIGN OF FREQUENCY SELECTIVE SURFACE

The FSS structure is designed with metallic cross dipole element having length 15mm and width 1.5mm, the periodicity in both x and y direction is 29.7mm. Dimension of the FR4-epoxy substrate is 150mm X 150mm X 1.6mm as shown in Fig.1, having 4.4 relative permittivity. The FSS unit cell is given in Fig.2.

Revised Manuscript Received on June 10, 2020.
* Saptarsika Das
Saptarsika Das*, Department of Electronics, Rishi Bankim Chanra College, Naihati, India. Email: saptarsika@gmail.com
Anirban Bhattacharya, Department of Electronics, Rishi Bankim Chanra College, Naihati, India. Email: bh.anirban@gmail.com
Santanu Mondal, Institute of Radio Physics and Electronics, University of Calcutta, Kolkata, India. Email: santanumondal2008@rediffmail.com
Partha Pratim Sarkar, DETS, University of Kalyani, Nadia, India. Email: parthabe91@yahoo.co.in

Design of Frequency Selective Surface as Multiband Absorber

Saptarsika Das *[1,2], Ramesh Chandra Tiwari[1], L Lolit Kumar Sing[3] and Partha Pratim Sarkar [4]

[1]Department of Physics, Mizoram University, Mizoram-796004, India

[2]Department of Electronics, Rishi Bankim Chandra College, Naihati, West Bengal-743165, India

[3]Department of Electronics and Communication Engineering, Mizoram University, Mizoram-796004, India

[4]Department of Engineering and Technological Studies, University of Kalyani, West Bengal-741235, India

Abstract- The different studies and surveys concerning the ill effects of electromagnetic radiation has proved that electromagnetic wave is extremely harmful to plant kingdom and animal kingdom including human beings. Frequent usage of mobile phones and other electronic gadgets are responsible for exposure to excessive electromagnetic radiation. The electromagnetic wave is unavoidable in existing situation. So there is no other alternative than to take protective measure from harmful effect of electromagnetic radiation. Design and application of reflective FSS may be a protection to a particular person but it will affect neighbouring people. The design and application of absorbing type FSS solely can be an appropriate measure as a protective device from harmful electromagnetic radiation. Present study describes design of multi absorbing band FSS structure.

1. Introduction

The rapid development of technology is a boon to mankind despite of living amidst electromagnetic pollution. Electromagnetic pollution which is also known as radiation pollution is harmful for human health. Human exposure to electromagnetic radiation results in the absorption of electromagnetic waves by body fluids. The absorption causes localised heating effects within the body which end in drying up of fluids around eyes, brain, joints etc. [1]. The localised heating effects become more adverse if the body is exposed to other sources of heat simultaneously, the body cooling system fails to cope with the excessive heat that consequences to heat stroke. The interaction of electromagnetic field with metallic implants within the body influenced the normal operation of the implants by generating some external pulses [2]. Long time exposure to electromagnetic radiation increases the activity of free radicals that are responsible for changes in enzymes involved in oxidative process and effect genes [3]. Radio frequency exposure increases calcium fluxes into the cell which disrupt synapse formation culminated neurodegeneration. Electromagnetic field team up with toxic chemicals contribute to brain diseases. Sleeping disorder, skin rashes, ear tumour, concentration problem, headaches are the aftermaths of prolong exposure to electromagnetic radiation [4]. The above facts foreshowed the slow devastating effects

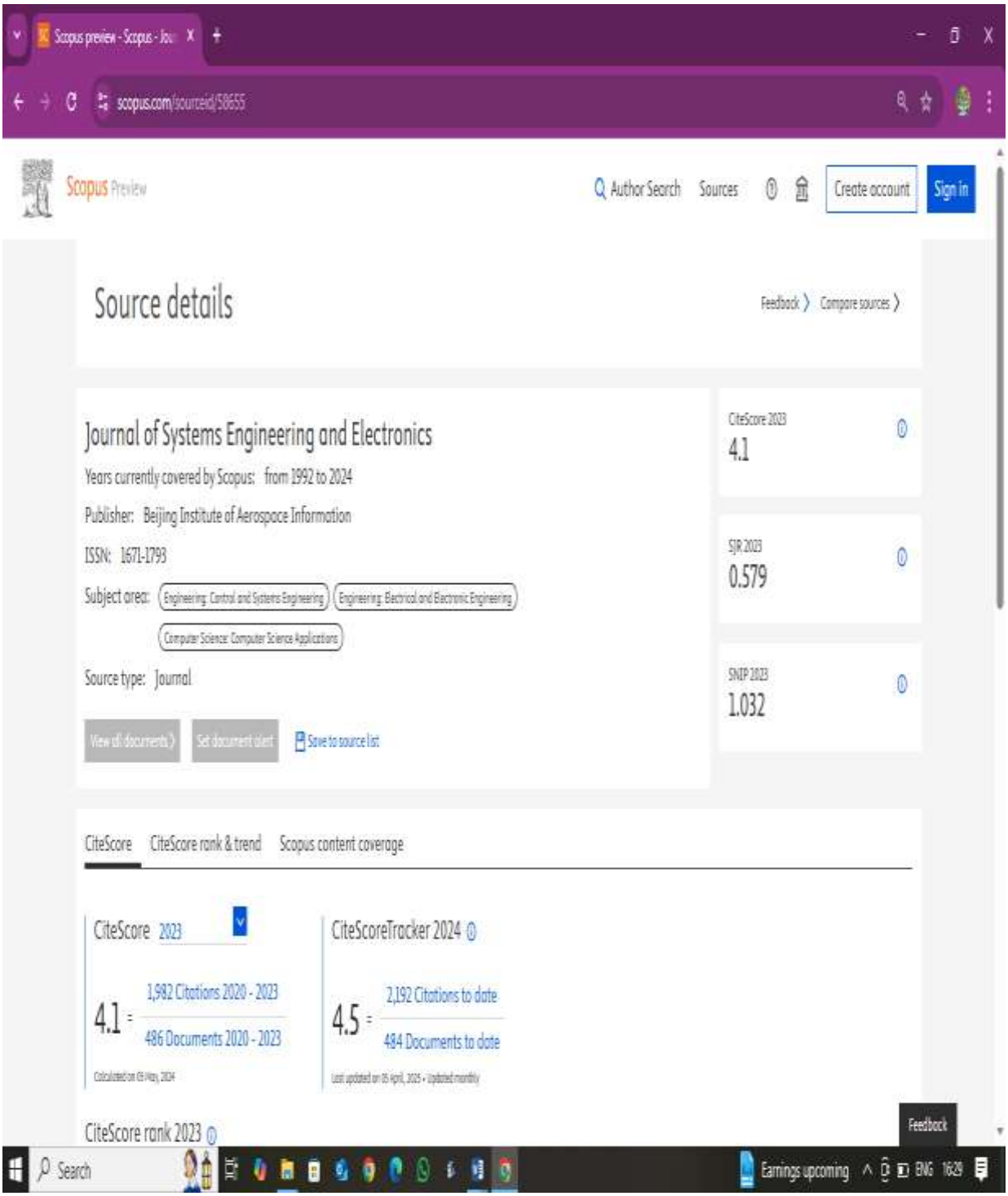
Scopus preview - Scopus - Jou
scopus.com/sourceid/58655
Scopus Preview
Author Search
Sources
Create account
Sign in
Source details
Feedback
Compare sources
Journal of Systems Engineering and Electronics
Years currently covered by Scopus: from 1992 to 2024
Publisher: Beijing Institute of Aerospace Information
ISSN: 1671-1793
Subject area: Engineering: Control and Systems Engineering
Engineering: Electrical and Electronic Engineering
Computer Science: Computer Science Applications
Source type: Journal
View all documents
Set document alert
Save to source list
CiteScore 2023
4.1
SJR 2023
0.579
SNIP 2023
1.032
CiteScore
CiteScore rank & trend
Scopus content coverage
CiteScore 2023
4.1 = 1,982 Citations 2020 - 2023 / 486 Documents 2020 - 2023
Calculated on 05 May, 2024
CiteScoreTracker 2024
4.5 = 2,192 Citations to date / 484 Documents to date
Last updated on 05 April, 2025 • Updated monthly
CiteScore rank 2023
Feedback
Search
Earnings upcoming
ENG
16:29

Published by:
https://tarzresearch.com/

Tarz Research Journal
ISSN: 1869-7720
Vol. 11 Issue 3, March-2025

Design of compact frequency selective surface comprising of slot and slit loaded square patch elements

Saptarsika Das [*1], Ramesh Chandra Tiwari[1], L Lolit Kumar Singh[2] and Partha Pratim Sarkar [3]

[1]Department of Physics, Mizoram University, Mizoram-796004, India
[2]Department of Electronics and Communication Engineering, Mizoram University, Mizoram-796004, India
[3]Department of Engineering and Technological Studies, University of Kalyani, West Bengal-741235, India

Abstract. The authors emphasized on conventional method of cutting slits and slots in the patch to reduce the resonant frequency resulting in effective size reduction of the Frequency Selective Surface. A compactness of 97.28% has been achieved by the structure presented in this paper by modifying a square patch incorporating slits and slots. The lowest resonant frequency attained by the structure is 1.78 GHz after modification and 10.80 GHz before modification. The compactness of 97.28% attained at such a low resonant frequency is the major contribution of the work. The multiband obtained by the structure establish its importance as band stop filter in L, C and X bands. This paper methodically fulfils the demand of miniaturized multifunctional spatial filter in a wireless communication system.

Keywords. Compact, Frequency Selective Surface, Multiband, Square Patch.

1 Introduction

Wireless communication expansion accelerates the demand of high and efficient transmission capacity to enhance the system's capability. Additionally, miniaturized multifunctional filter is the major requirement to build a light weight system. The frequency selective property of the frequency selective surface (FSS) in spatial domain meets the requirement of the filter in modern communication systems. The gain of the microstrip antenna can also be enhanced using such filters. So, compact multifunctional FSS is of high demand as spatial filters. FSS is a two dimensional array of elements that transmit or reflect a particular frequency band in free space. The stop band FSS efficiently separates the unwanted signal and thus reduced

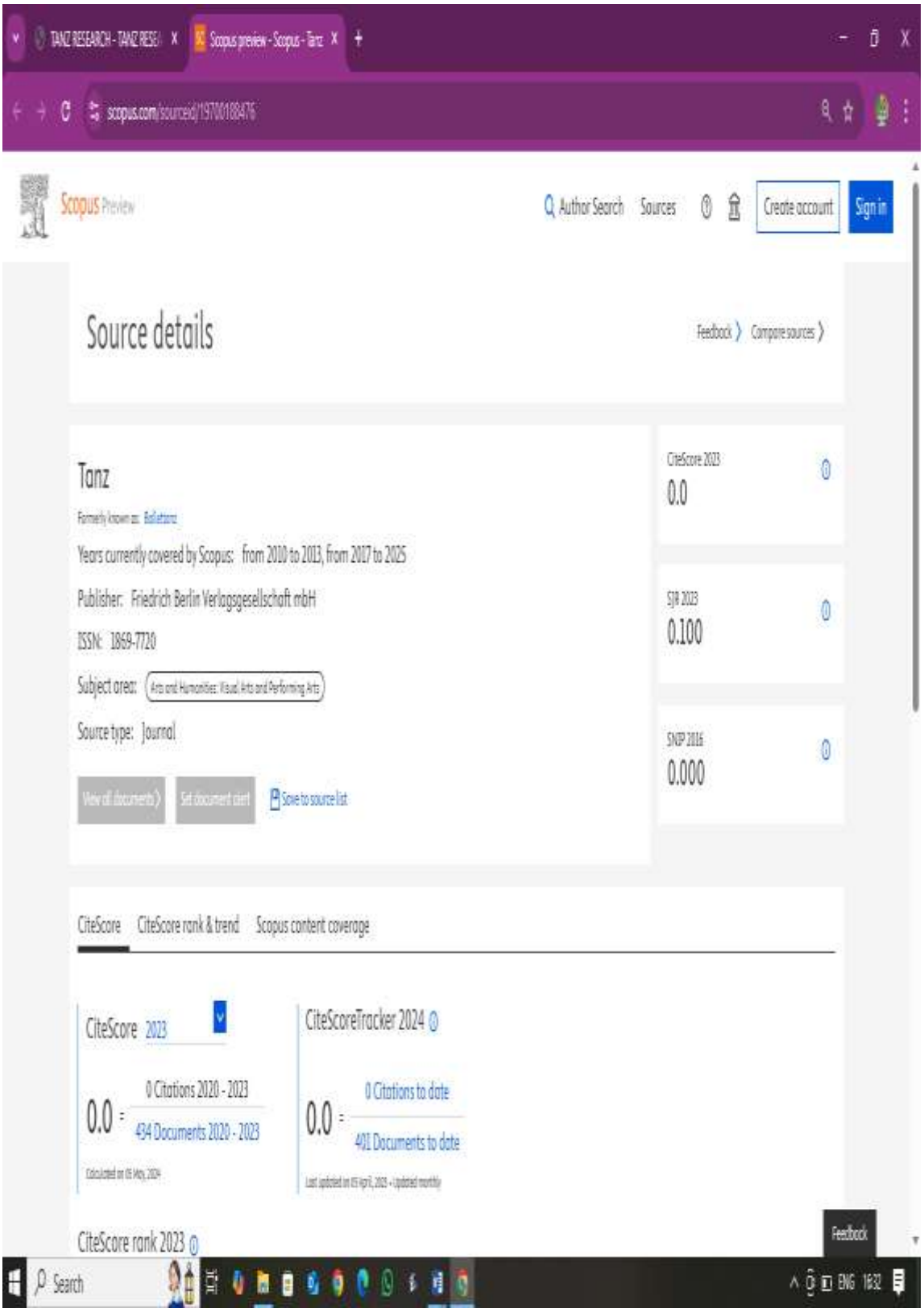
TANZ RESEARCH - TANZ RESE
Scopus preview - Scopus - Tanz
scopus.com/sourceid/19700188476
Scopus Preview
Author Search
Sources
Create account
Sign in
Source details
Feedback
Compare sources
Tanz
Formerly known as: Ballettanz
Years currently covered by Scopus: from 2010 to 2013, from 2017 to 2025
Publisher: Friedrich Berlin Verlagsgesellschaft mbH
ISSN: 1869-7720
Subject area: Arts and Humanities: Visual Arts and Performing Arts
Source type: Journal
View all documents
Set document alert
Save to source list
CiteScore 2023
0.0
SJR 2023
0.100
SNIP 2016
0.000
CiteScore
CiteScore rank & trend
Scopus content coverage
CiteScore 2023
0.0 = 0 Citations 2020 - 2023 / 434 Documents 2020 - 2023
CiteScoreTracker 2024
0.0 = 0 Citations to date / 401 Documents to date
CiteScore rank 2023
Feedback
Search
ENG 16:32

JIS UNIVERSITY

INSTITUTION'S INNOVATION COUNCIL

Azadi Ka Amrit Mahotsav

G20 भारत 2023 INDIA

CERTIFICATE

This is to certify that

Saptarsika Das

has presented the paper entitled "*Design of a Compact Tri-band Frequency Selective Surface*" in 1st International Conference on Recent Innovation in Science, Communication & Computation 2024 organized by Department of Computer Science and Engineering of JIS University on 19th & 20th April 2024.

Prof. (Dr.) Dharmpal Singh	Mr. Radhakrishna Jana	Prof. Sandip Roy	Prof. H.S. Maji
Convener , RISCC 2024	Co- Convener , RISCC 2024	HOD of CSE, JIS University	Dean Academic, JIS University

First International Conference on Sustainable Technologies (ICST-2024)

12-15th December 2024,

Organized by
Microsystem Design-Integration Lab
Bidhan Chandra College, WB, India

PARTICIPATION CERTIFICATE

This **Participation Certificate** is presented to

Mrs. Saptarsika Das of Mizoram University

for presenting the following title (Oral/Poster):

Design of a Multiband FSS Absorber

in First International Conference on Sustainable Technologies (ICST-2024)
12-15th December 2024,

Dr. Amit Banerjee,
Convener, ICST-2024

Prof. Amit K. Chakraborty,
Organising Chair, ICST-2024

Dr. Falguni Mukhopadhyay,
Patron, ICST-2024

PARTICULARS OF THE CANDIDATE

Name of Candidate	: Saptarsika Das
Degree	: Ph.D
Department	: Physics
Title of Thesis	: Design, Analysis and Characterization of Different Types of Frequency Selective Surfaces and Absorber
Date of Admission	: 15th September 2021
Approval of Research Proposal	
1.DRC	: 22nd March 2022
2.BOS	: 8th April 2022
3.School Board	: 7th June 2022
MZU Regn No	: 2200050
Ph.D Regn No	: MZU/ Ph.D./ 1935 of 15.09.2021
Extension (if any)	: NIL

Head of the Department

ABSTRACT

DESIGN, ANALYSIS AND CHARACTERIZATION OF DIFFERENT TYPES OF FREQUENCY SELECTIVE SURFACES AND ABSORBER

AN ABSTRACT SUBMITTED IN PARTIAL FULFILLMENT OF THE REQUIREMENTS FOR THE DEGREE OF DOCTOR OF PHILOSOPHY

SAPTARSIKA DAS

MZU REGISTRATION NO.: 2200050

Ph.D. REGISTRATION NO.: MZU/Ph.D./1935 of 15.09.2021

DEPARTMENT OF PHYSICS

SCHOOL OF PHYSICAL SCIENCE

AUGUST, 2025

DESIGN, ANALYSIS AND CHARACTERIZATION OF DIFFERENT TYPES OF FREQUENCY SELECTIVE SURFACES AND ABSORBER

BY

SAPTARSIKA DAS

DEPARTMENT OF PHYSICS

SUPERVISOR

Prof. RAMESH CHANDRA TIWARI

JOINT SUPERVISOR

Prof. L. LOLIT KUMAR SINGH

Submitted

In partial fulfillment of the requirement of the Degree of Doctor of Philosophy in Physics of Mizoram University, Aizawl

Abstract

Frequency Selective Surface (FSS) is a two dimensional array of elements which operates on the resonating principle of a filter. There are two types of FSS- Patch type FSS and Aperture type FSS. The patch type FSS resembles bandstop filter as it reflects a specific frequency range of the incoming electromagnetic wave at resonant frequency depending on the geometry of the FSS element, permittivity of the FSS substrate, periodicity etc. Similarly, aperture type FSS resemble bandpass filter as it passes certain range of the incoming electromagnetic wave at resonance. The unique feature of an FSS to stop or pass a desired band of frequency of the electromagnetic spectrum has been utilised to replace the electronic filters in microwave and optical systems. This substitution corresponds to the application of the FSS as sub-reflector, radome, polariser. FSS enhances the gain and directivity of the antenna when integrated with microstrip antenna by reducing back lobe losses. It has advance applications as power and energy limiters, isolaters etc. FSS being light weight, low cost and easy to fabricate with wide range of application fascinate researchers to carry out an extensive study. Focusing on the explored territory discussed in the literature, it has been observed that the FSS need improvement according to the call of time. Thus, the objective of the thesis has been outlined to study the FSS theoretically, to improve the parameters like roll-off, insertion loss, flatness of the band in case of planar and curved FSS, to reduce the size of the FSS in lower frequency range, to design a cost effective FSS absorber without using any absorbing material. Hence, FSS is the cynosure of the presented thesis, concentrating on its versatile application field.

In **chapter 1,** the fundamentals of FSS are put forward to understand the characteristic behaviour of an FSS. Its dependence on structure of the unit cell elements. The methods applied to theoretically analyse an FSS and the softwares used for the purpose. The areas that substantiate the importance of FSS as spatial filter. A thorough literature survey has been done to track down the objective of our work. In this chapter the objective and organisation of thesis are also presented,

In **chapter 2,** theoretical study of a cross dipole structure of dimension 15 mm X 1.5 mmembossed on FR4-epoxy substrate of thickness 1.6 mm, having periodicity of 29.7 mm in both the plane of two dimensionhas been presented following the method of moment numerical technique. A MATLAB coding has been established following the numerical methodology to generate the transmission characteristics of the FSS prototype. The designed structure is simulated by ANSOFT version 2.2 and the experimental study of the fabricated prototype has been done by standard microwave test bench. The result obtained by the MATLAB programming presented in this chapter shows closest agreement with the experimental result than that obtained by the simulation software. Thus, the numerical approach and MATLAB programming presented in this chapter analyse an FSS structure effectively in compare to the available software. Moreover,the result obtained by simulation using software is dependent on the choice of number of steps in the frequency range of study or on typeof choosing a mess; whereas, the algorithm developed by us is independent of such type of consideration.The work is published in Scopus indexed journal.

In **chapter 3,** an aperture type planar and curve FSS have been designed with concentric annular ring element. The aim of this chapter is to design a planar and curve FSS with agood roll-off at both the edges of the transmission characteristic curve having flat band and low insertion loss. Air is considered as dielectric medium and 7.6 mm has been optimized as the air gap between the two layers. Firstly, the planar FSS has been designed by using HFSS software, which is then fabricated and tested using standard microwave test bench. It has been observed that the simulated and measured results of the designed planar FSS are in good agreement. A wide flatband of 4 GHz has been obtained in the frequency range of 6.7 GHz to 10.7 GHz with low insertion loss with respect to -10 dB. The planar FSS attain a percentage bandwidth of 45.96% with a sharp left and right roll-off of 45 dB/GHz and 73.33 dB/GHz respectively. The comparative study of the designed planar FSS with the documented work in the literature set forth the fact that the bandwidth achieved by the designed planar FSS presented in this chapter is the best. The roll-off attained by the structure is sharpest in compare to all the documented work.

All these parameters, ie. roll-off, insertion loss and flatband, cannot be attained easily for a curved structure; as for each element, surface current and scattering from the edges diverges significantly. For designing the curve FSS the elemental dimension, periodicity and air gap of both the layers are kept same as that of the planar FSS. Semi cylindrical form has been chosen to study the curve structure, where the radius of layer 1 is 100mm and that of layer 2 is 107.6 mm. The length of the semi cylinder has to be limited to 310 mm considering the fact that high computational resources should be taken into account. Taking account of the fact that unit cell simulation is not possible for curved FSS, the entire composite structure of the curved FSS has been simulated by CAD FEKO simulation software. The simulated and measured result of the designed curve FSS are in good agreement. The curve FSS composite attain a bandwidth of 4.2 GHz in the frequency range of 7 GHz to 11 GHz. The structure attain 45.16% fractional bandwidth with right and left roll-off of 32.09 dB/GHz and 16.66 dB/GHz respectively. The comparative study of the designed conformal structure presented in this thesis with the contemporary works enlisted in the literature put forward the facts that the fractional bandwidth and the roll-off attained by the designed structure are the best and sharpest respectively. It is notable that the bending of the planar FSS into semi cylindrical form exhibits insignificant fractional bandwidth alteration.This novel feature puts forward the designed FSSs from the present state of art. Both the planar and curve FSS are capable to efficiently reduce electromagnetic interference and noise without deteriorating the signal strength due to the sharp roll-off depicted by them. Since planar FSS is incompatible for application with the curve structure as the studied parameters degrade highly, the curved FSS fulfills the purpose and is compatible with any conformal structure. The presented studies outline applications in satellite communication systems, radome systems and electronic warfare systems.The work is published in SCI indexed journal.

In **chapter 4,** focus has been given to reduce the size of the FSS at lowest resonant frequency by incorporating slit and slot in the patch. Three patch type simple elements are modified to obtain compactness. Firstly, a circular patch of radius 9.8 mm having periodicity of 20 mm X 20 mm has been embossed on FR4-epoxy of

thickness 1.6 mm, which is then modified step by step by introducing circular slot and swastika shaped slot.The reference patch resonated at 9.36 GHz. The final modified circular patch type FSSachieved multiple band in the frequency range of 2.5 GHz to 11.5 GHz. The lowest frequency attained by the modification of the patch is 2.82 GHz, that is a compactness of 90.92% has been accomplished by modifying a circular patch incorporating circular slots and swastik shaped slot.

Secondly, 11mm X 11 mm square patch has been modified by introducing square loop and circular slots. FR4-epoxy substrate of thickness 1.6 mm is used as substrate.The periodicity of the structure has been kept 12 mm in both x and y direction. The reference patch resonated at 19.37 GHz.The modification of the square patch attains three stopband in the frequency range of 3 GHz to 18 GHz. The lowest resonant frequency achieved by the modified square patch is 3.41 GHz. Hence, the size of the FSS has been reduced to 96.90%.

Finally, a square patch of dimension 16mm X 16mm printed on FR4-epoxy substrate of thickness 0.8 mm having periodicity of 23 mm in x and y direction, has been modified by introducing rectangular slits and slots. The modified structure is fabricated and measured.The reference square patch resonates at 10.80 GHz. The final modification of the square patch results into three stop band in the frequency range of 1.6 GHz to 11 GHz. The lowest frequency attained by the structure by simulation is 1.72 GHz and by measurement it is 1.78 GHz. Hence, the compactness achieved by the modification of the square patch by introducing slits and slots is 97.28%.The modification of square patch by loop type slots is presented in an international conference and the modification of the square patch by introducing slits and slots is published in scopus indexed journal. The study documented in this chapter have a significant role in real world application. Compact FSS helps to produce portable gadgets. FSS's compactness determines the compactness of composite structure (Antenna + FSS).

In **chapter 5,** focus has been given to design an FSS absorber without using any absorbing material, that is aim to reduce the total cost of the FSS composite. A three layer FSS absorber is designed considering the periodicity of 25 mm in both the

plane of two dimension. The bottom layer is designed by modifying a 24mm X 24 mm square patch on FR4-epoxy substrate. Two square patches of dimension 6.5 mm X 6.5 mm and 9.5 mm X 9.5 mm are imprinted on both sides of the substrate to design the middle layer. Two square patches of dimension 15 mm and 9.4 mm have been embossed on both sides of the substrate to design the upper layer. Three absorption band have been attained by the designed three layer FSS absorber in the frequency range of 8 GHz to 11 GHz. The maximum absorption coefficient attain by the FSS absorber is above 90% for all the three bands, with the maximum of 99.62%;and the respective minimum absorption coefficient is above 80%.

A two layer FSS absorber is designed with periodicity of 22 mm in both the plane of two dimension.The substrate thickness of bottom layer is 1.6 mm and that of top layer is 0.8 mm. A modified 16 mm X 16 mm square patch and a modified 18 mm X 18 mm square patch have been imprinted on both side of the substrate to design the bottom layer of the FSS absorber. A superstrate of dimension 9.7 mm X 9.7 mm is added to the bottom layer.The designed FSS absorber achieved minimum and maximum percentage of absorption of 83% and 97% respectively in the frequency range of 6.5 GHz to 9.1 GHz.

The design of FSS absorber presented in this chapterdoesnot use any absorbing material which makes it a cost effective FSS absorber. The designed absorbers have high absorption coefficient, which can be utilised for radiation shielding and absorption purpose. The FSS absorbers examined in this chapter demonstrate their value in concealing radar systems and can also be employed to obfuscate defense systems. In order to lessen the negative effects of electromagnetic radiation, the absorbers can also be utilized in window screens in homes and hospitals. Long-term exposure to electromagnetic radiation poses health risks, which can be reduced by utilizing FSS absorbers to absorb the unwanted radiation. In summary, the research on FSS absorbers that has been discussed here is a prime example of the current technical demands.

Conclusively, this research work successfully completed the objectives outlined from the investigation of the literature.